Streptophyta I

Chlorophyta x Streptophyta

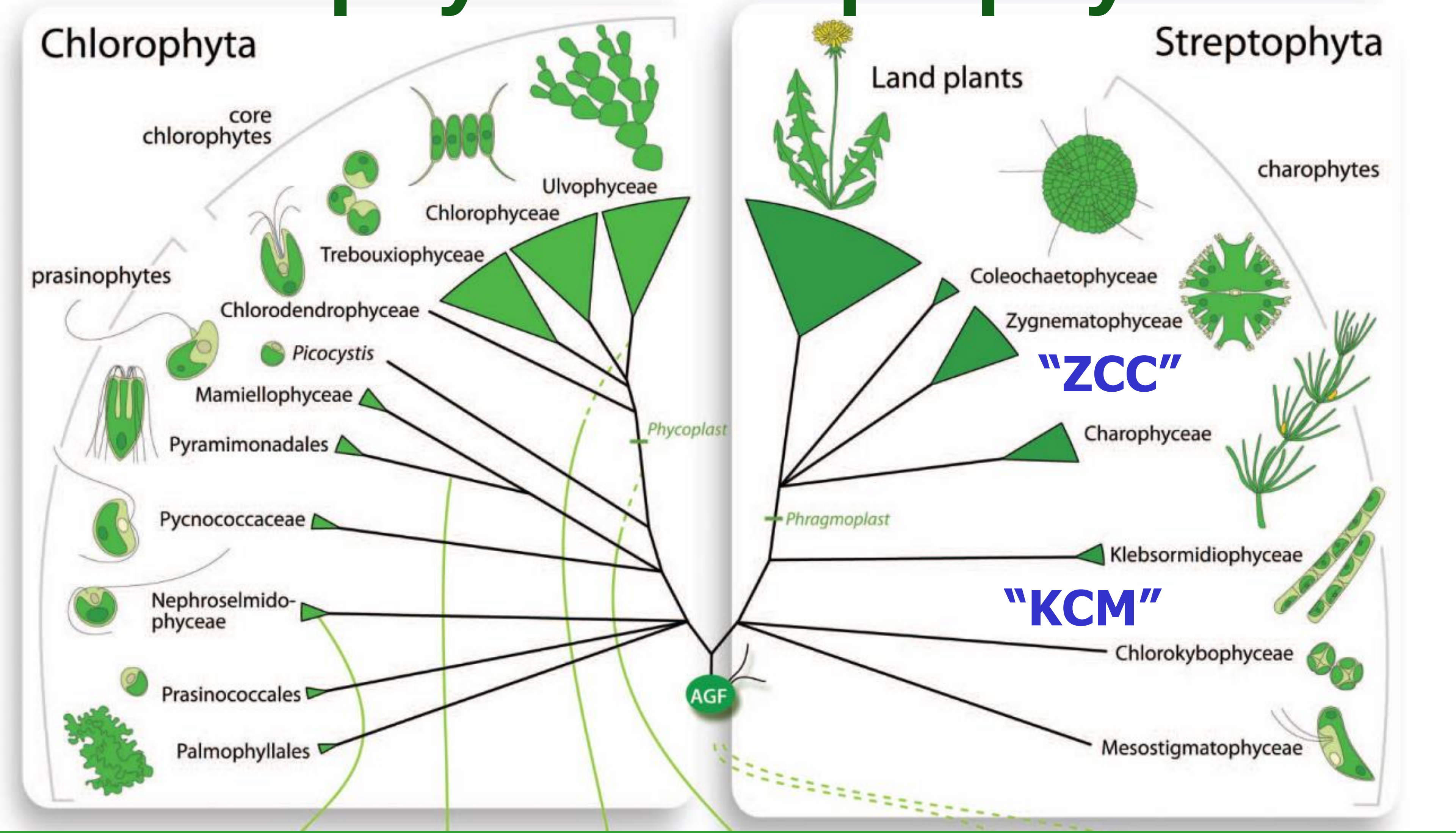

Leliaert et al. (2012)

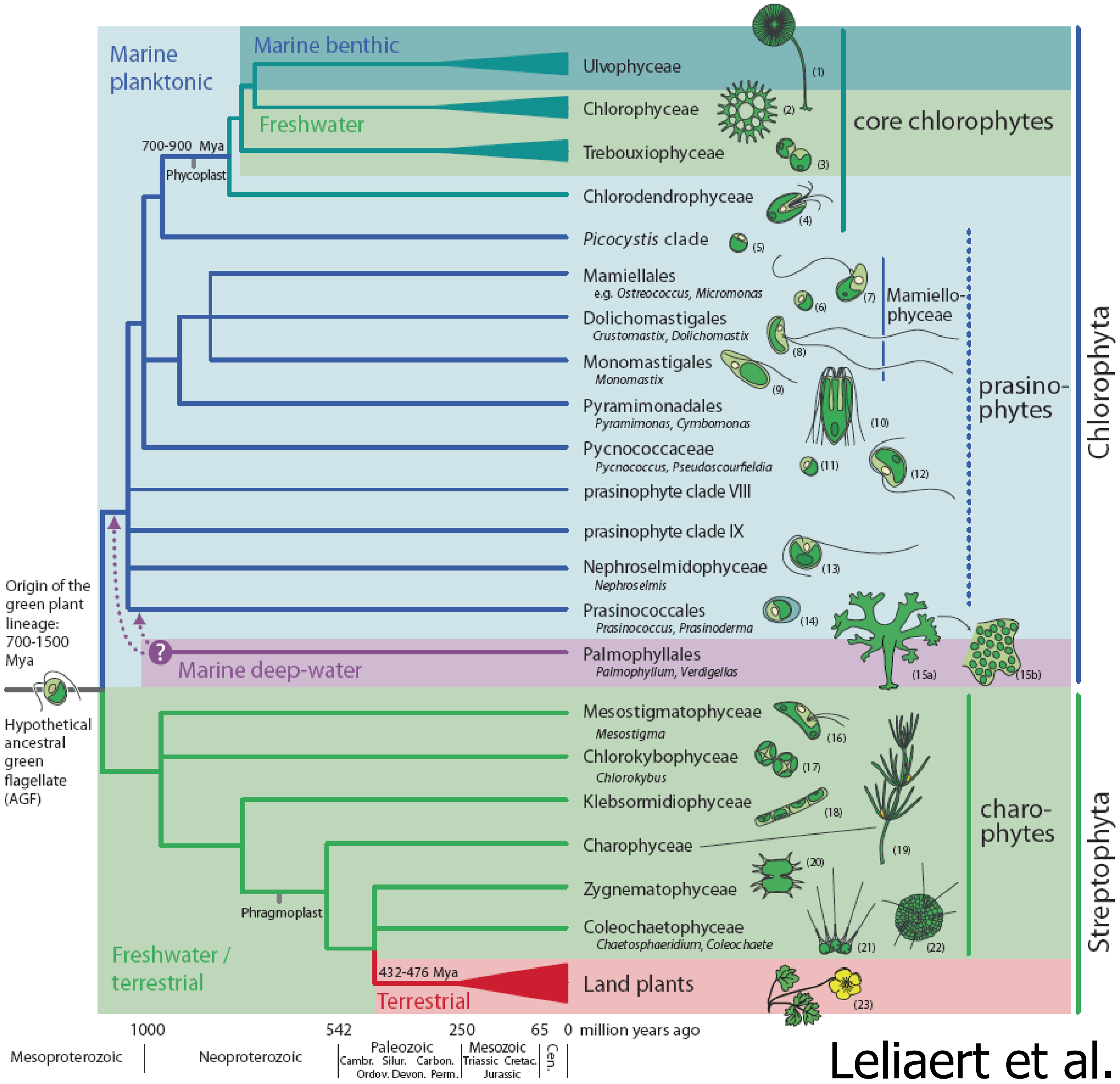

Leliaert et al. (2011)

Chlorophyta x Streptophyta

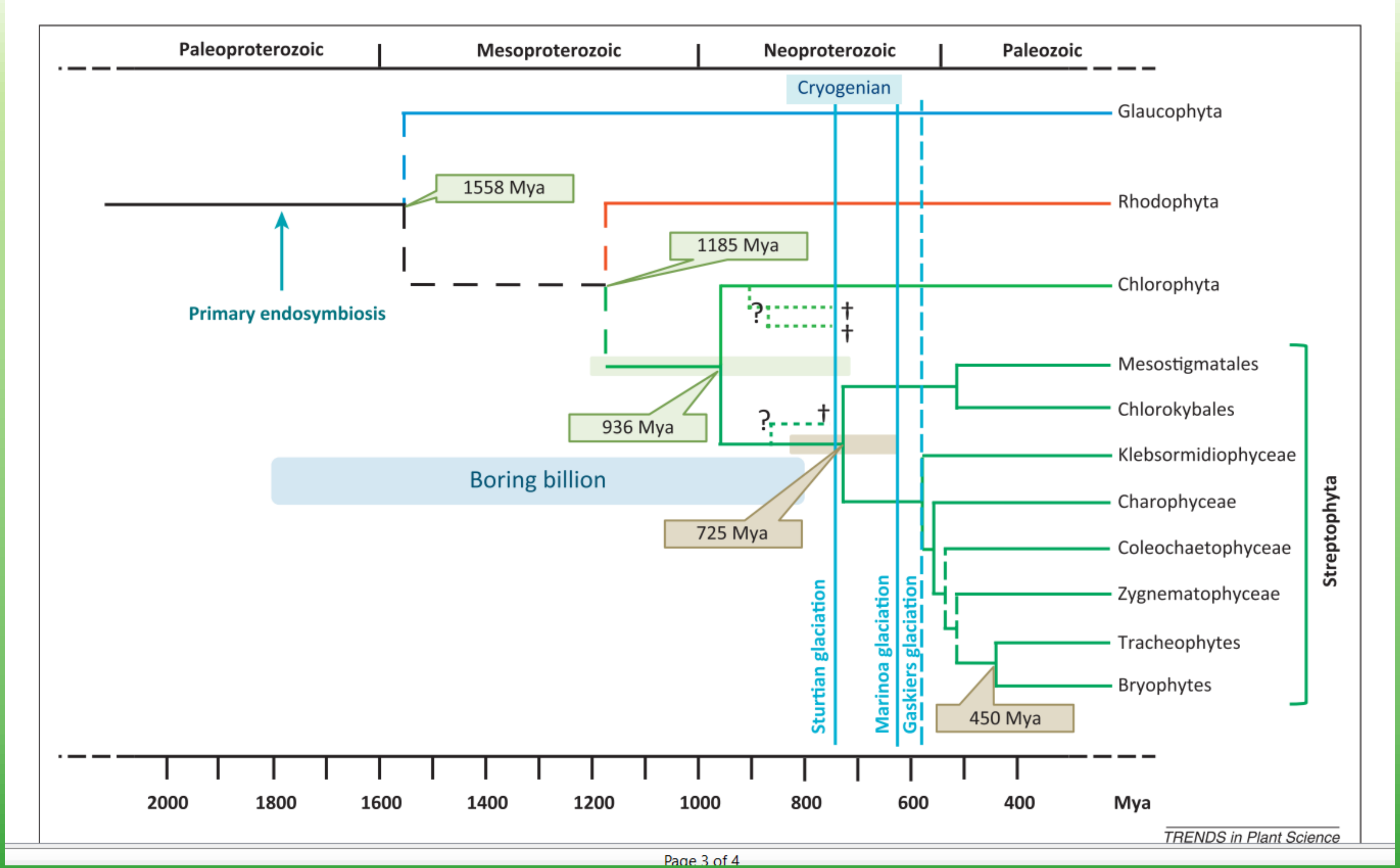

Becker (2013)

Chlorophyta x Streptophyta

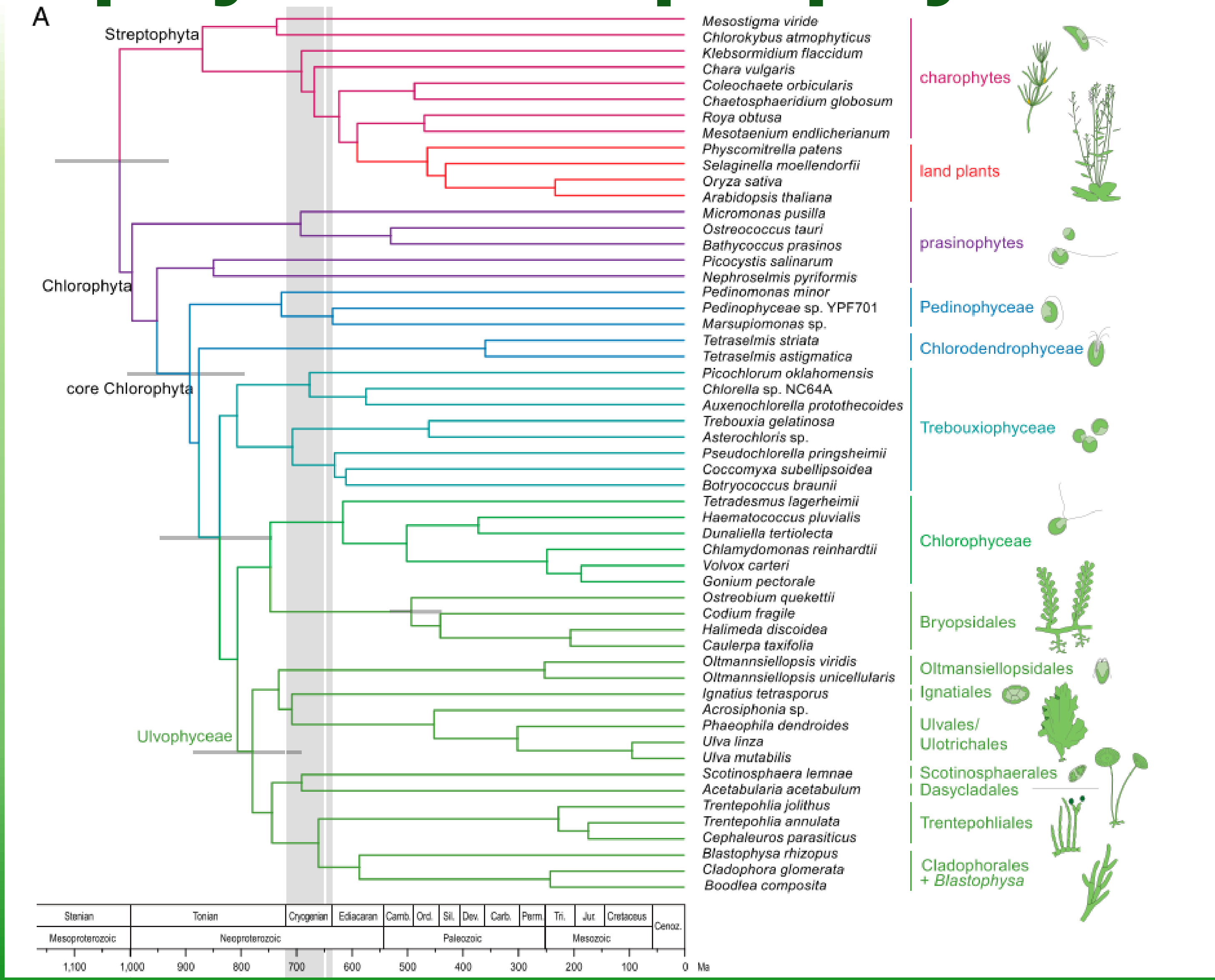

Cortona et al. (2020)

Most recent phylogeny

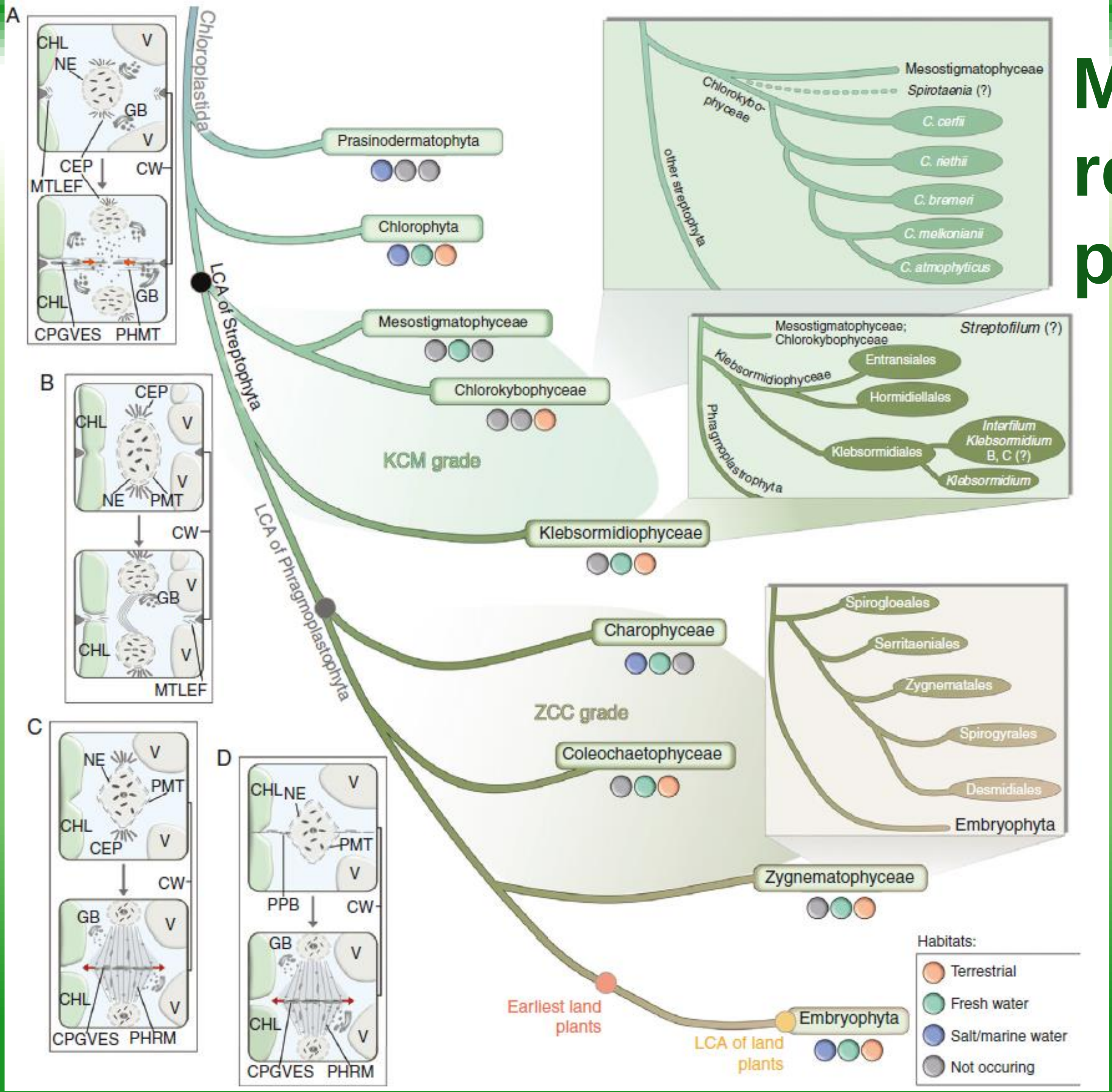

Bierenbroodspot et al. (2024)

Streptophyta phylogeny including *Streptofilum* lineage

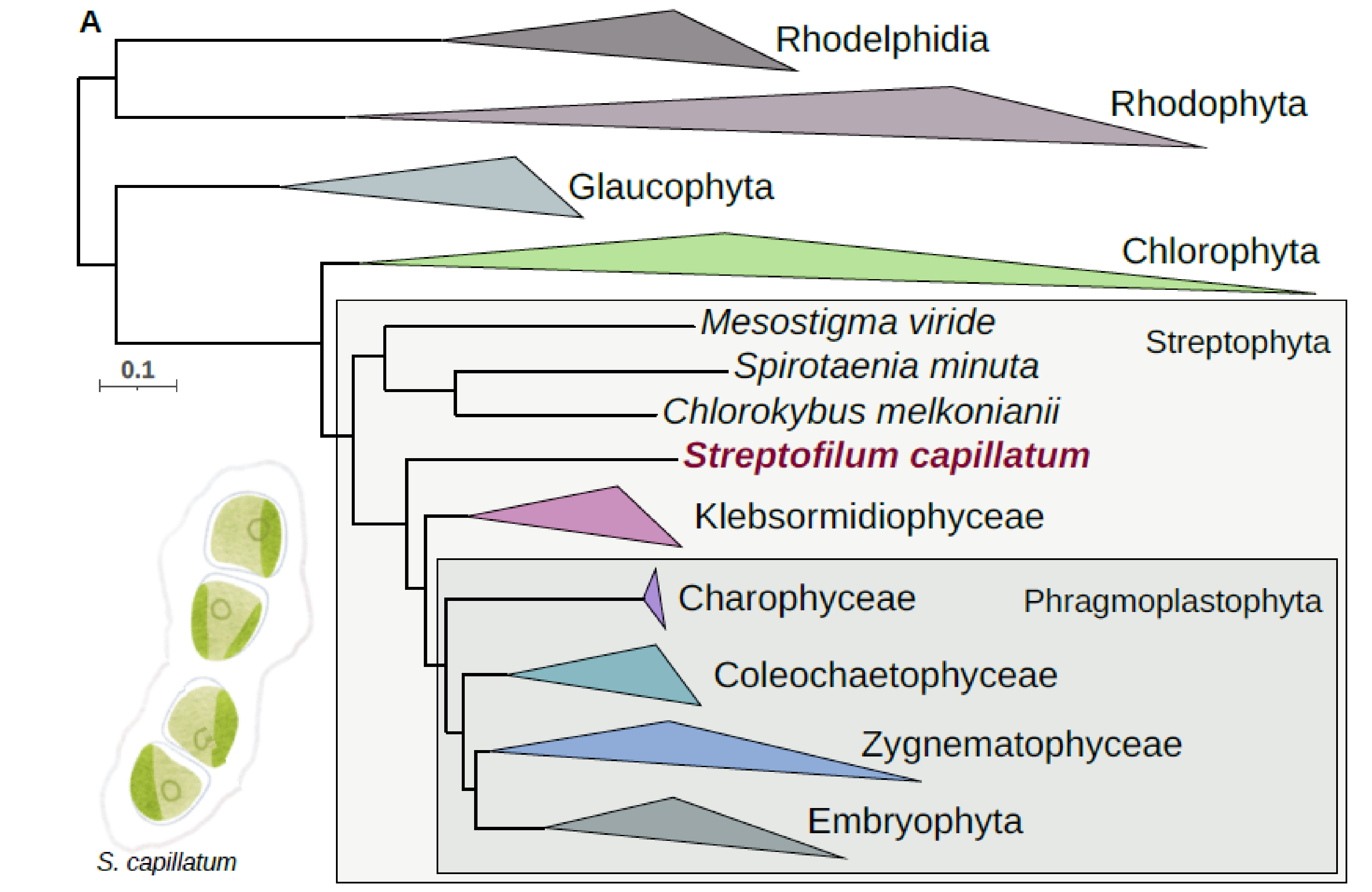

Žárský & Eliáš (2025)

Streptophyta - new traits

Lateral flagella

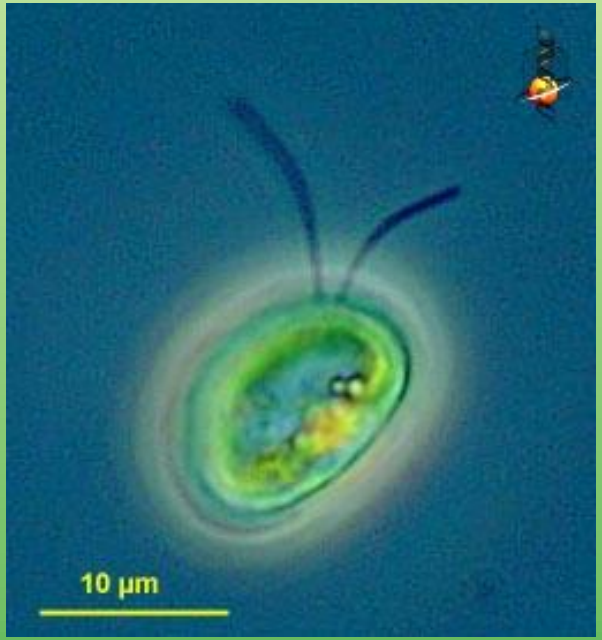

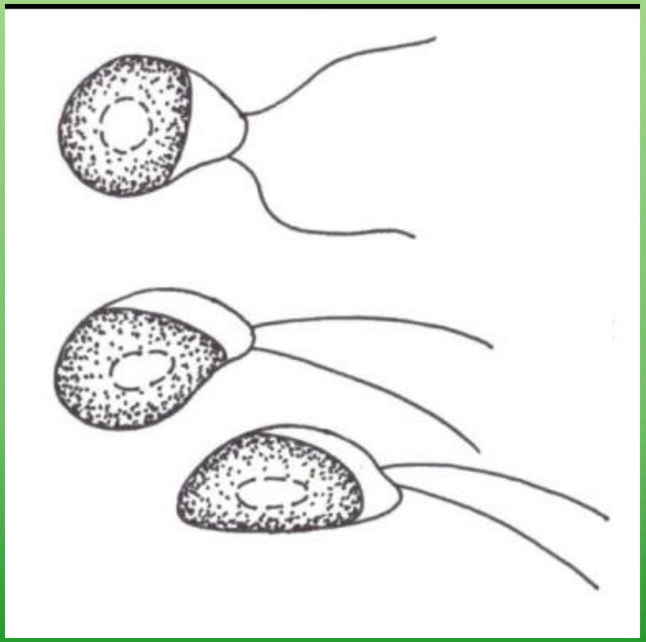

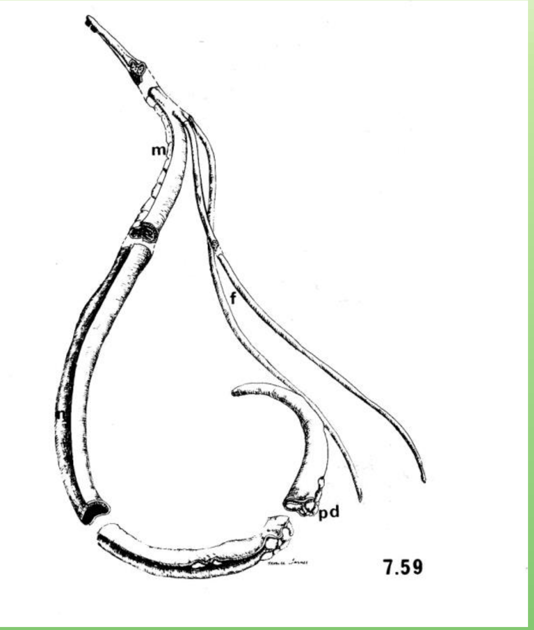

Streptophyta - new traits

MLS – multi-layered structures associated with the flagellar bases

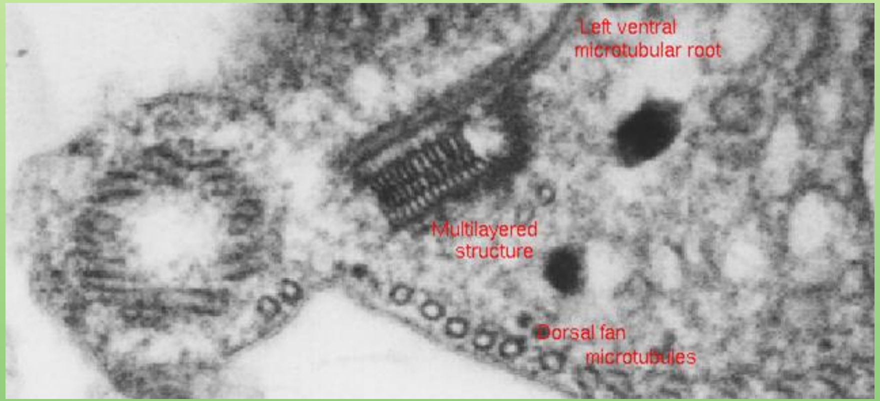

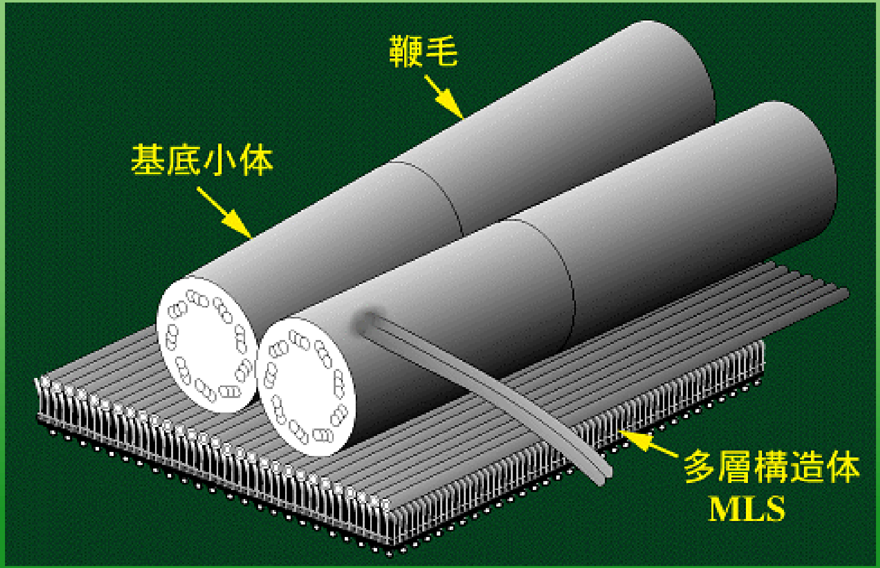

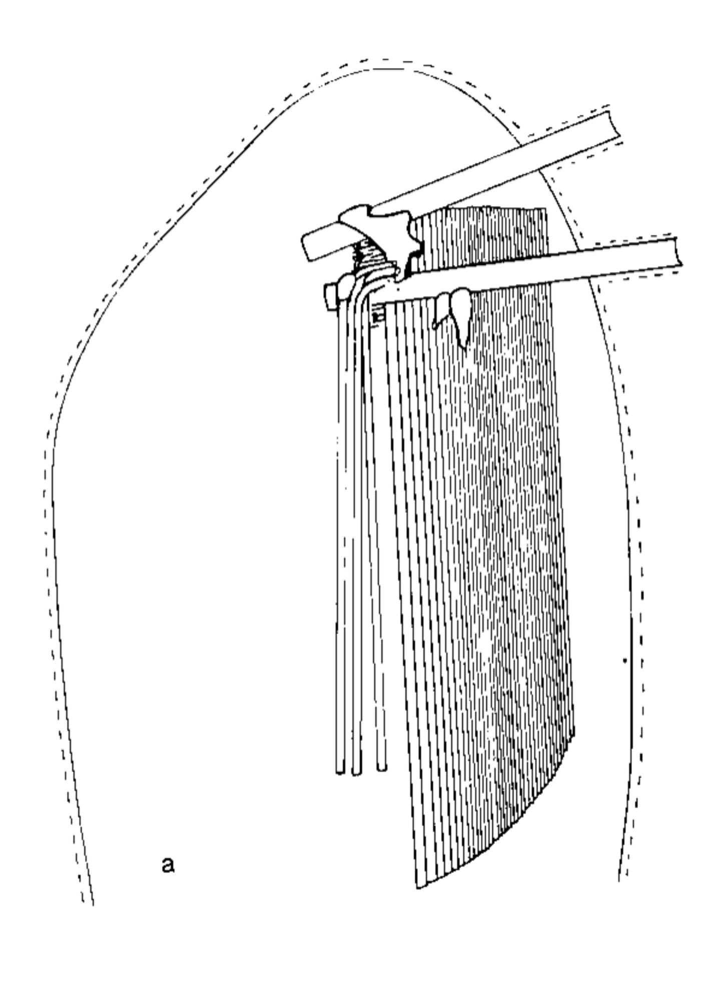

Streptophyta - new traits

- Open mitosis
- phragmoplast

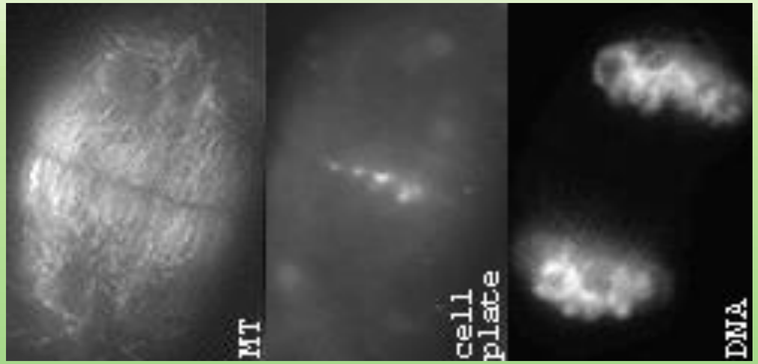

Microtubular orientation during cell division:

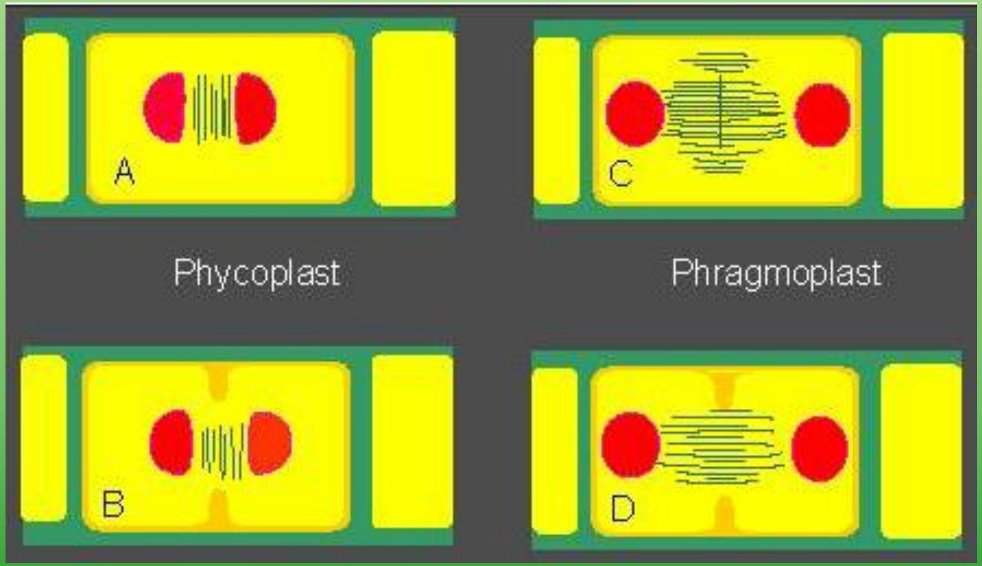

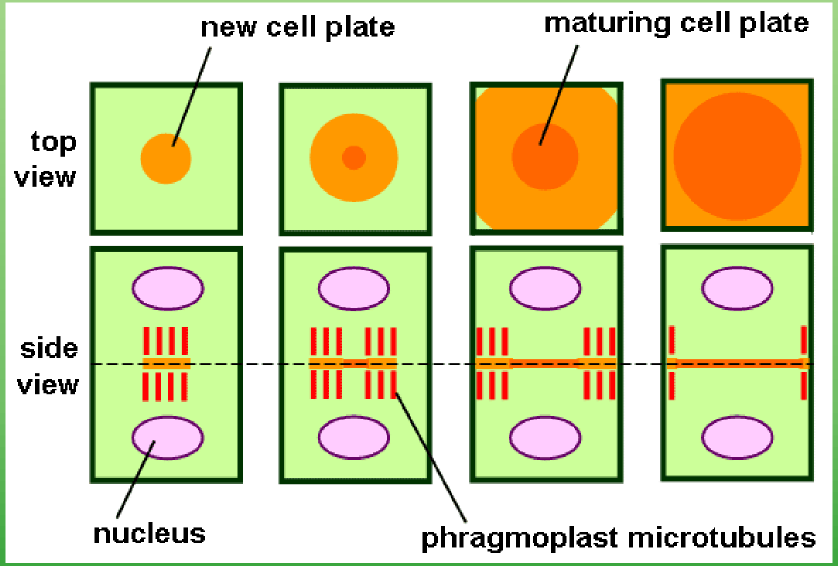

Streptophyta - new traits

Phragmoplast and cell division

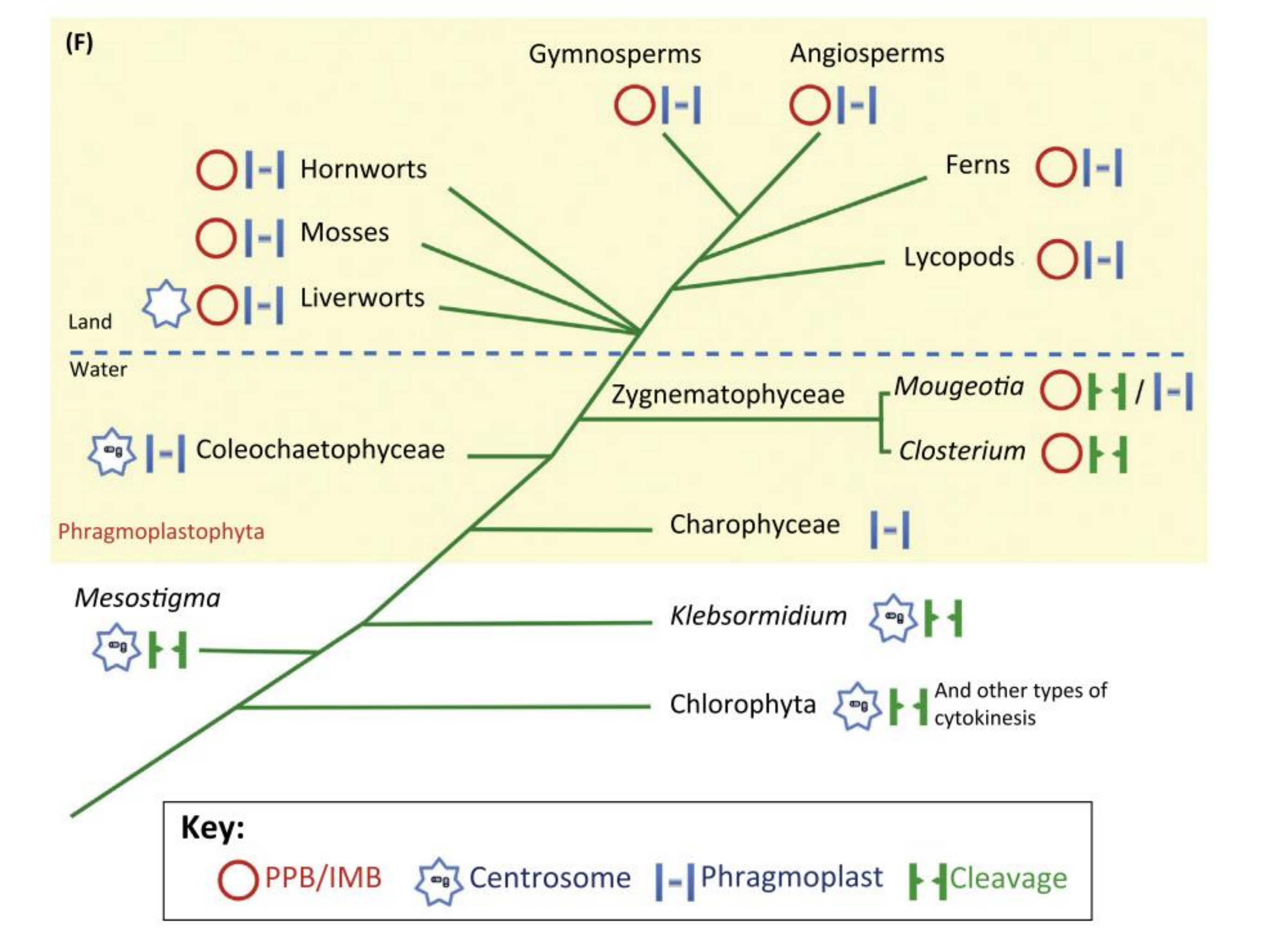

Buschmann & Zachgo (2016)

Streptophyta – new traits

$RuP_2 + CO_2 + H_2O \rightarrow 2 \times$ 3-phospho glycerate

$RuP_2 + O_2 \rightarrow$ 3-phospho glycerate + phosphoglycolate

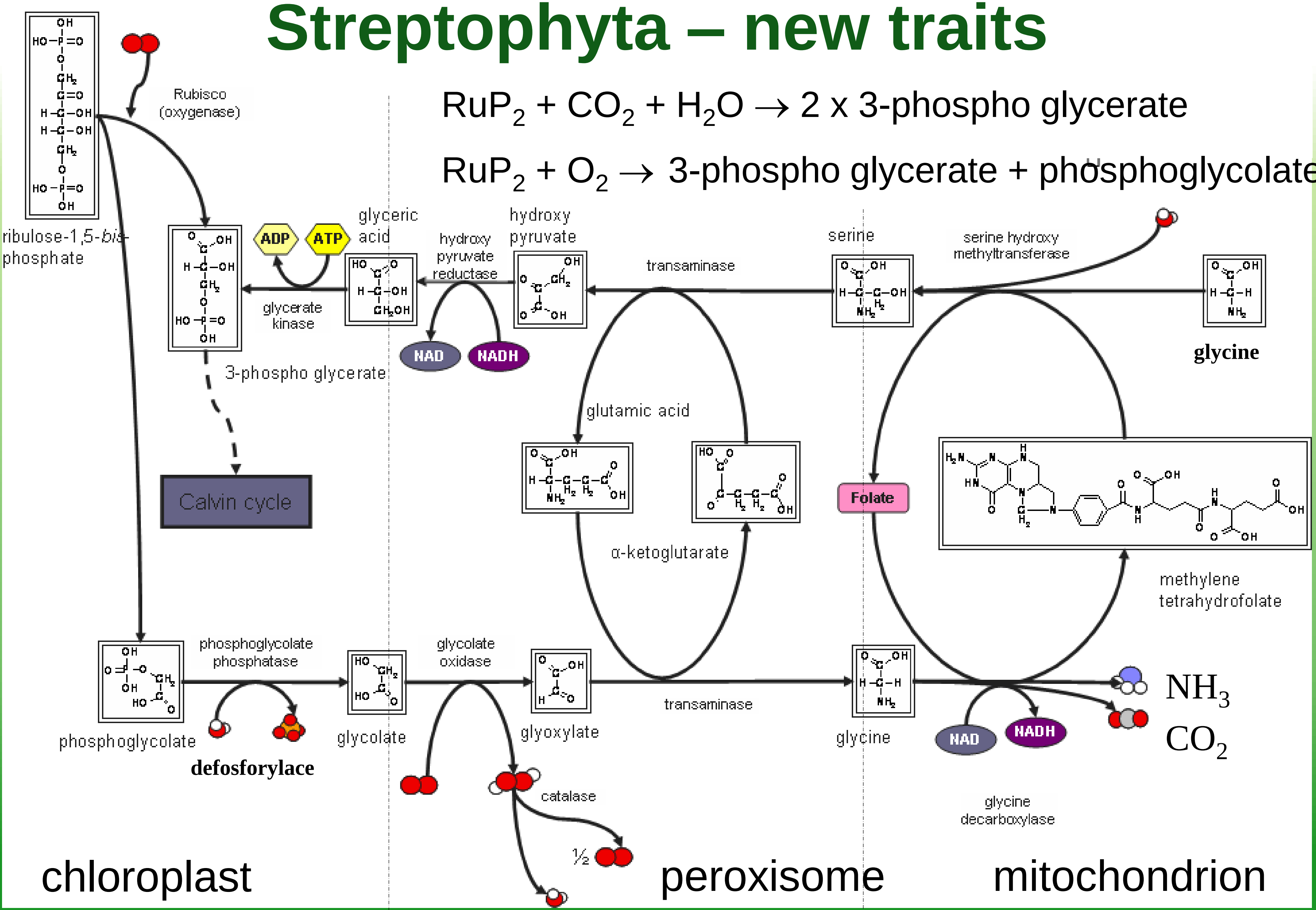

Streptophyta – new traits

thylakoids form grana

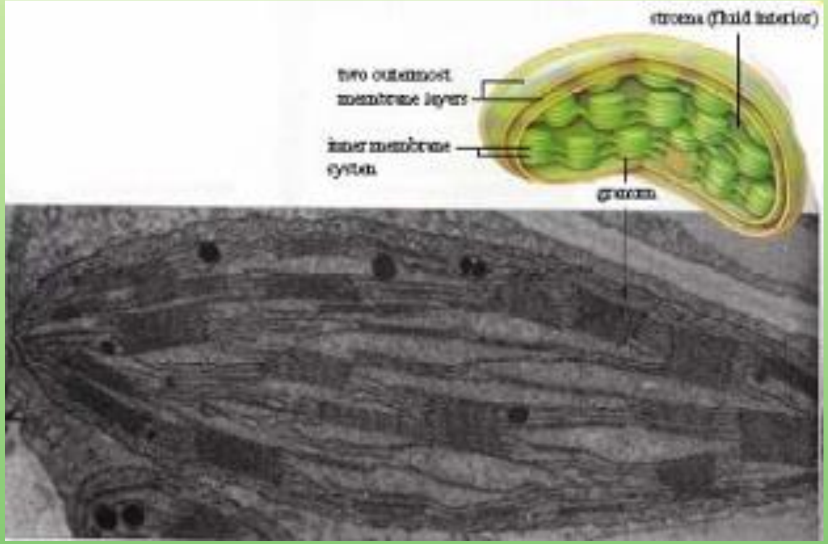

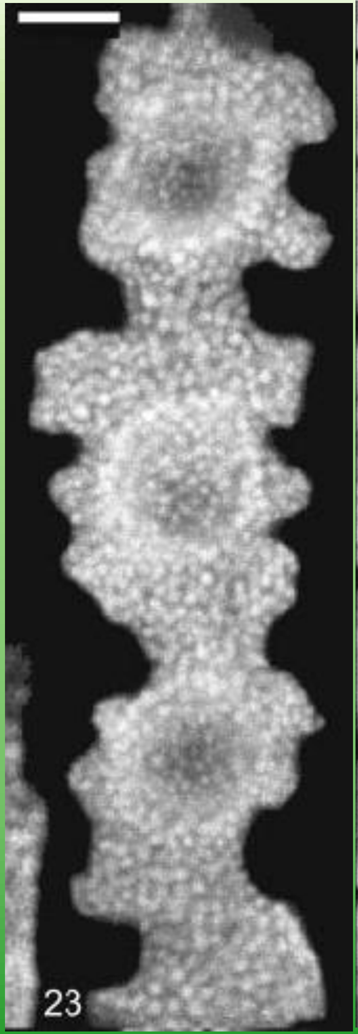

Chara

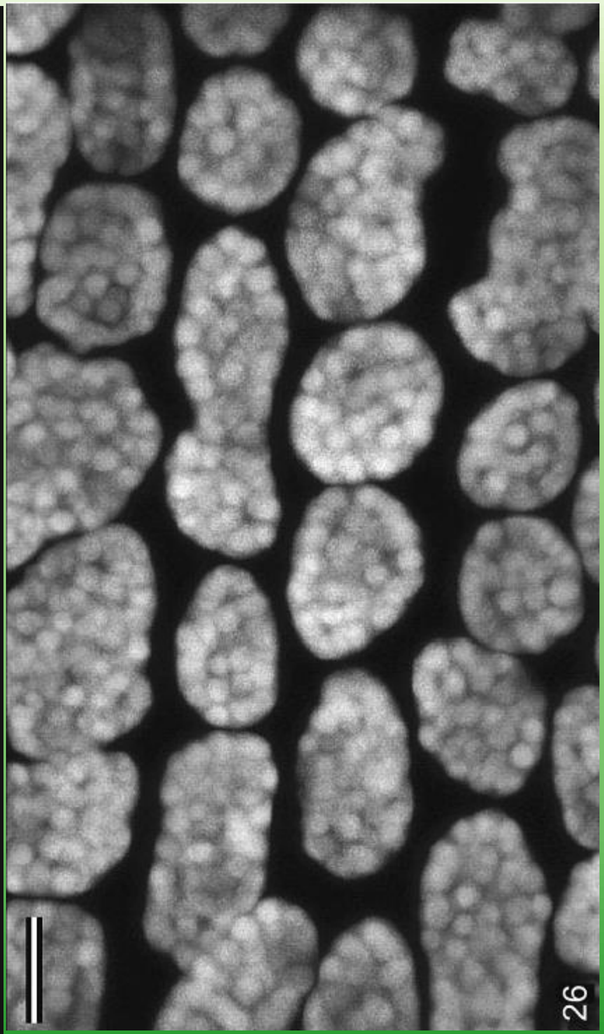

Coleochaete

Streptophyta – new traits

Plasmodesmata

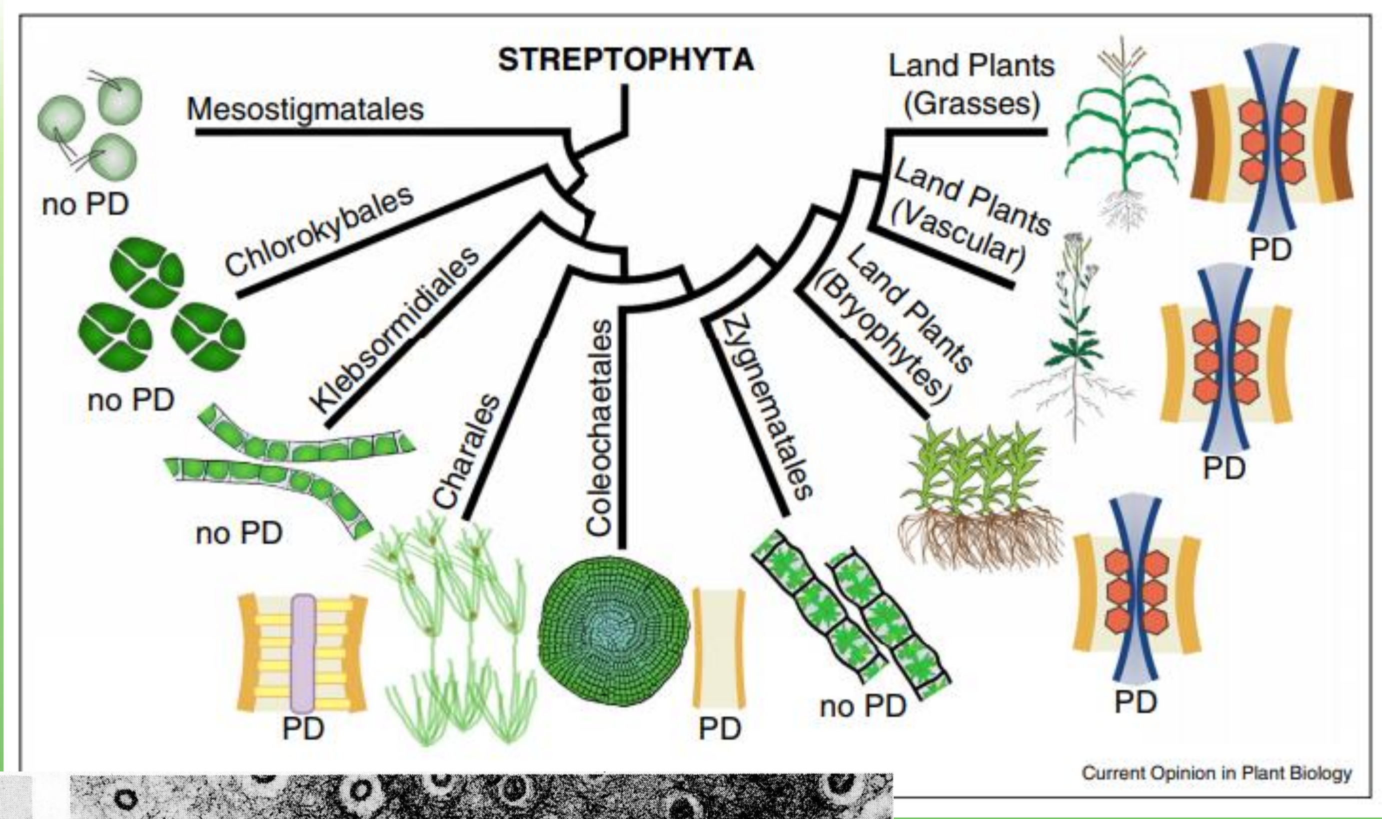

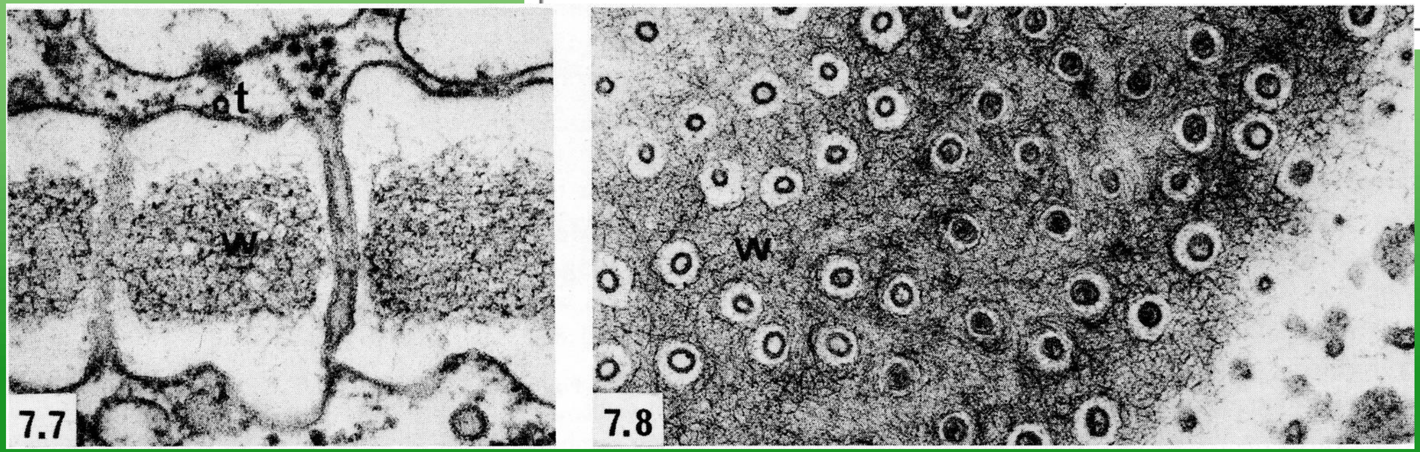

Brunkard & Zambryski (2016)

Streptophyta – new traits

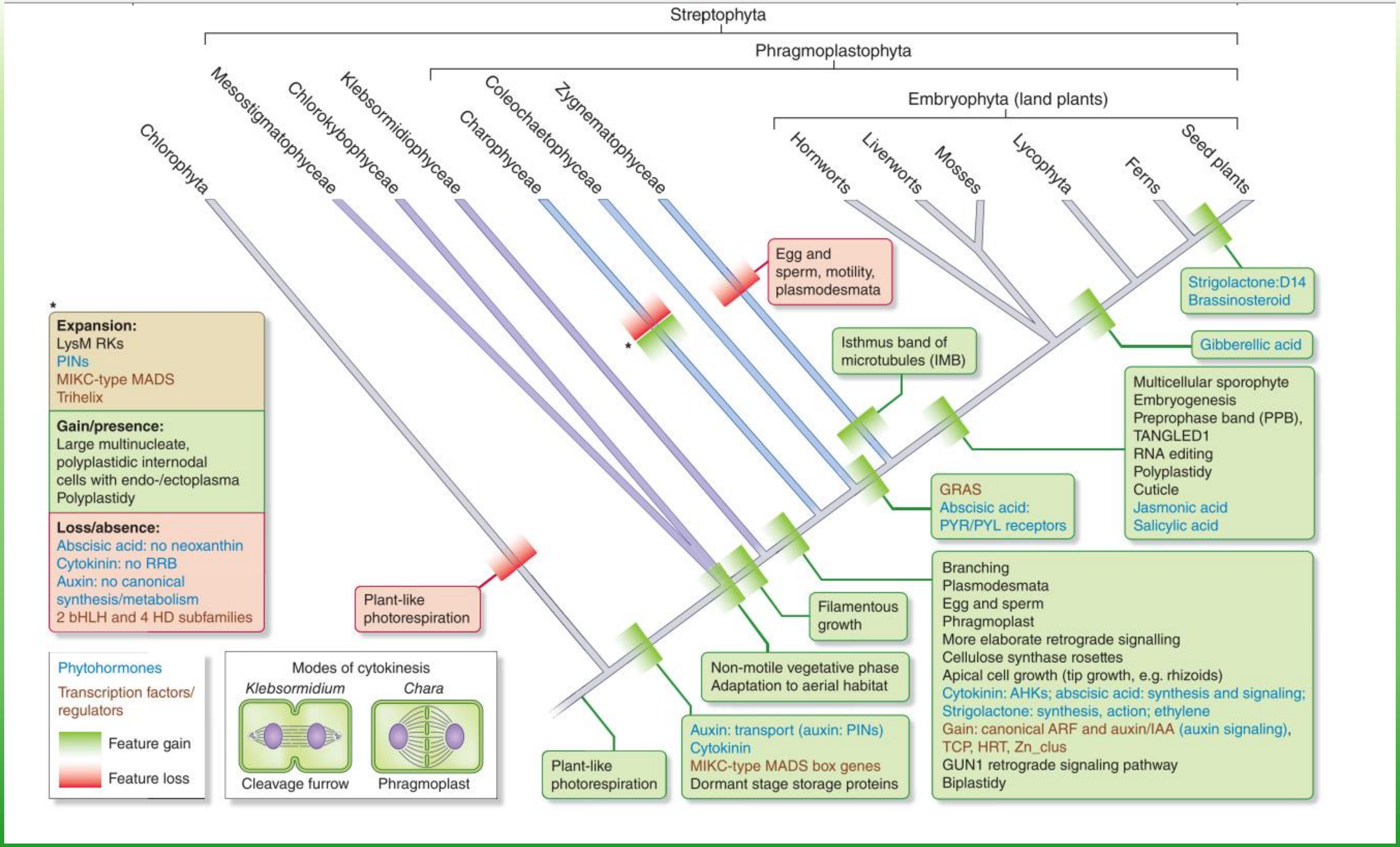

Nishiyama et a. (2018)

Mesostigmatophyceae

Mesostigma viride

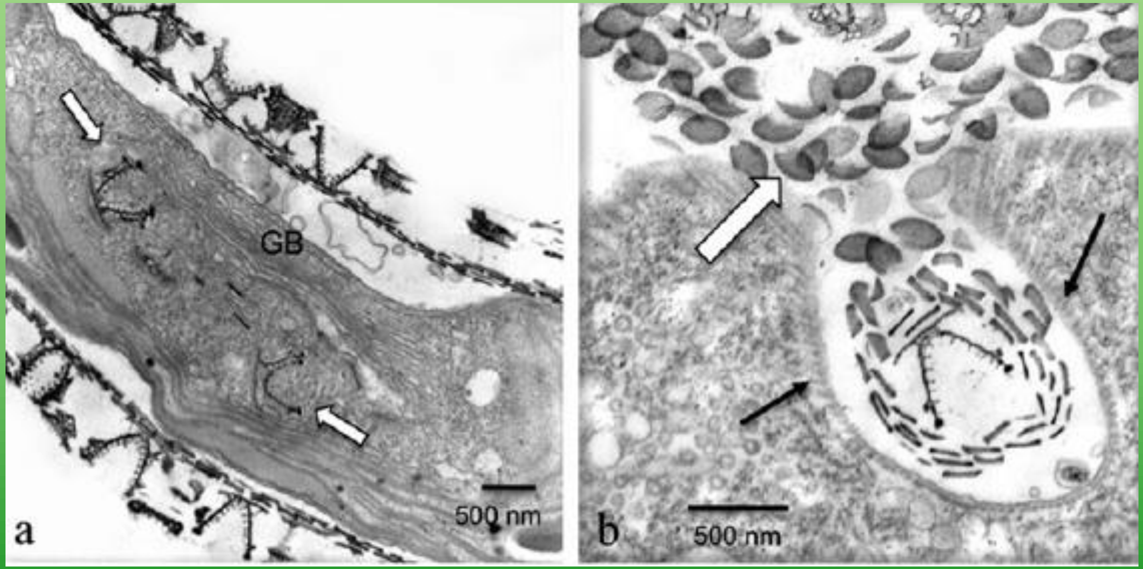

Mesostigmatophyceae

BMC Plant Biology
BioMed Central
Research article
Open Access

EST analysis of the scaly green flagellate *Mesostigma viride* (Streptophyta): Implications for the evolution of green plants (Viridiplantae)

Andreas Simon†[1], Gernot Glöckner†[2], Marius Felder[2], Michael Melkonian[1] and Burkhard Becker*[1]

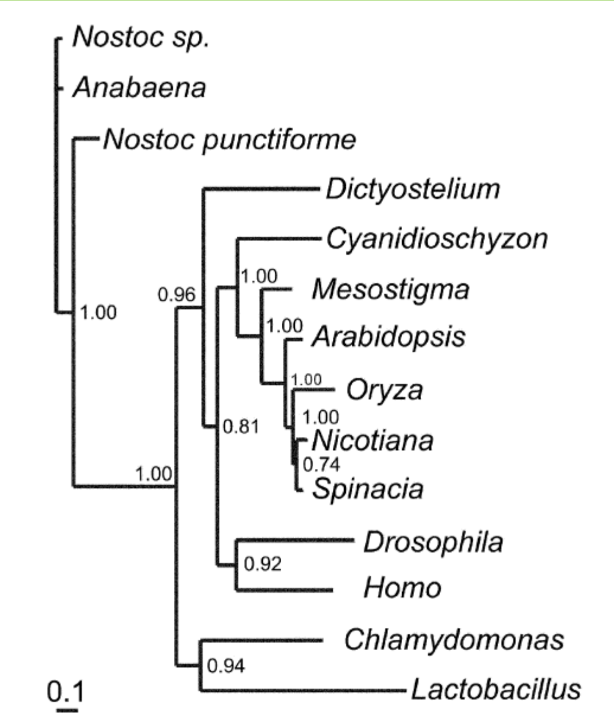

Figure 4
Phylogenetic tree of glycolate oxidase and glycolate oxidase-like genes. The tree shown was derived by Bayesian inference analysis from 402 amino acid positions using a mixed model for amino acid substitutions and a gamma correction for rate variation among sites. The Bayesian inference utilized MRBAYES, Ver. 3.0 * with posterior probabilities derived from 100000 generations and discarding a burnin of 1000. The tree obtained with a parsimony analysis using PHYLIP gave essentially the same topology.

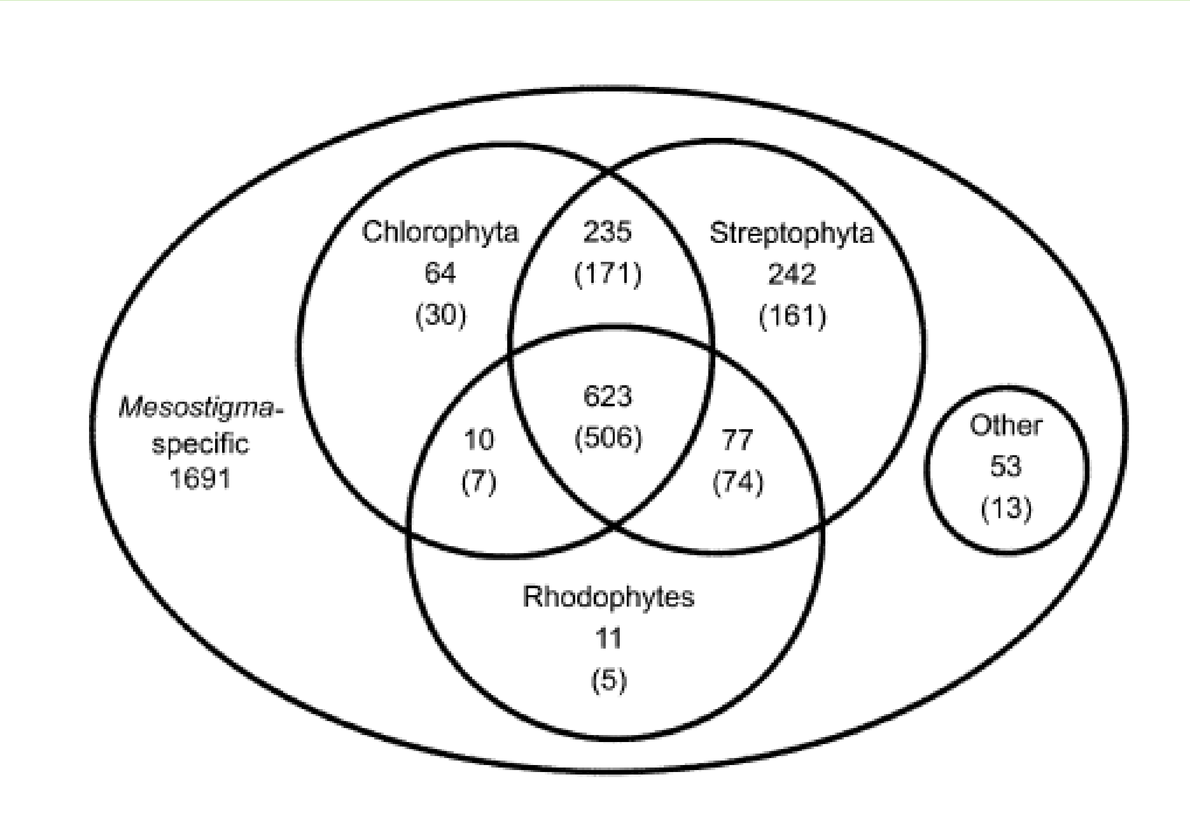

Streptofilum

Mikhailyuk et al. (2018)

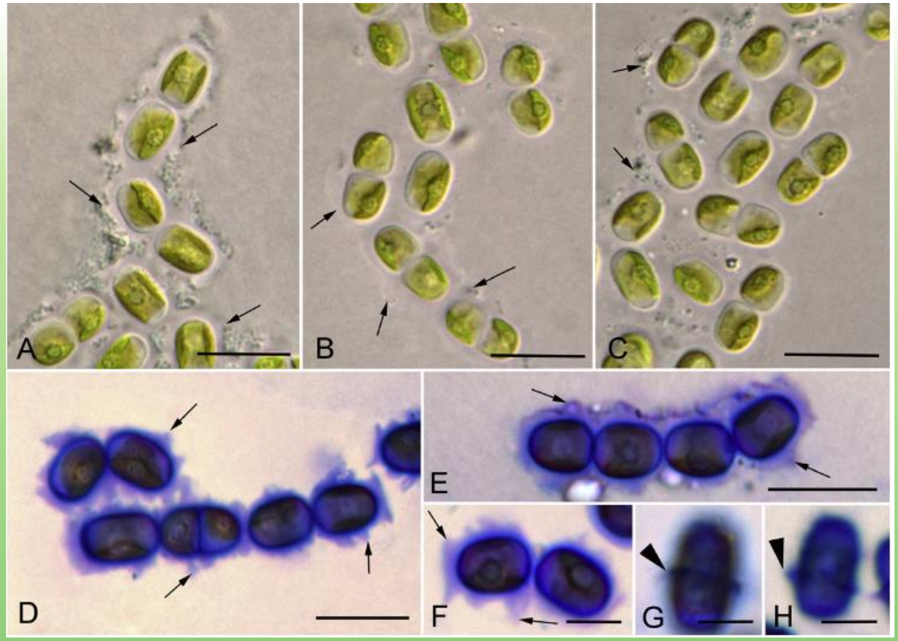

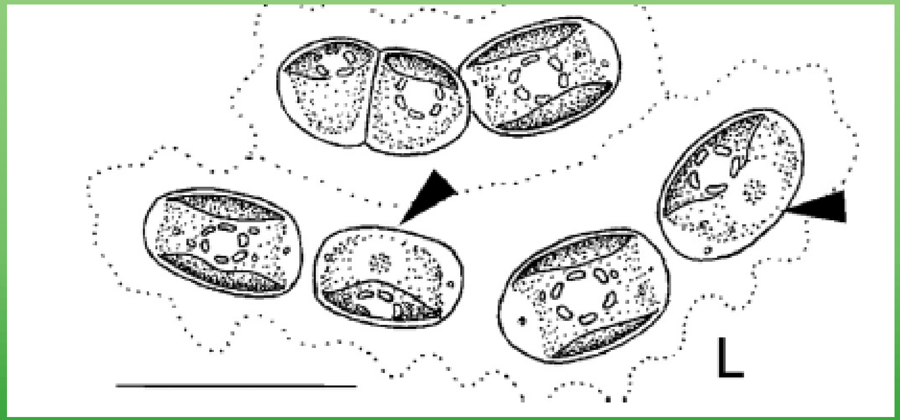

Chlorokybophyceae

Chlorokybus atmophyticus

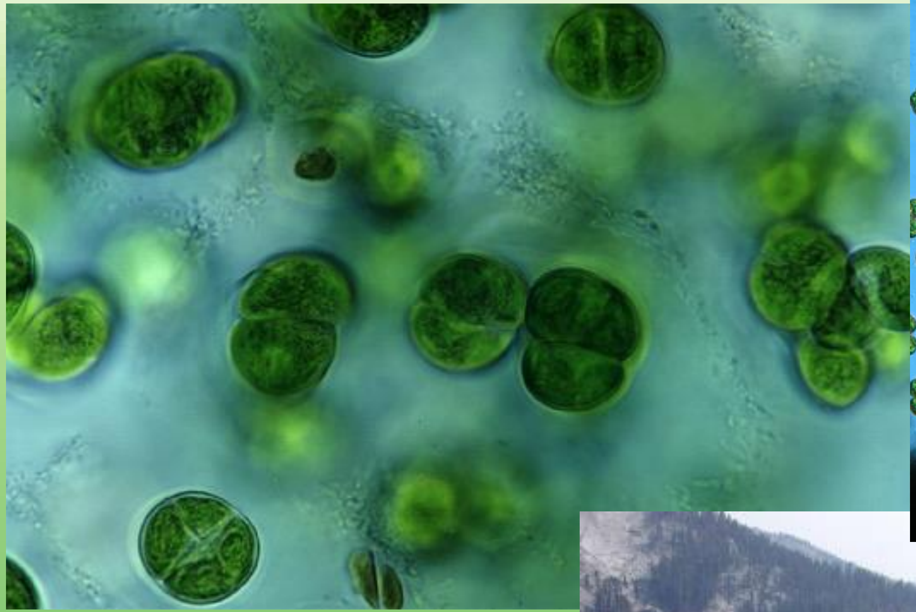

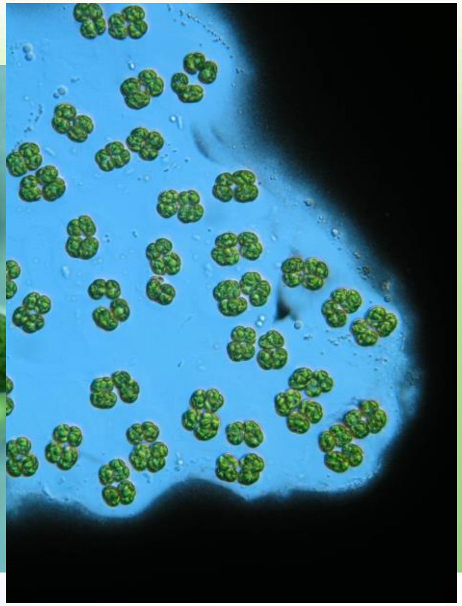

Klebsormidiophyceae

Klebsormidium

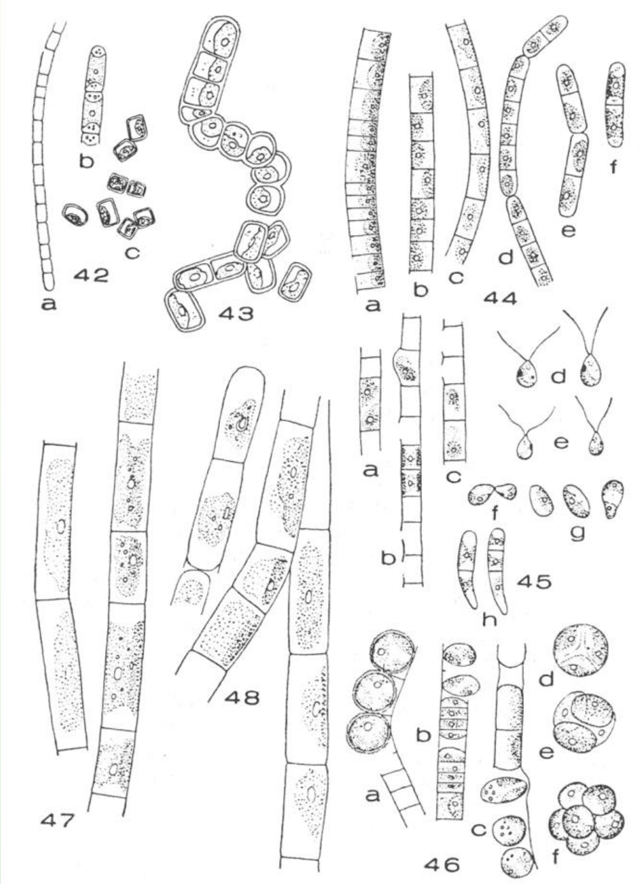

gamet, h — młode rośliny (według Wille); 46 — *Ch. flaccidum*: a — aplanospory spoczynkowe, b, c — powstawanie aplanospor, d, e, f — podziały aplanospory (według Wille); 47 — var. *nitens* (według Chodata); 48 — var. *crassum* (według Chodata)

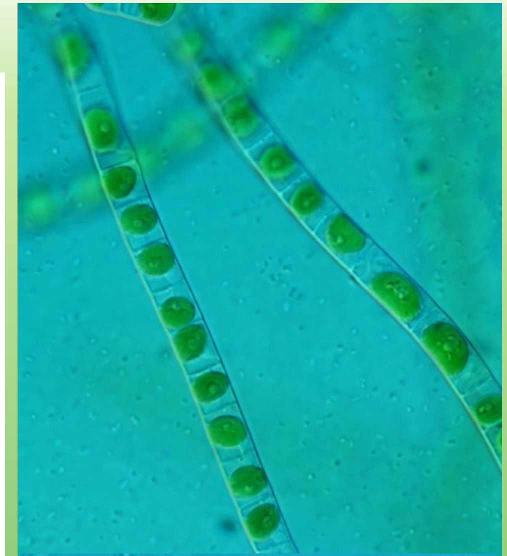

Klebsormidiophyceae

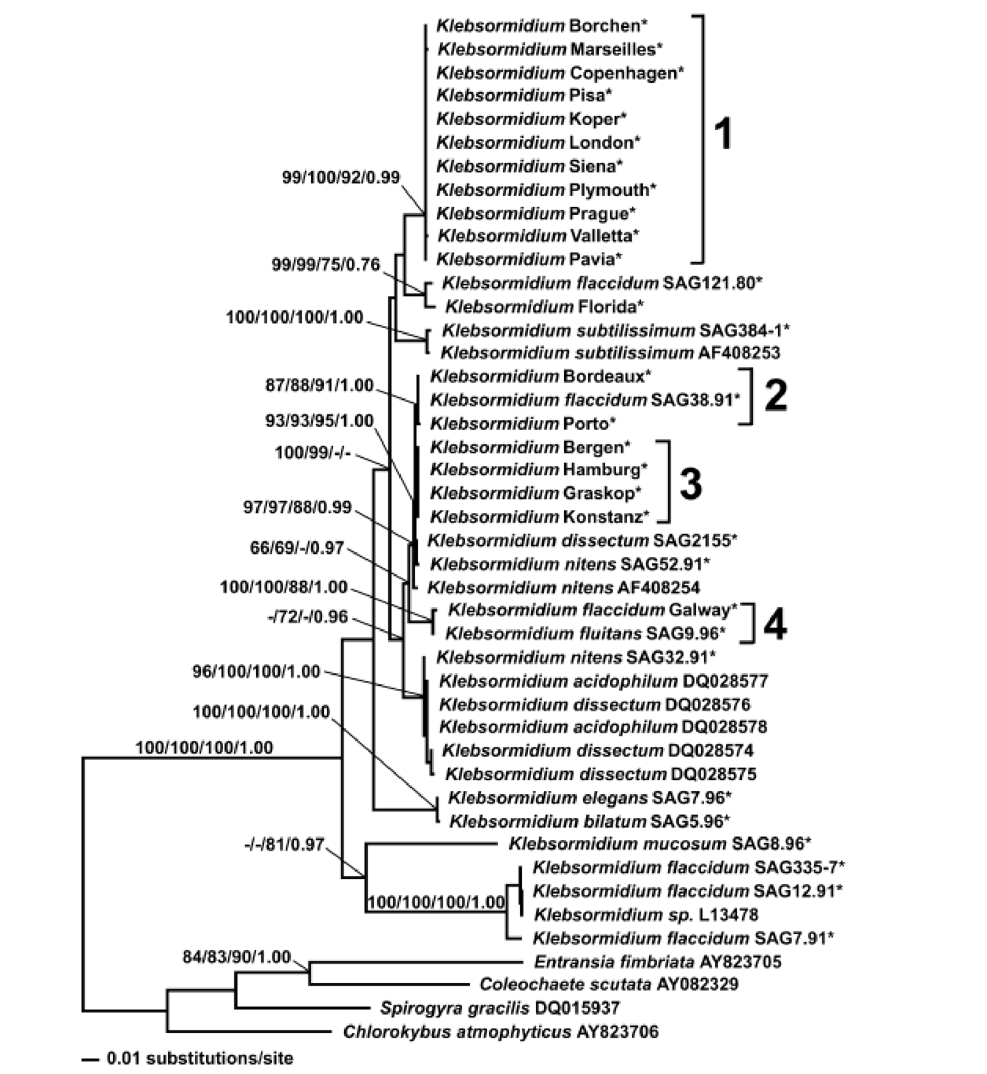

Rindi et al. (2008)

Ecological differentiation

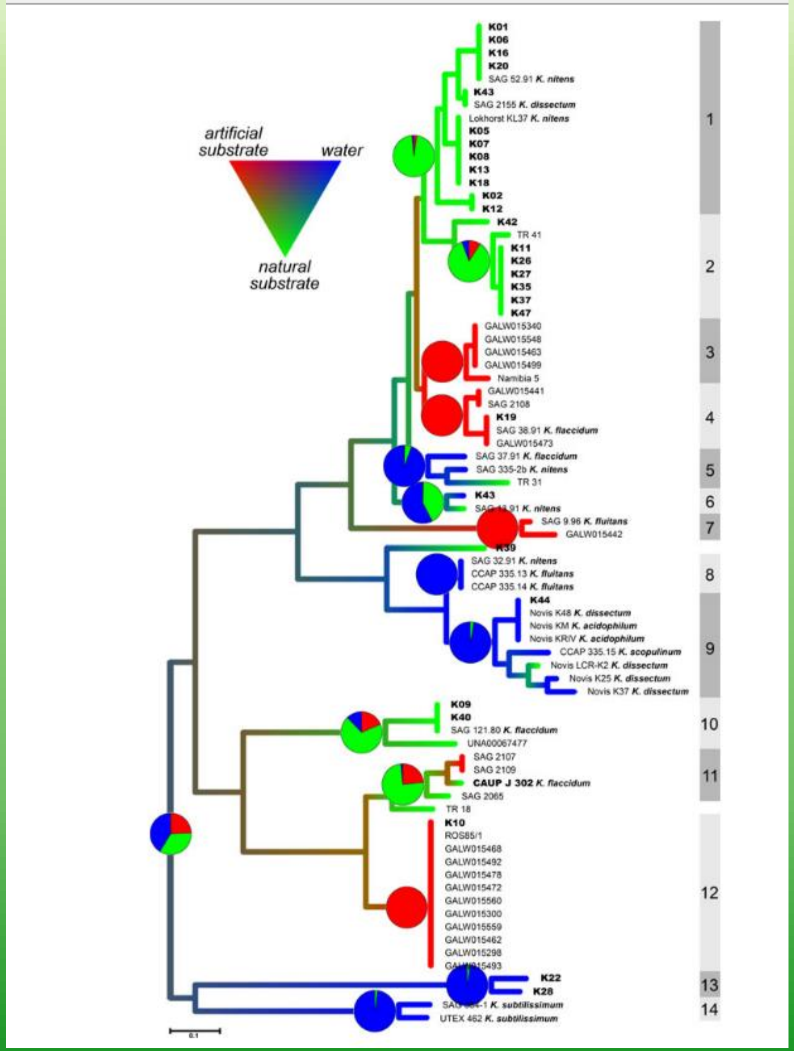

Škaloud & Rindi (2013)

Klebsormidiophyceae

Stress adaptations

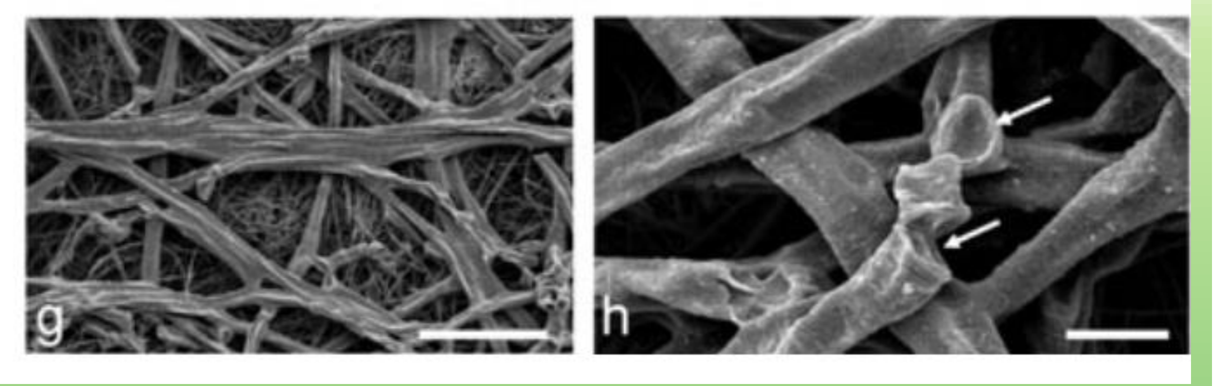

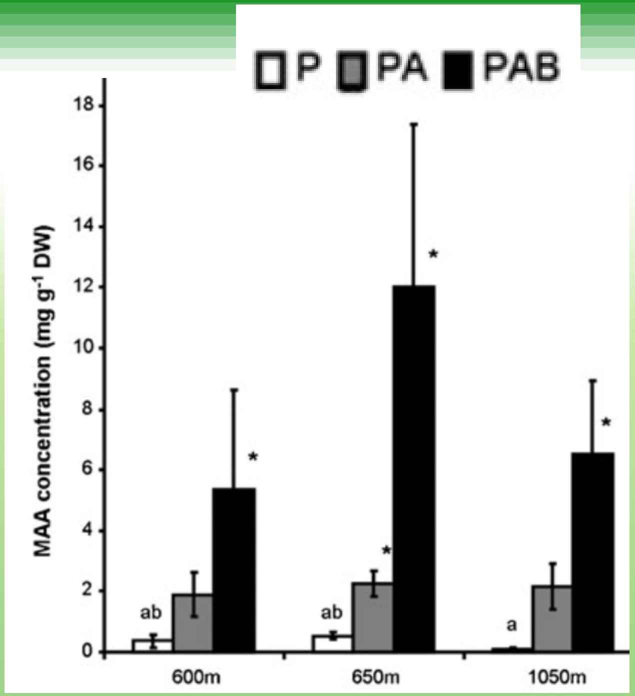

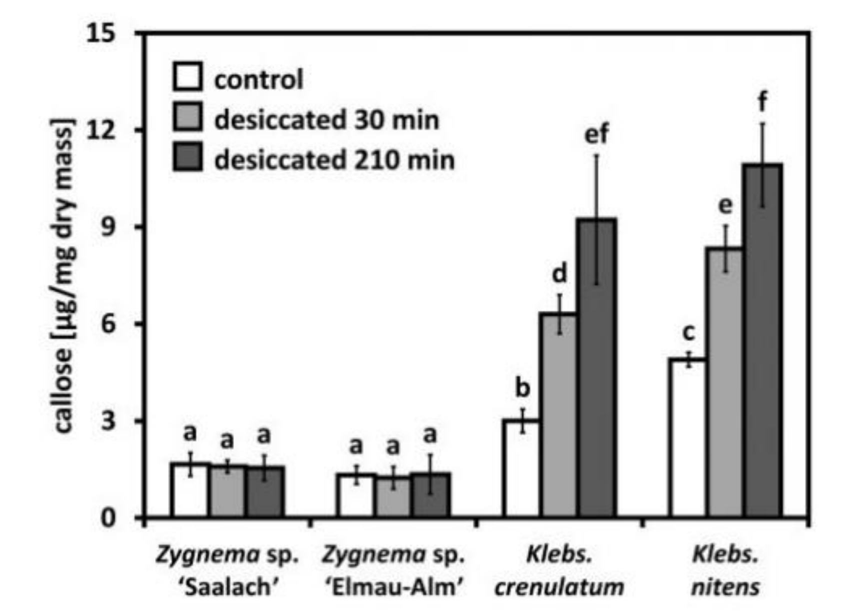

Callose in the cross cell walls

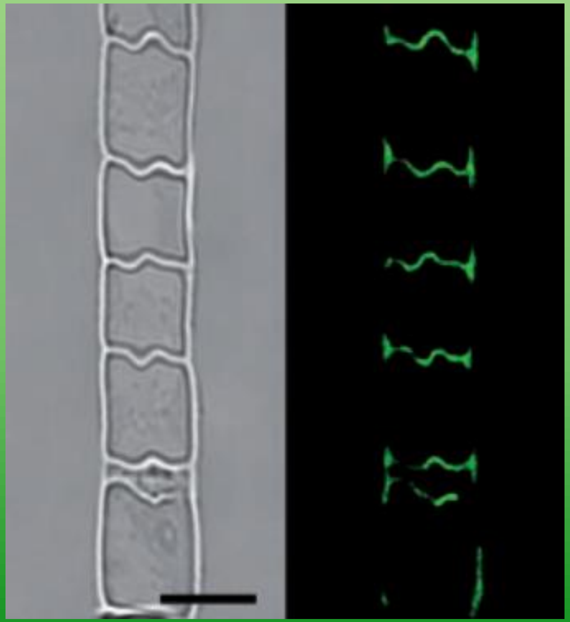

Holzinger et al. (2011); Herburger & Holzinger (2015), Kitzing et al. (2014)

Klebsormidiophyceae

Interfilum

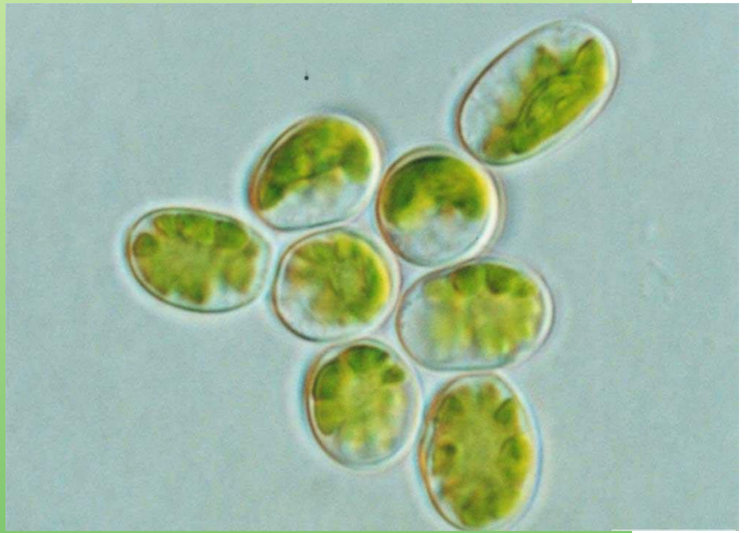

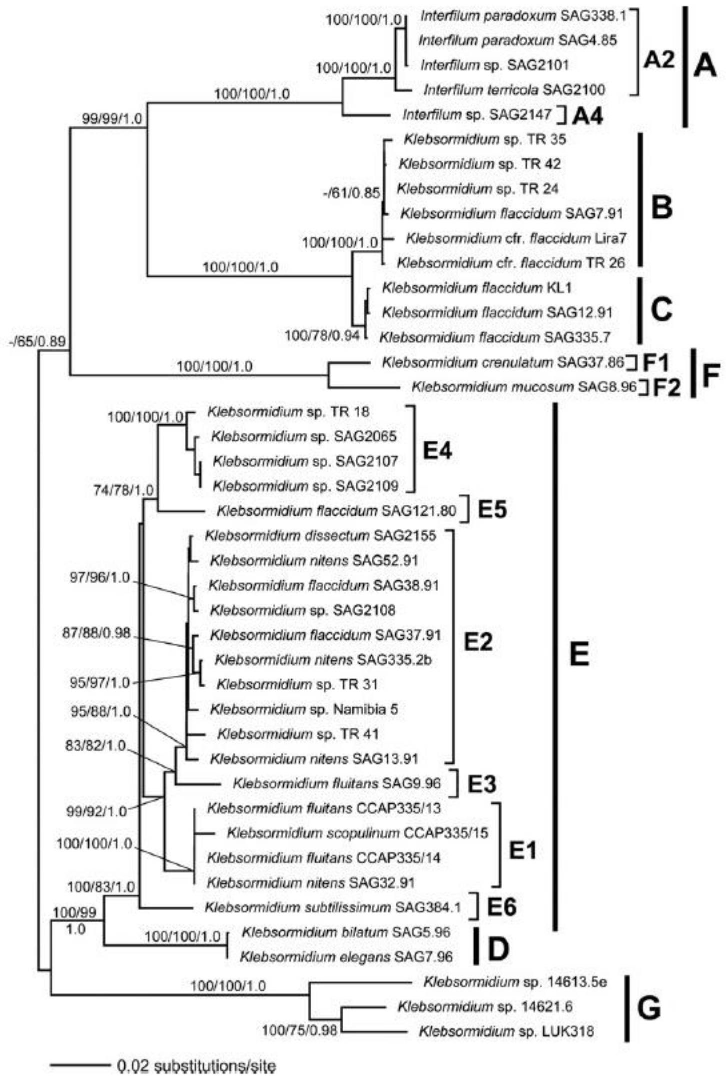

Fig. 3. Phylogram inferred from Maximum-Likelihood analysis of the concatenated dataset *rbc*L-ITS rRNA in the Klebsormidiales, with bootstrap support (BP) and Bayesian Posterior Probabilities (PP) indicated at the nodes. From left to right and from top to bottom the support values correspond to Neighbor Joining BP, Maximum-Likelihood BP and Bayesian PP. BP values lower than 60% and PP lower than 0.8 are not reported.

Klebsormidiophyceae

Entransia

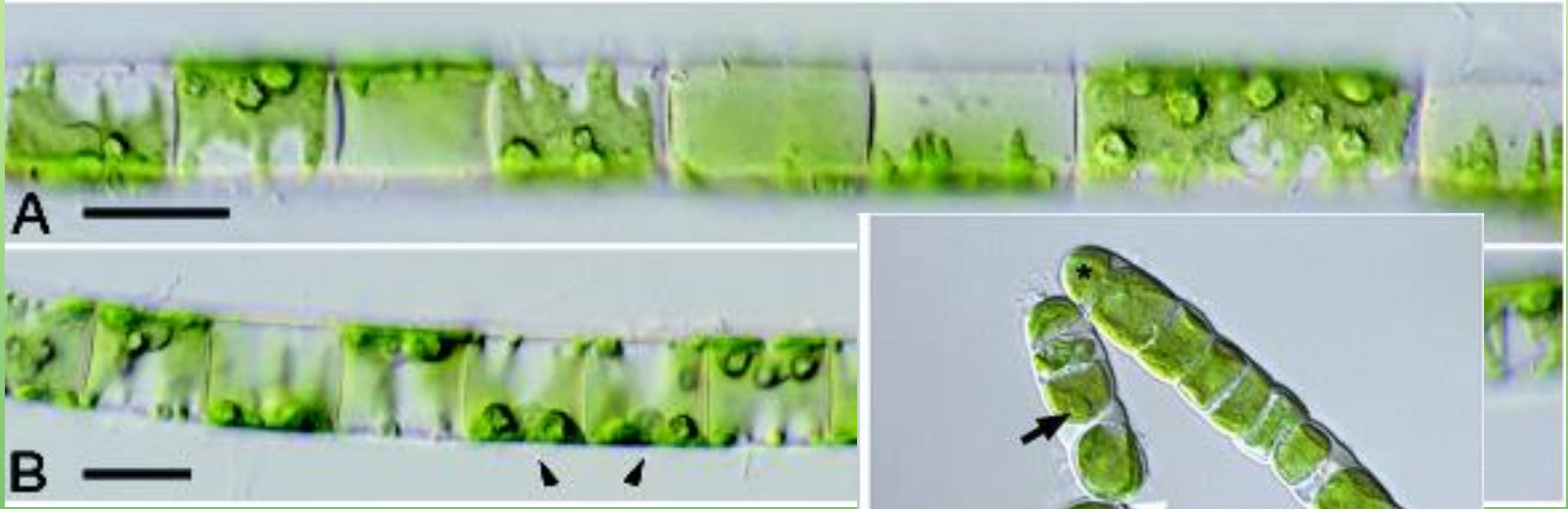

Hormidiella

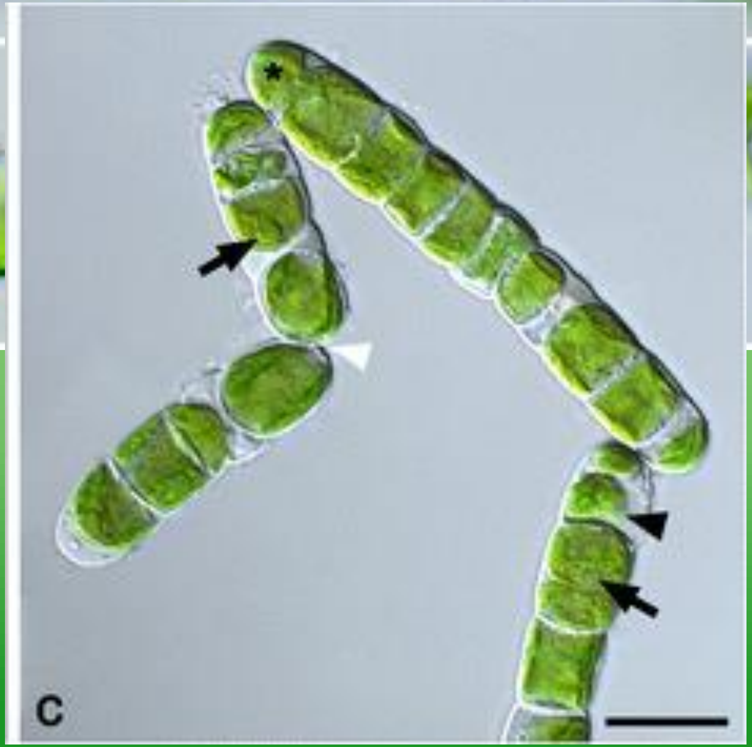

Klebsormidiophyceae

Streptosarcina

Mikhailyuk et al. (2018)

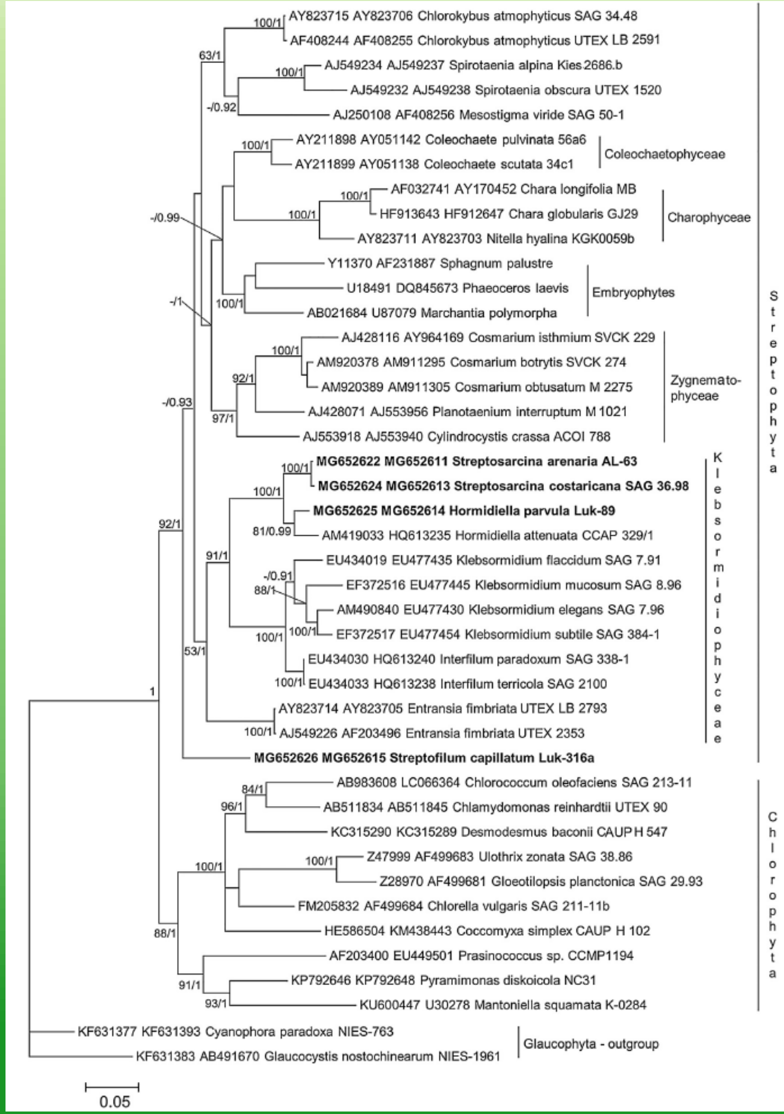

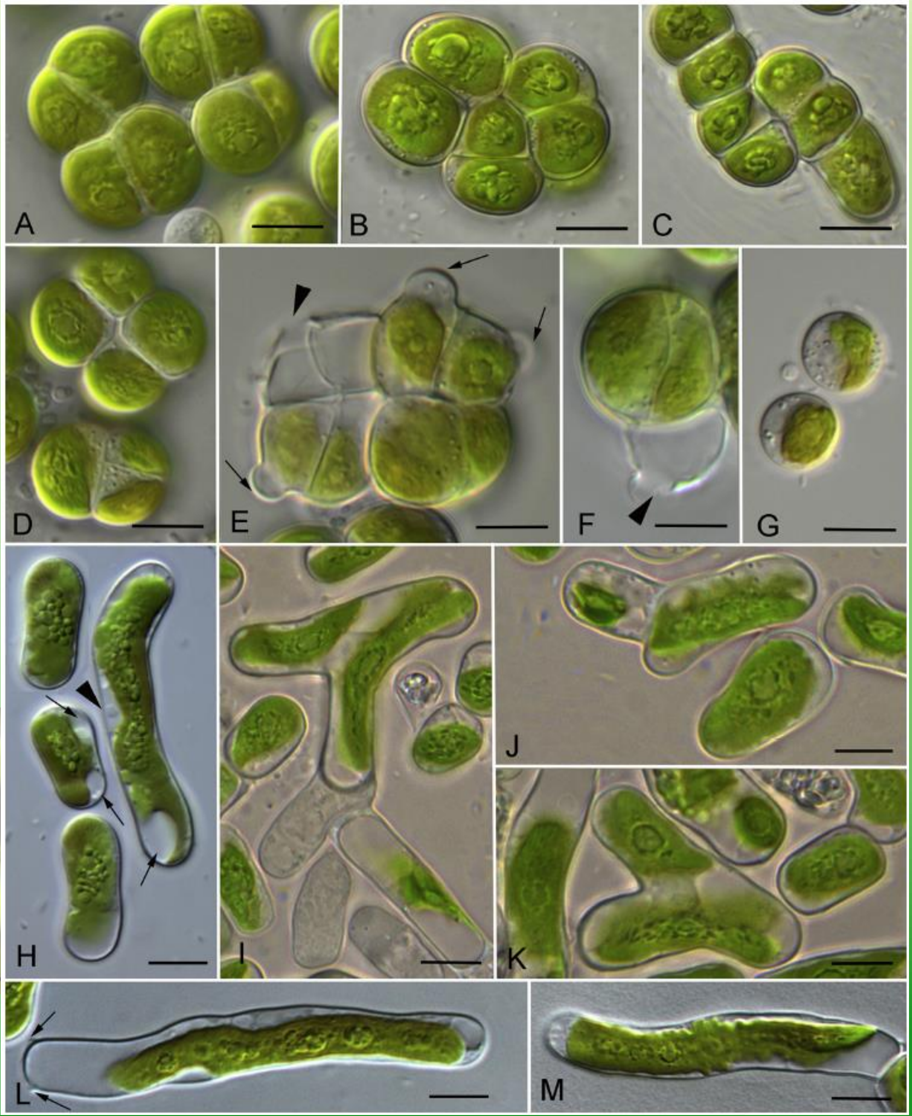

Coleochaetophyceae

Coleochaete

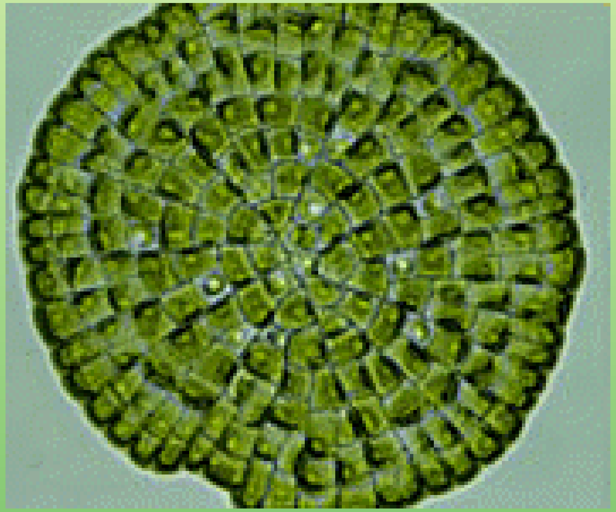

C. orbicularis

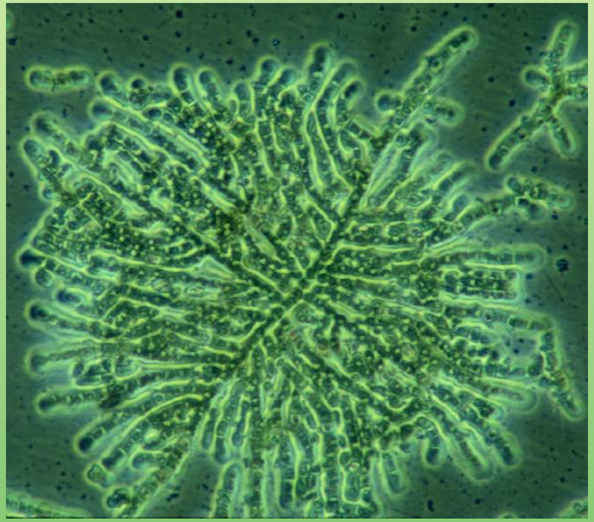

C. irregularis

Coleochaetophyceae

- Asexual reproduction: zoospores covered with polysaccharide scales
- Sexual reproduction: oogamy, haplontic life cycle

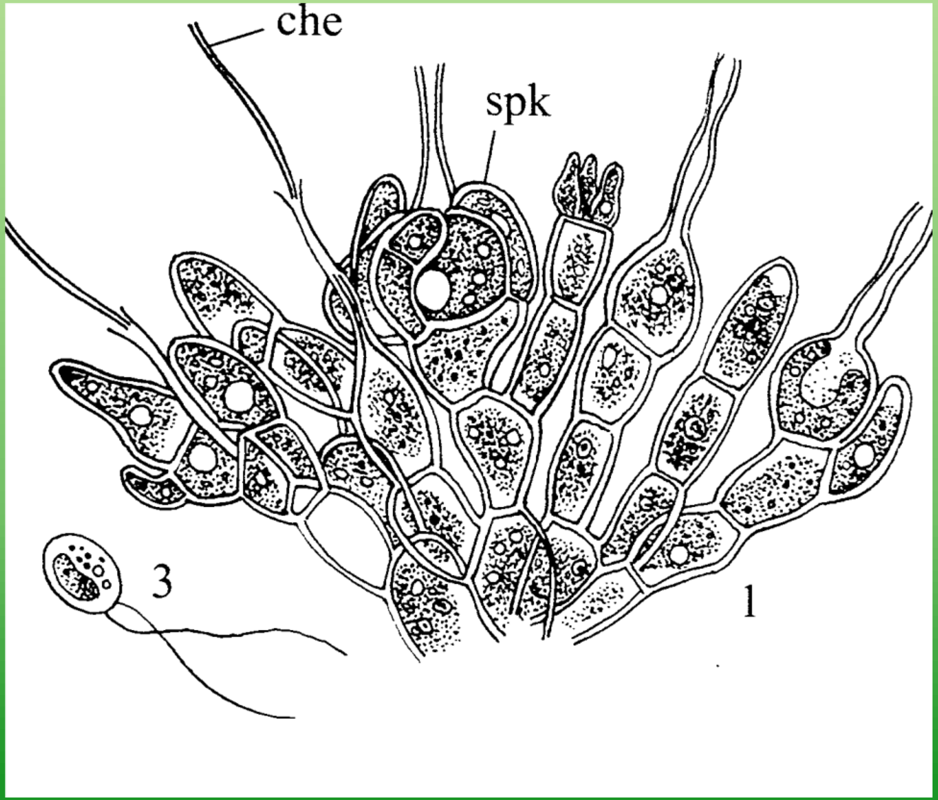

Coleochaetophyceae

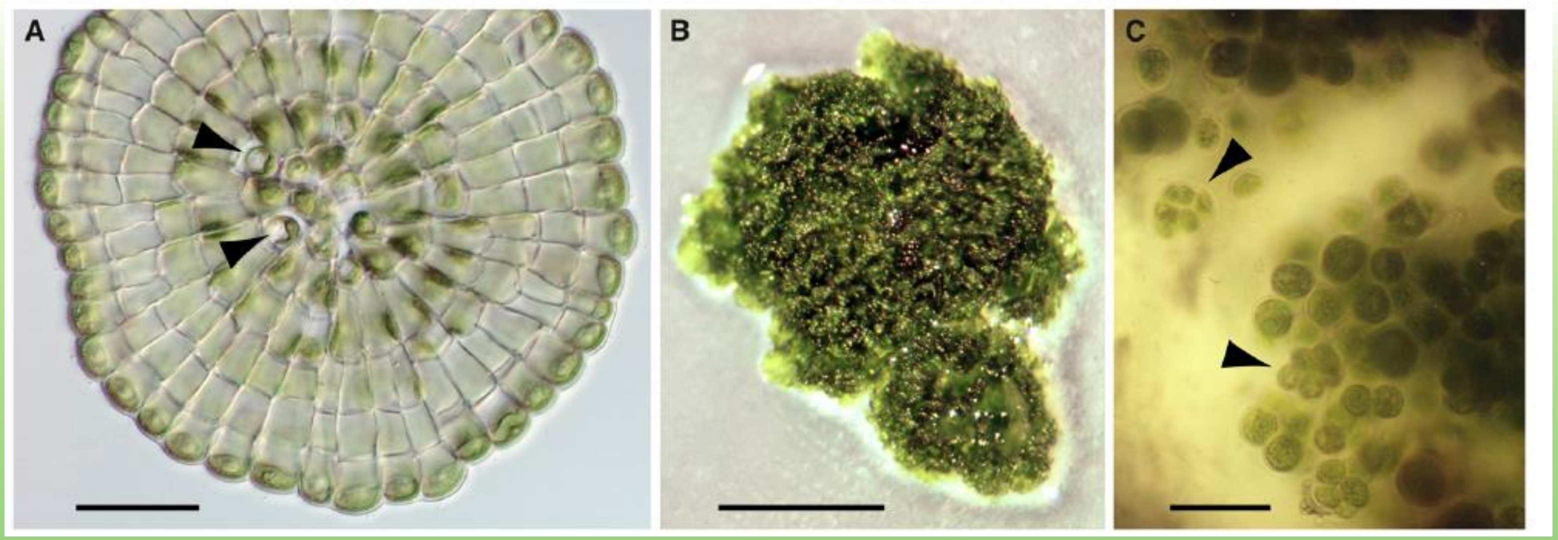

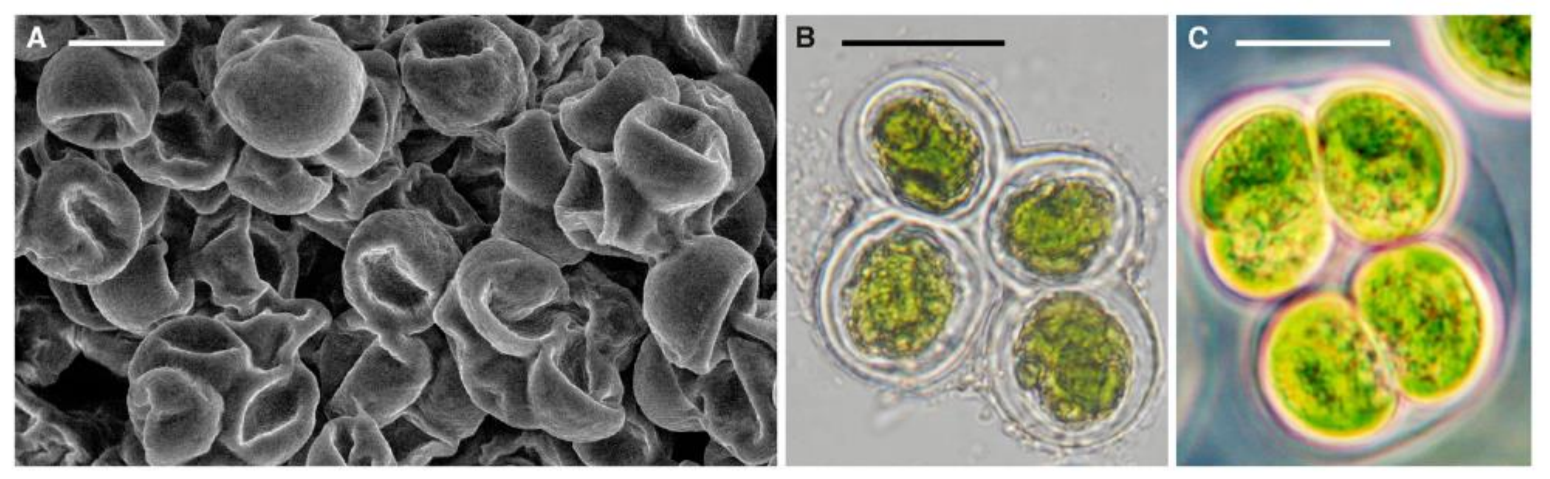

Graham et al. 2012

Coleochaetophyceae

Chaetosphaeridium

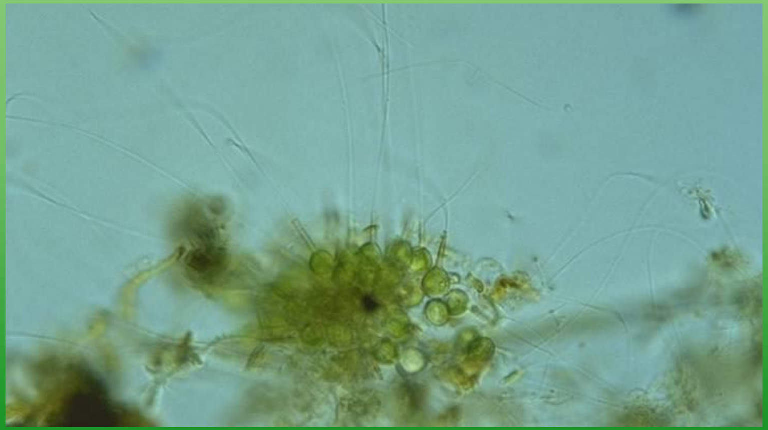

Charophyceae

Morphology

Macroscopic, branched thallus

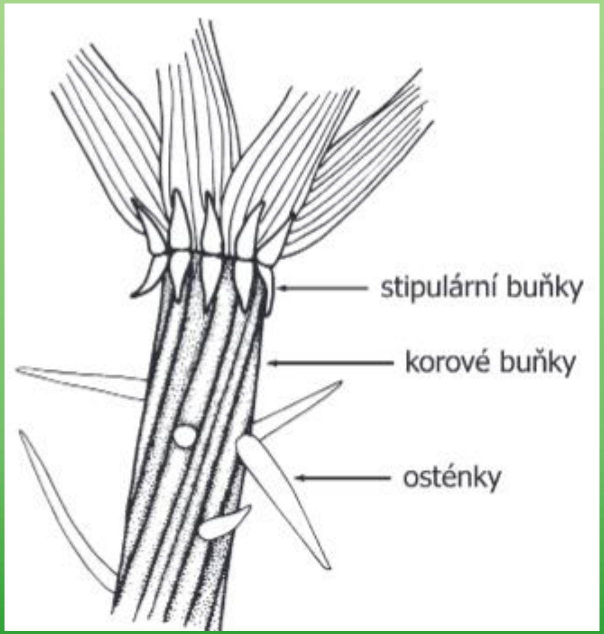

Kaštovský et al. (2018)

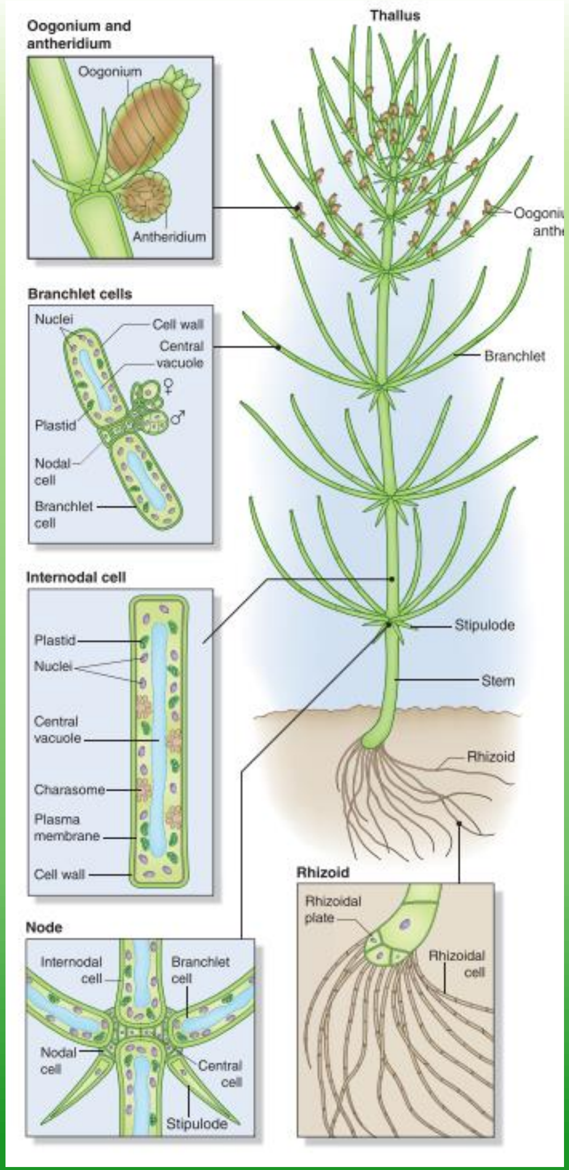

Nishiyama et al. (2018)

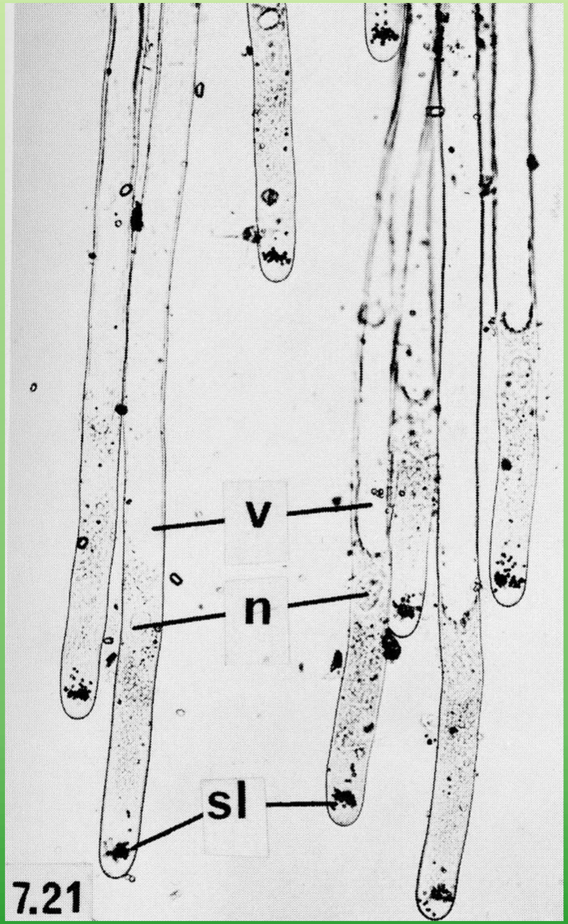

Morphology

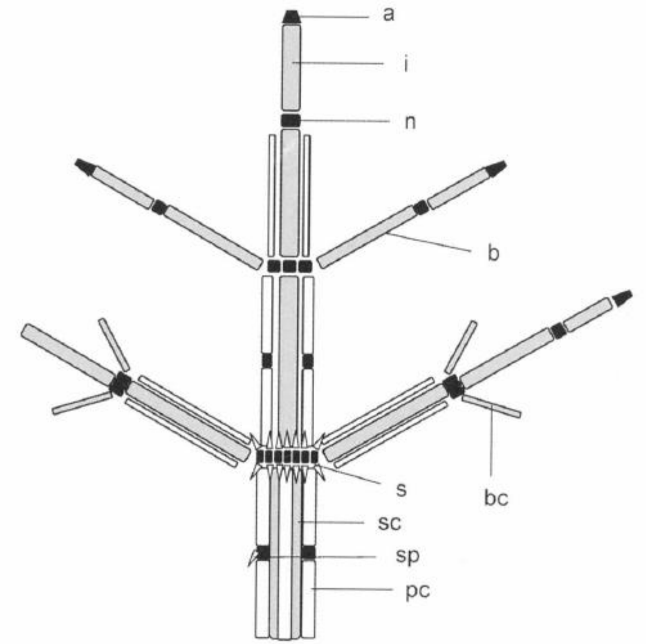

Fig. 11-6. Charales. Structure of a characean shoot, schematically. The apical cell (a) divides alternating into a large, multinucleated cell (i) which does not divide further, and a small, meristematic cell (n) (black). Nodes (n) and internodes (i) alternate along the shoot. Whorls of branchlets (b) are formed on the nodes. Within the genus *Chara*, all spp. possess bract cells (bc). Cortex cells (white) and 2 tiers of stipulodes (s) are present in most spp. Primary cortex cell rows (pc) with small meristematic (black) and large multinucleated (white) cells in alternating order. The small (black) cells form 1 (diplostichous spp.) or 2 (triplostichous spp.) secondary cortex cell rows (sc) between the primary cortex cell rows. In most *Chara* spp., primary cortex possesses spine cells (sp). Density, length and shape of spine cells are diagnostic characters as is the size of primary and secondary cortex cell rows. (Orig., drawing by M. Schnittler and I. Blindow.)

Morphology

calcification

charasome

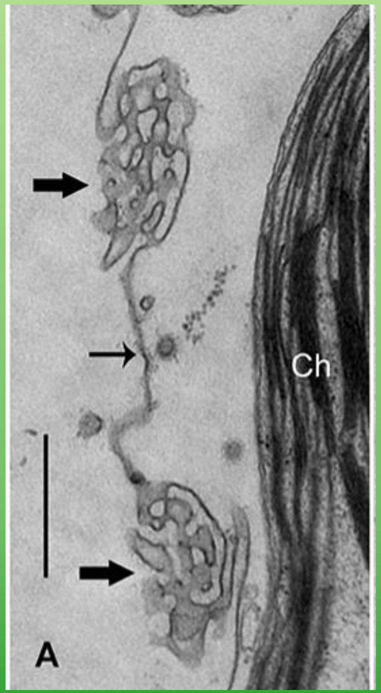

Hoepflinger et al. (2017)

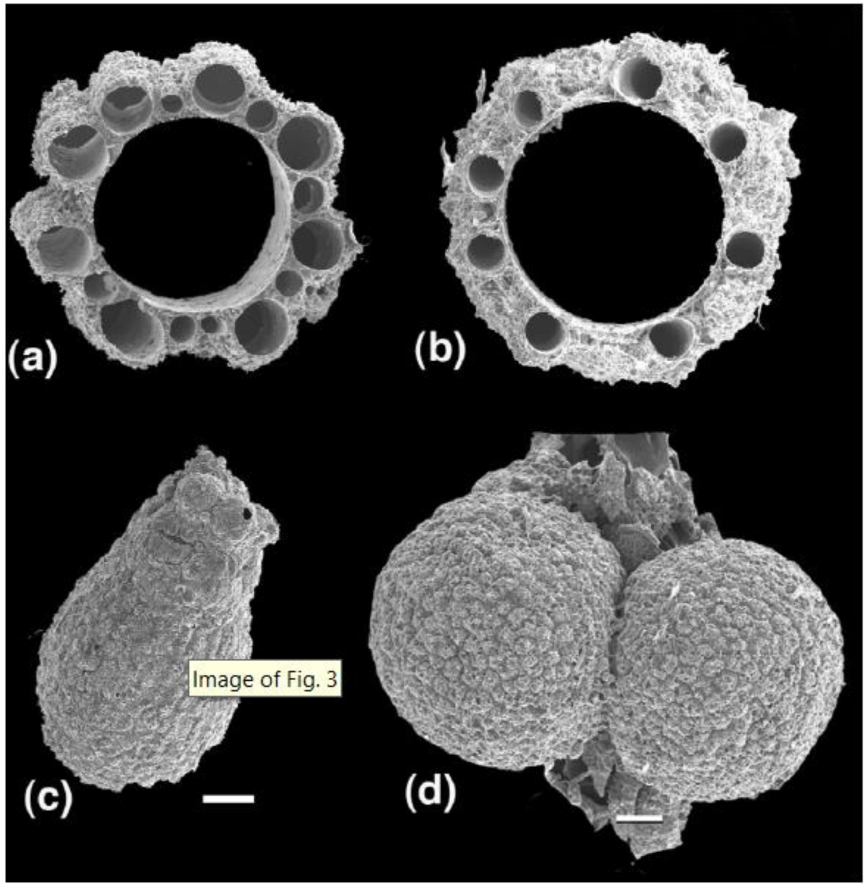

Fig. 3. External carbonate deposits (encrustations) on *Chara*. (a) Section of a diplostichous internode, *Chara vulgaris*; (b) section of a haplostichous internode, *Chara imperfecta*; (c) encrustation around the continuous integument of an oogonium including the coronular cells; (d) encrusted geminated antheridia. Scale bars: 100 µm.

Soulié-Märsche & García (2015)

Life cycle

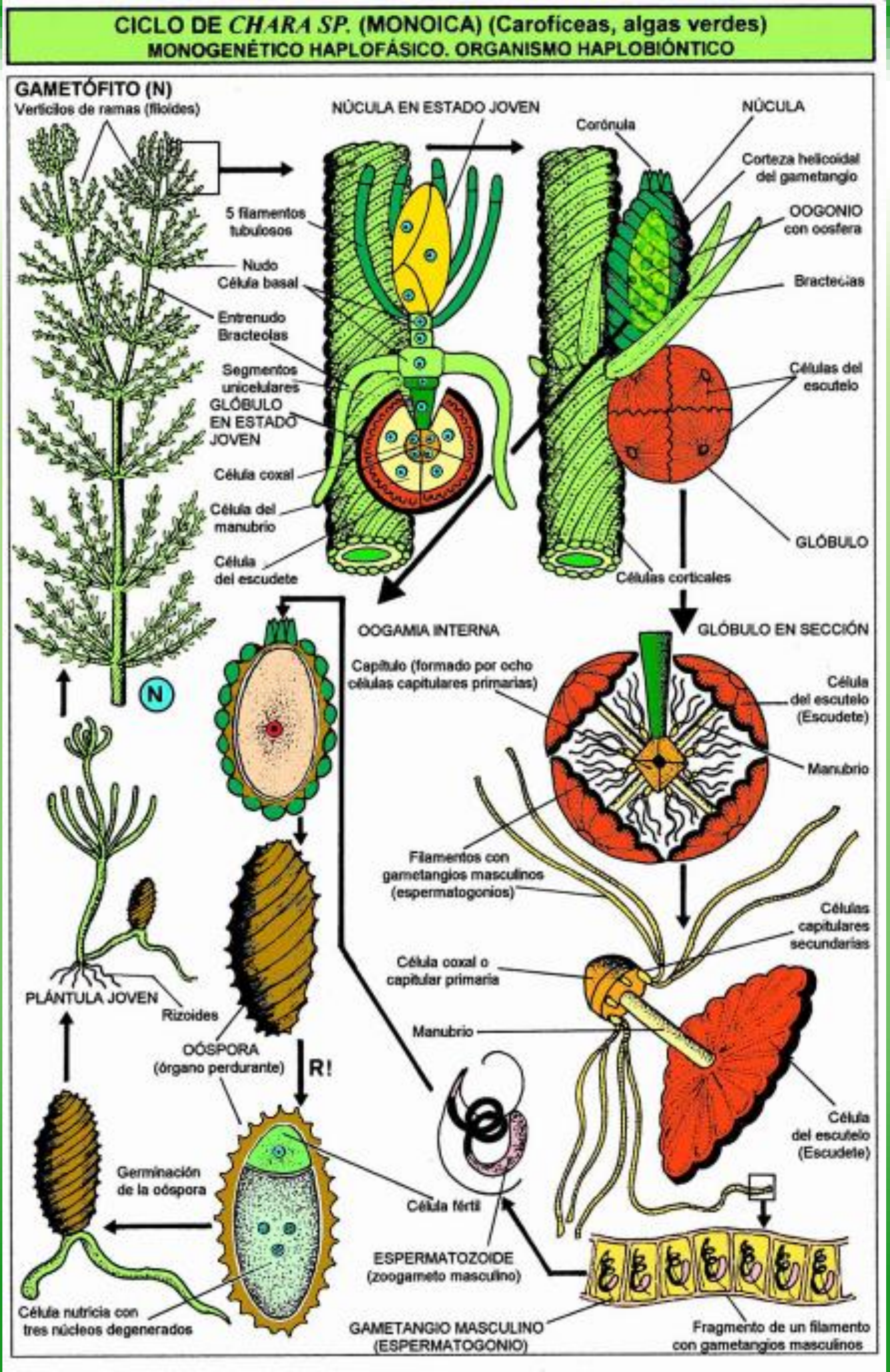
CICLO DE CHARA SP. (MONOICA) (Carofíceas, algas verdes)
MONOGENÉTICO HAPLOFÁSICO. ORGANISMO HAPLOBIÓNTICO
GAMETÓFITO (N)
Verticilos de ramas (filoides)
NÚCULA EN ESTADO JOVEN
Corónula
NÚCULA
Corteza helicoidal del gametangio
OOGONIO con oosfera
5 filamentos tubulosos
Nudo
Célula basal
Entrenudo
Bracteolas
Segmentos unicelulares
GLÓBULO EN ESTADO JOVEN
Célula coxal
Célula del manubrio
Célula del escudete
Células del escutelo
GLÓBULO
Células corticales
N
OOGAMIA INTERNA
GLÓBULO EN SECCIÓN
Capítulo (formado por ocho células capitulares primarias)
Célula del escutelo (Escudete)
Manubrio
Filamentos con gametangios masculinos (espermatogonios)
Células capitulares secundarias
Célula coxal o capitular primaria
Manubrio
PLÁNTULA JOVEN
Rizoides
OÓSPORA (órgano perdurante)
R!
Célula del escutelo (Escudete)
Germinación de la oóspora
Célula fértil
ESPERMATOZOIDE (zoogameto masculino)
Célula nutricia con tres núcleos degenerados
GAMETANGIO MASCULINO (ESPERMATOGONIO)
Fragmento de un filamento con gametangios masculinos

Life cycle

Antheridium

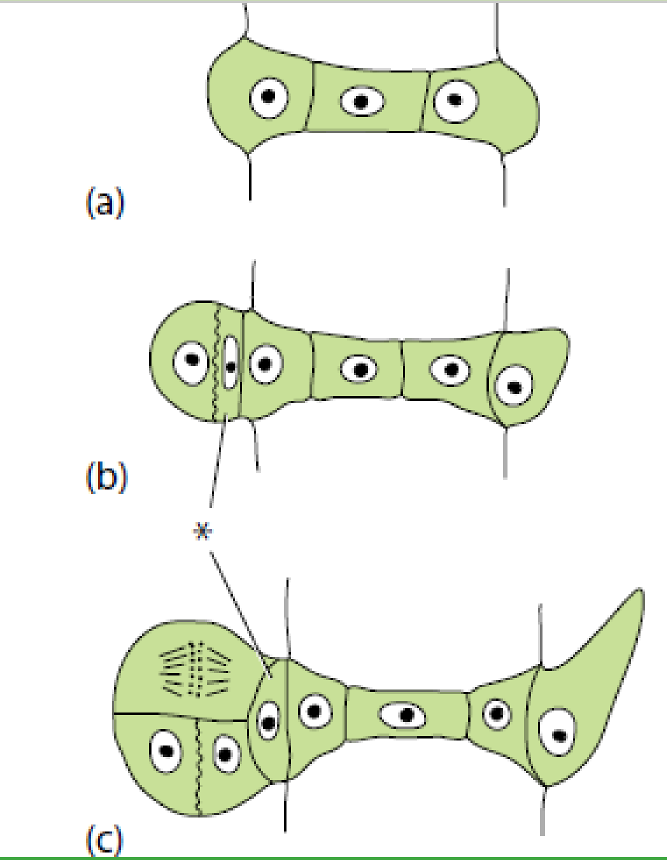

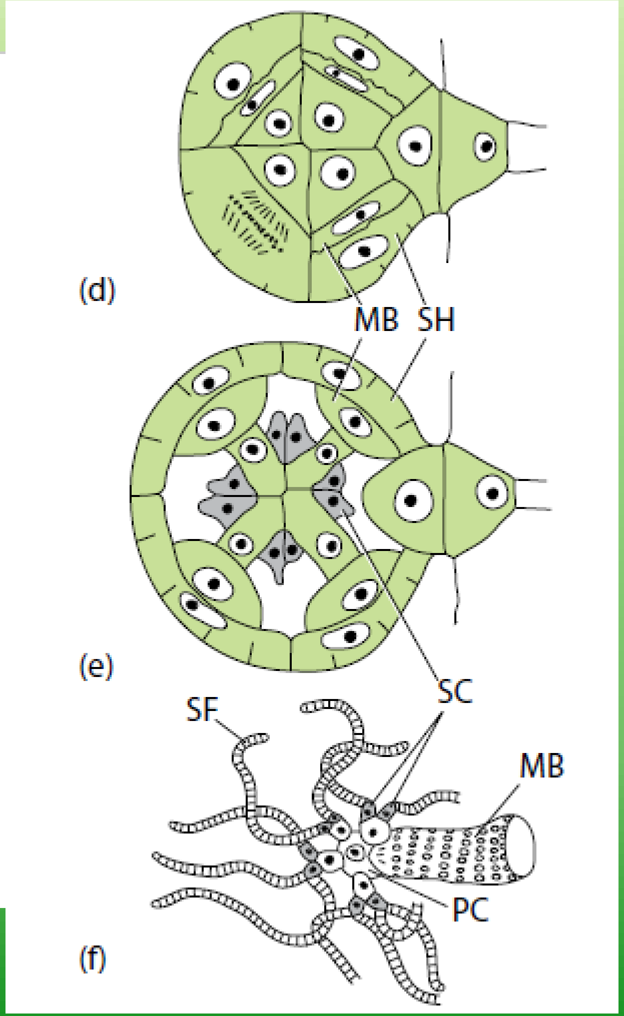

SH – shield
MB – manubrium
PC - primary capitula
SC – sec. capitula
SF – spermatogenous filaments

Life cycle

Spermatozoids

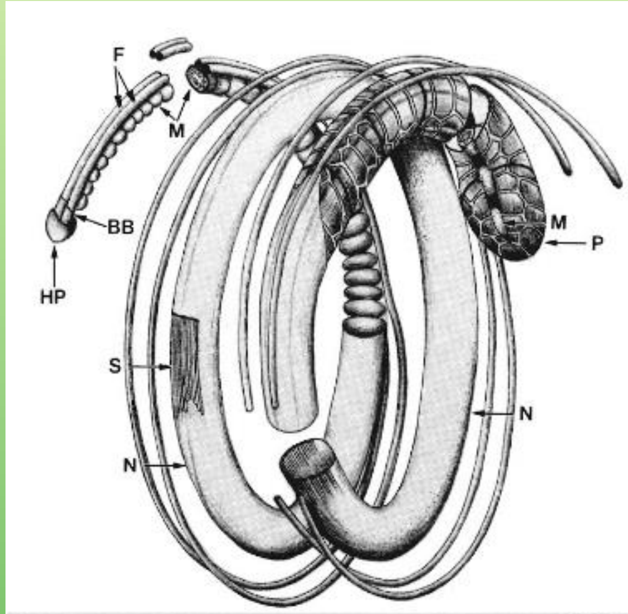

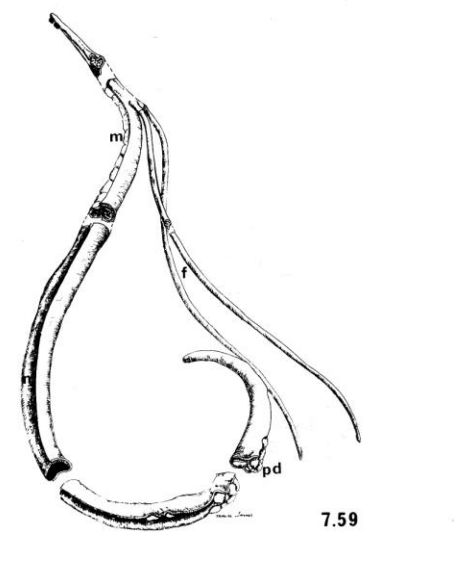

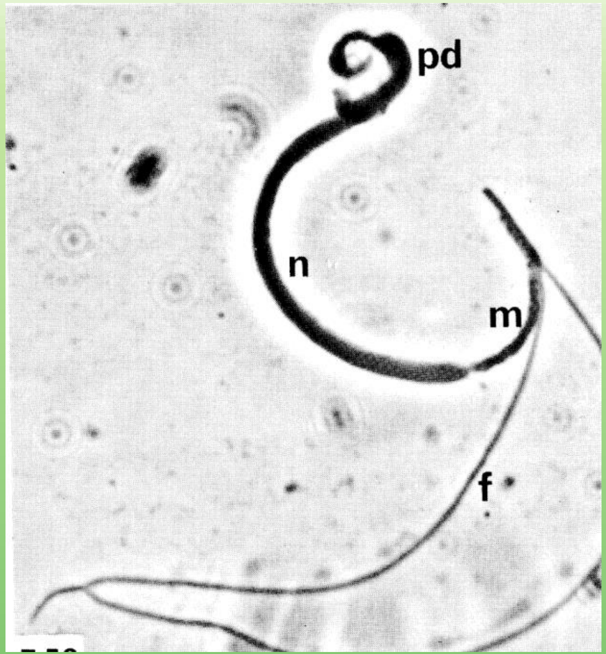

pd - reduced chloroplast
n – nucleus
m – mitochondria
f - flagellum

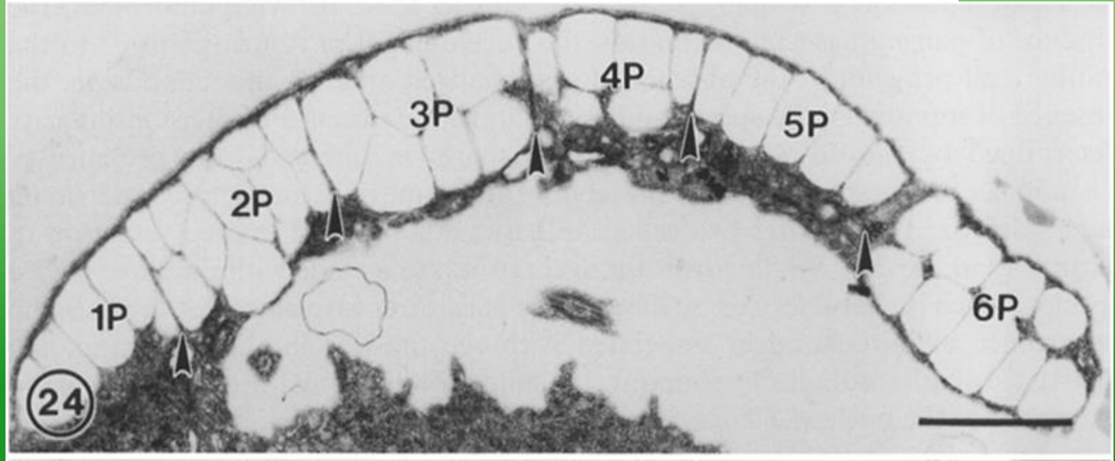

Duncan et al. (1997)

Life cycle

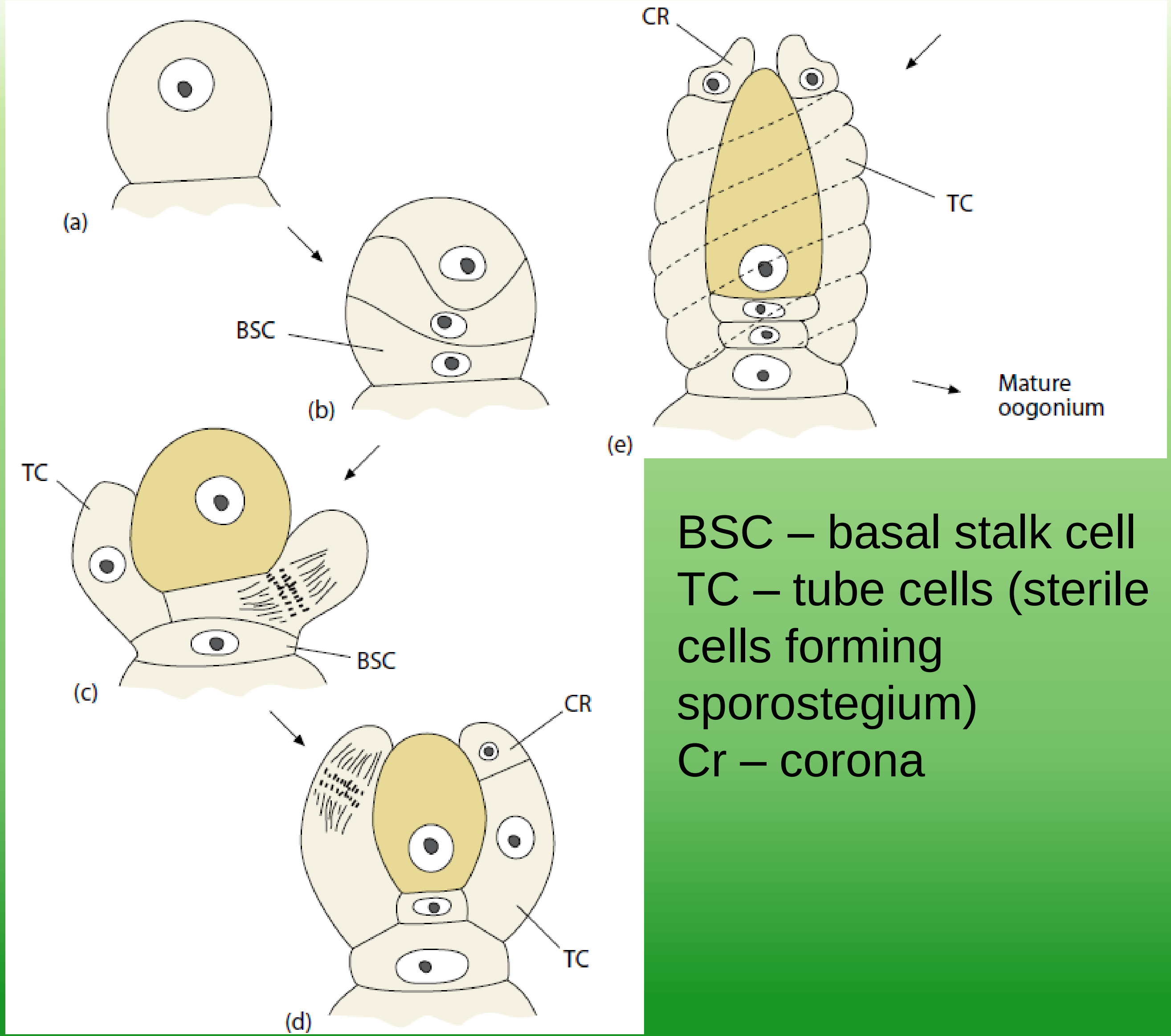

BSC – basal stalk cell
TC – tube cells (sterile cells forming sporostegium)
Cr – corona

Oogonium

Life cycle

Oogonium

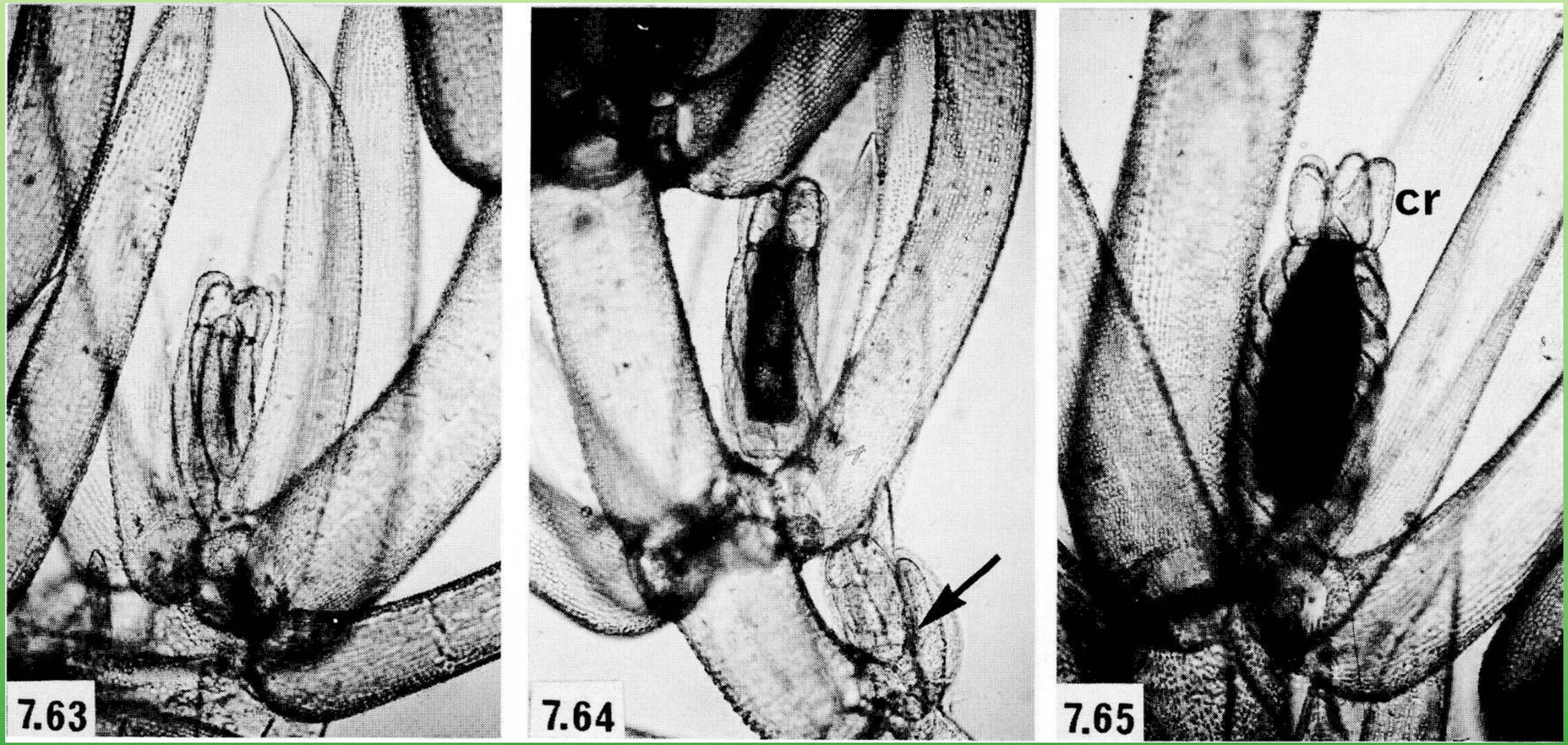

Life cycle

Oospore and gyrogonite

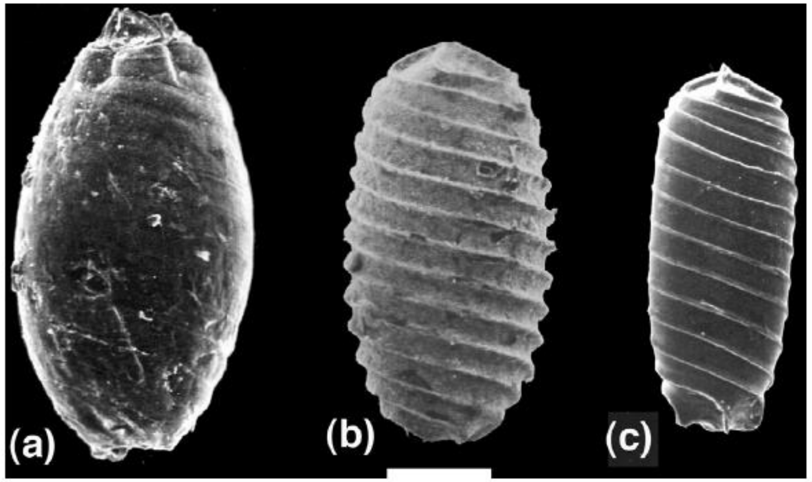

Fig. 1. Developmental stages of the fertilised female fructifications of the Chareae (example genus *Chara*). (a) Fertilised oogonium (=oosporangium) covered by the oogonial integument, coronular cells preserved on top; (b) gyrogonite, after removing the remaining cellulosic walls of the oosporangium; (c) organic-walled oospore, after removing the $CaCO_3$ of the gyrogonite. Scale bar: 250 µm.

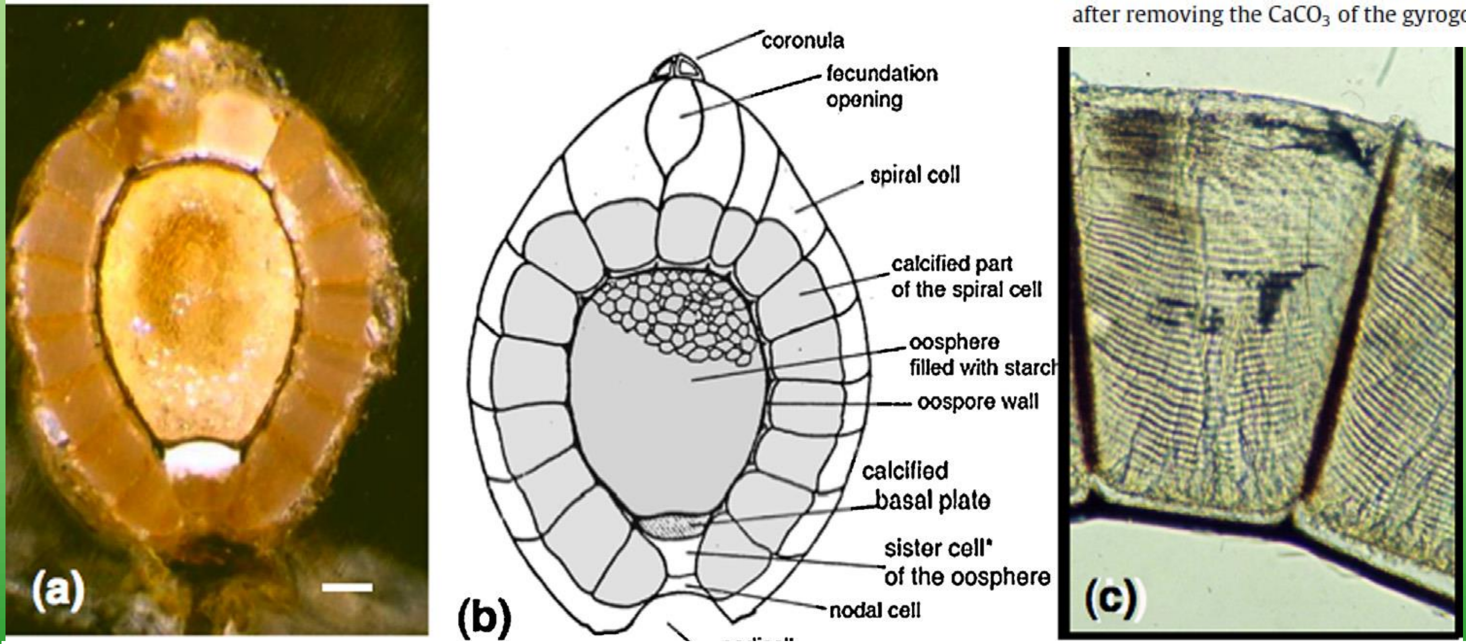

Fig. 2. Structure of the oosporangium of a gyrogonite-forming Characeae (example *Nitellopsis obtusa*). (a) Longitudinal section of a ripe oosporangium showing the relatively thick collapsed integument that covers the gyrogonite. (scale bar: 100 µm); (b) Terminology relating to the ripe oosporangia; *in *Nitellopsis* only the upper part of the sister cell becomes calcified, providing a typical, disc-shaped basal plug; (c) Thin section of the lime-shell enlarged, showing the multilayered structure of alternating organic and calcitic layers; outer oospore wall composed of ectosporostine. Note the presence of ectosporostine between two spiral cells.

Souillé-Märsche & García (2015)

Asexual reproduction

Thallus fragmentation, bubils

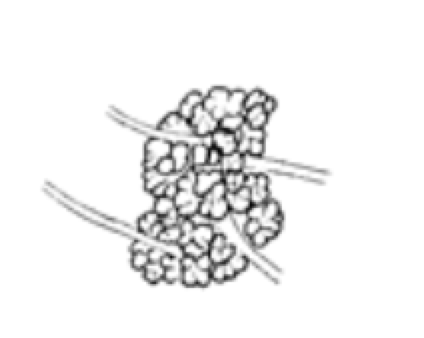

Chara delicatula

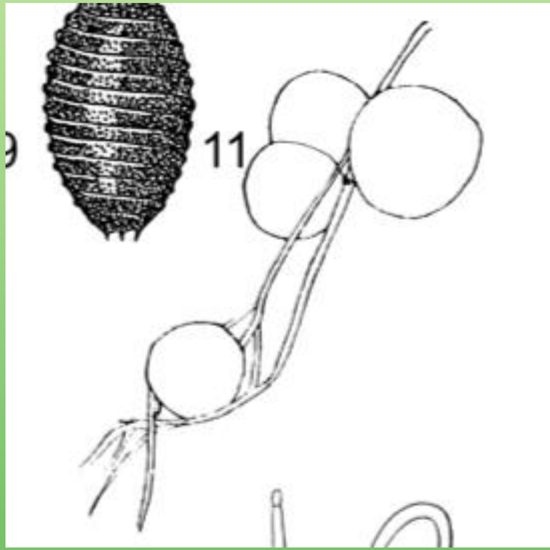

Chara aspera

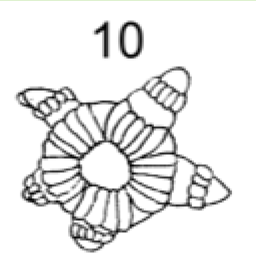

Nitellopsis obtusa

Systematics

6 genera:

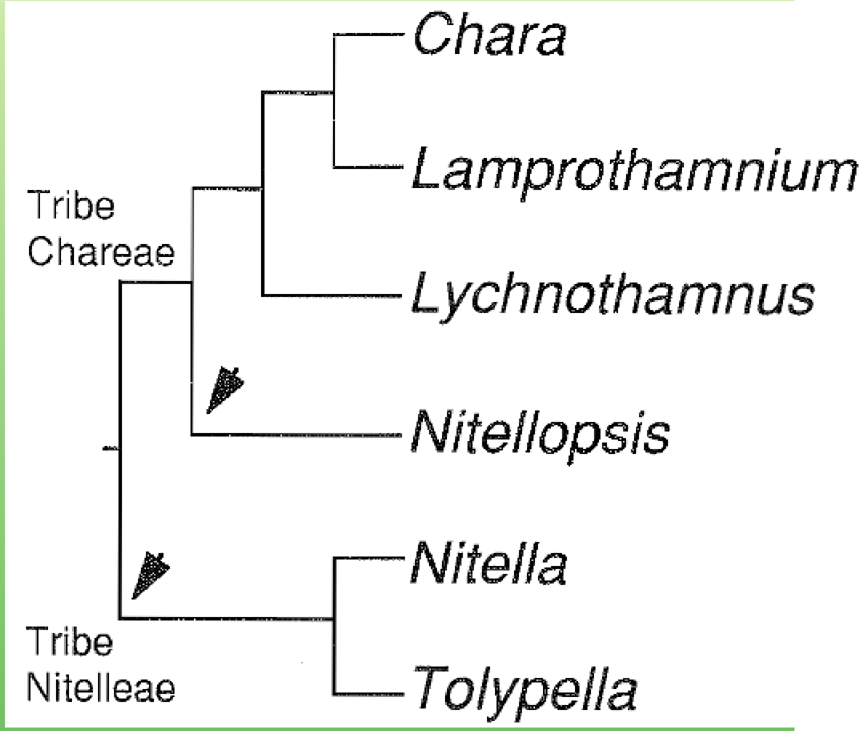

McCourt et al. (1996)

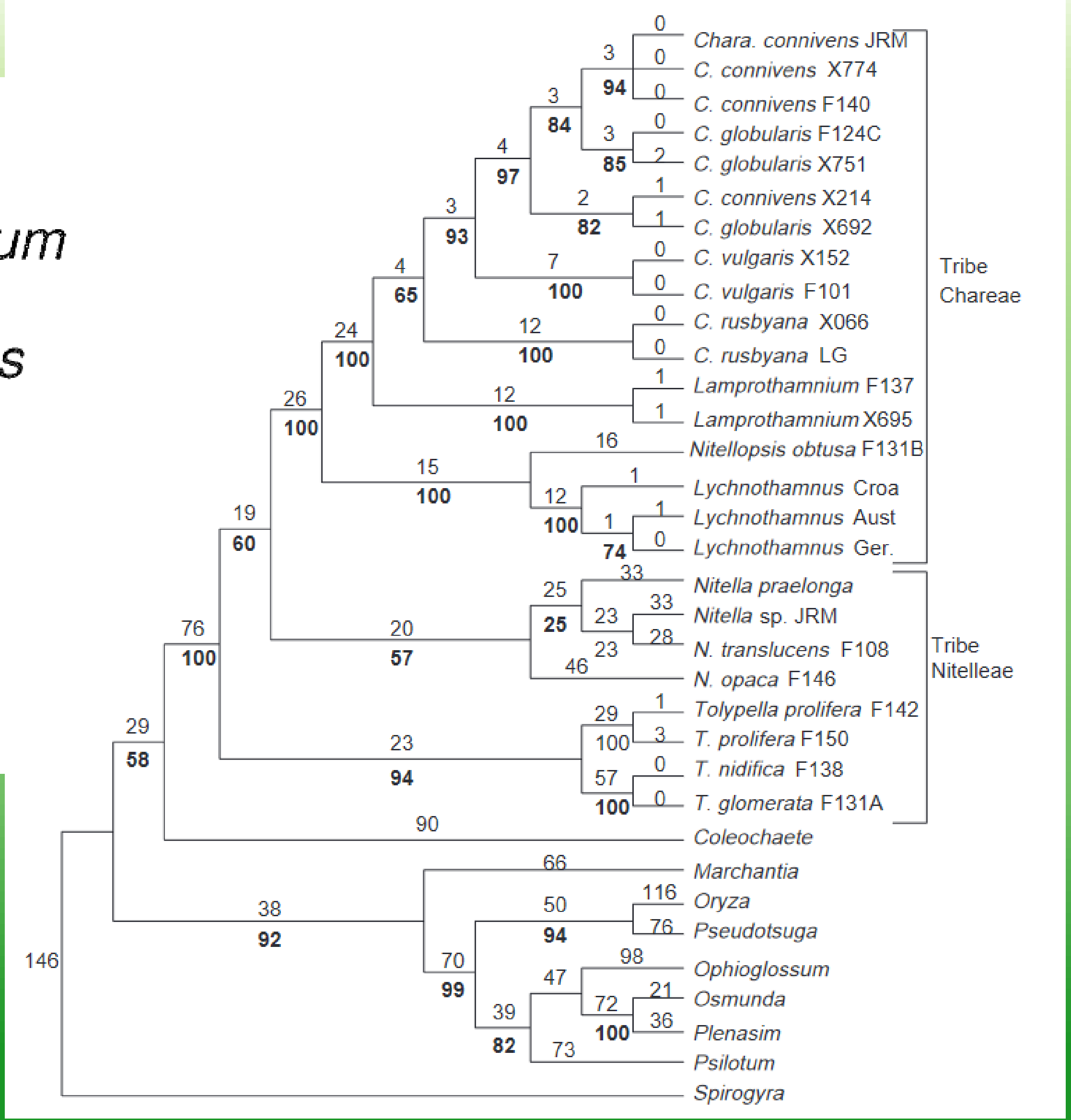

McCourt et al. (1999)

Genus *Chara*

Chara

- Cortex layer
- Corolna consists of 5 cells

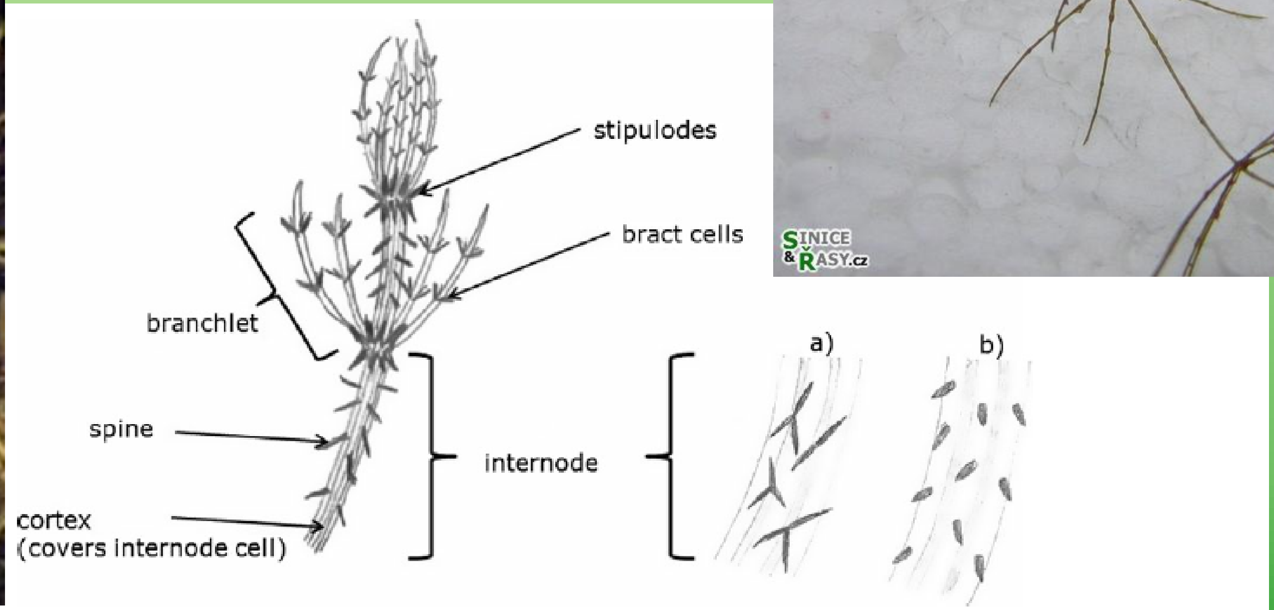

FIG. 1. Schematic drawing of the uppermost part of a *Chara* specimen; the cortex can be (i) haplostichous (number of cortex cell rows corresponds to the number of branchlets), diplostichous (twice as many cortex cell rows as the number of branchlets), or triplostichous (three times as many cortex cell rows as the number of branchlets), and (ii) aulacanthous (secondary cortex cell rows more prominent, spines on thinner cortex cells), tylacanthous (primary cortex cell rows more prominent, spines on thicker cortex cells), or isostichous (primary and secondary cortex cells equally prominent). (a) It shows an example of a diplostichous aulacanthous cortex with fasciculate spines (e.g., *C. hispida*), (b) illustrates an example of a diplostichous tylacanthous cortex with single spines (e.g., *C. baltica*).

Genus *Chara*

Chara braunii – species concept

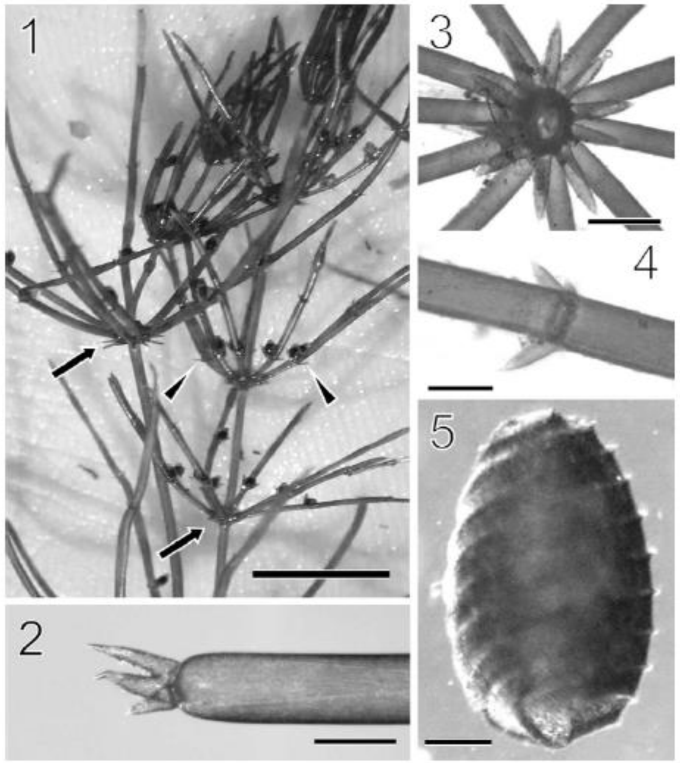

Figs 1–5. Diagnostic characters that were used for classifying infraspecific taxa of *Chara braunii* (Wood 1965; Zaneveld 1940).
Fig. 1. Upper portion of thallus. Arrows and arrowheads indicate positions of stipulodes and bract cells, respectively (SK005, Table 1). Scale bar = 1 cm.
Fig. 2. Terminal branchlet cells formed coronally (NIES-1590, Table 1). Scale bar = 300 mm.
Fig. 3. Axial sectional view of stipulodes (SK005). Scale bar = 1 mm.
Fig. 4. Bract cells (SK005). Scale bar = 500 μm.
Fig. 5. Oospore (SK005). Scale bar = 100 μm.

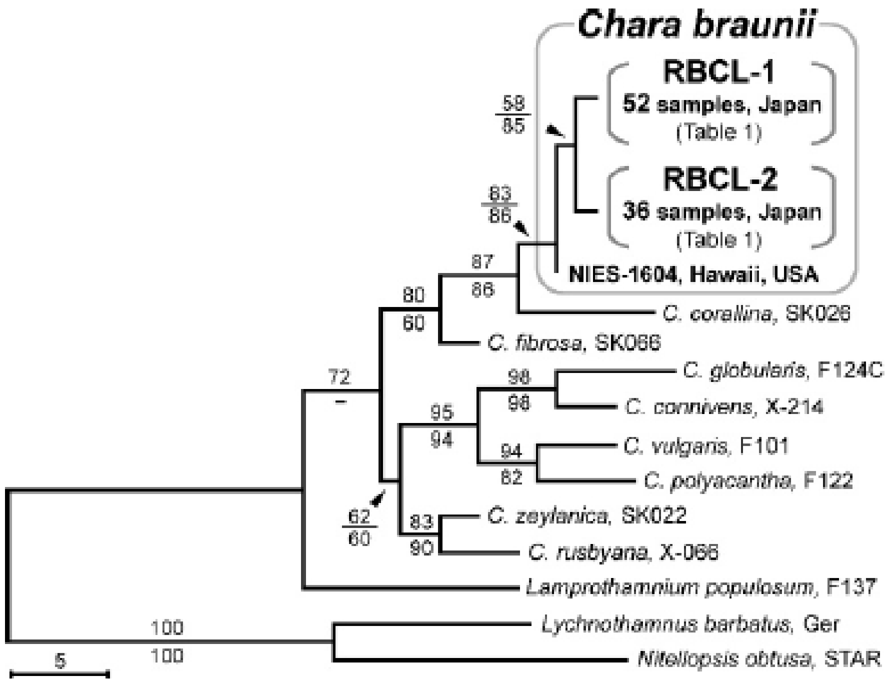

Fig. 10. Single MP tree based on 1194 bp in the coding regions of the *rbc*L genes of 100 samples representing nine species of the genus *Chara* (*C.*) and other charalean species (Table 1). Branch lengths are proportional to the nucleotide changes, which are indicated by the scale bar below the tree. Numbers above and below branches are bootstrap values (50% or more) based on 1000 replications of the MP and NJ (based on HKY + I distance) analyses, respectively.

Kato et al. (2008)

Chara braunii

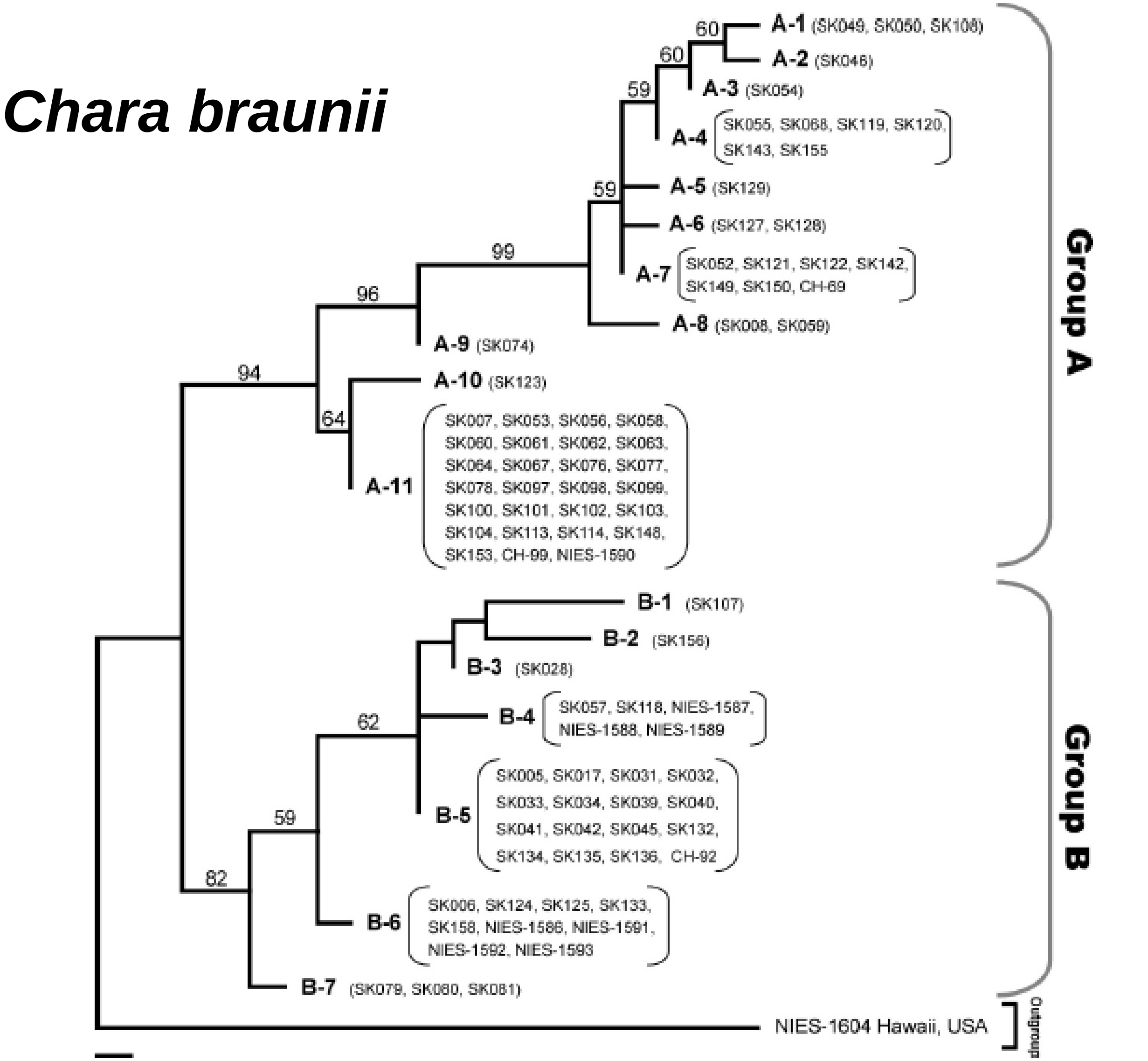

Fig. 11. Single MP tree based on 2393 bp in the coding regions of the *rbc*L (1194 bp) genes plus the intergenic spacer regions between *atp*B and *rbc*L genes (*atp*B-*rbc*L IGS) (1745 bp) from 89 samples of *Chara braunii* (Table 1). Branch lengths are proportional to the nucleotide changes, which are indicated by the scale bar below the tree. Numbers above branches are bootstrap values (50% or more) based on 1000 replications of the MP analysis.

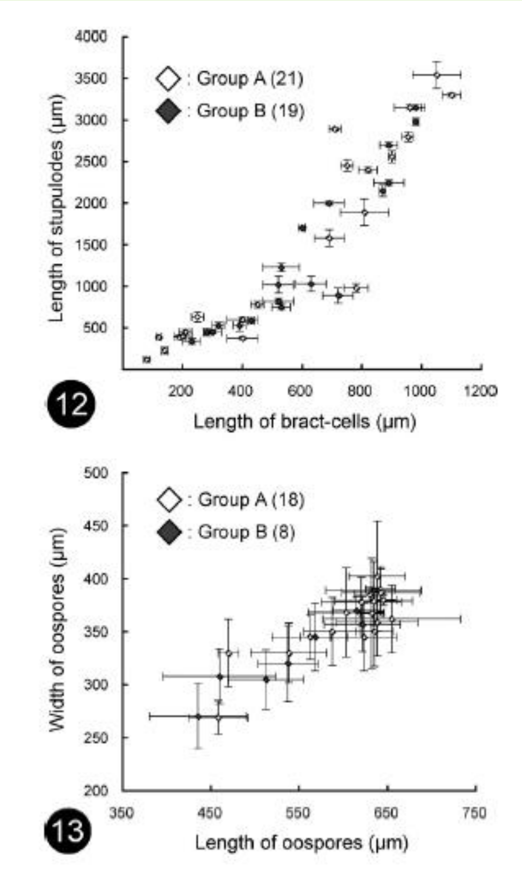

Chara

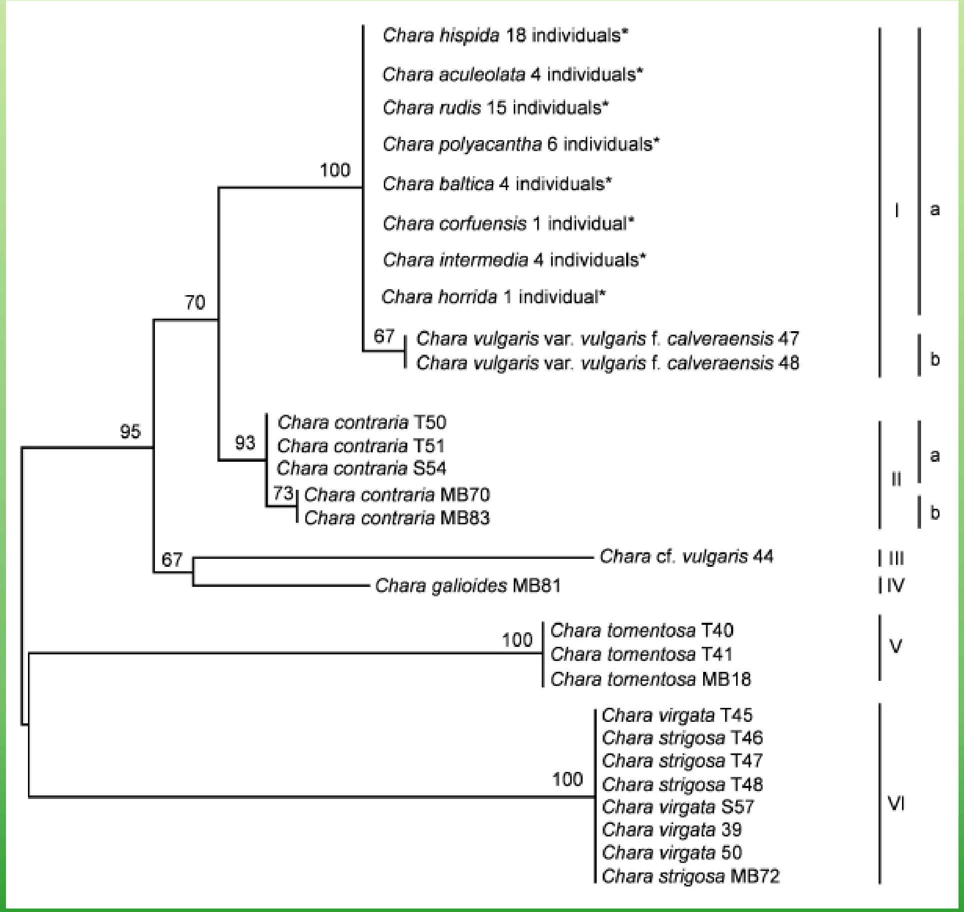

FIG. 3. Concatenated maximum likelihood (ML) tree of ITS2, *matK* and *rbc*L sequences of 73 *Chara* samples. Bootstrap values above 50% are shown in the tree. The bar indicates 1% sequence divergence. *= for sample ID see Table 1. The clusters belong to the following subsections according to Wood and Imahori (1965): I = Hartmania, II = Chara, III = Chara, IV = Grovesia, V = Chara, VI = Grovesia.

Schneider et al. (2015)

Chara

Multigene analysis

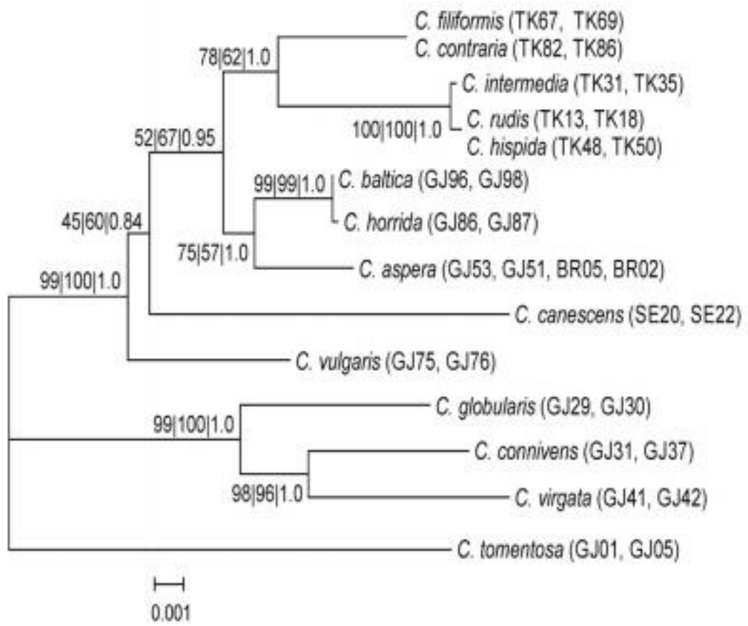

section	subsection	cortication						sex		spines			stipulode		branchlet		clade	
		1	2	3	tylacanth	aulacanth	isostich	monoecious	dioecious	>>axes	=axes	<axes	short	very short	ecorticate	most segments corticate		
Chara	Chara		x		x		x	x					x	x	x		C	
			x		x		x	x				x	x			x		
	Hartmania		x		x		x	x				x	x			x		
			x			x		x			x	x				x	D	
			x			x	x	x		x						x		3
			x		x		x	x		x	x	x	x			x	B	
			x			x	x	x		x	x					x		
Grovesia	Grovesia			x	x				x	x						x	A	
Desvauxia		x							x	x						x		
Chara	Chara		x			x	x	x				x	x	x		x		
Grovesia	Grovesia			x			x	x						x		x		
				x			x		x					x		x		2
				x	x			x				x	x			x		
Chara	Chara		x		x		x		x		x	x	x			x		1

''''

Fig. 2. Molecular phylogeny of *Chara* microspecies based on the concatenated *atp*B,*rbc*L, *matK*, 18S rRNA and nrITS-1 sequences using 6214 aligned positions combined with morphological characters. Additionally the sections and subsections of the macrospecies concept are indicated. The unrooted tree resulted from a maximum parsimony, a maximum likelihood and a Bayesian inference analysis; bootstrap percentage values and posterior probabilities (>50%) were determined and are given above the branches (MP|ML|BI). Sample IDs are indicated for every microspecies in parentheses. The scale bar indicates 0.1% sequence divergence.

Nowak et al. (2016)

Genus *Nitella*

Nitella

- No cortex nor stipuli
- Corona consists of 10 cells

Nitella

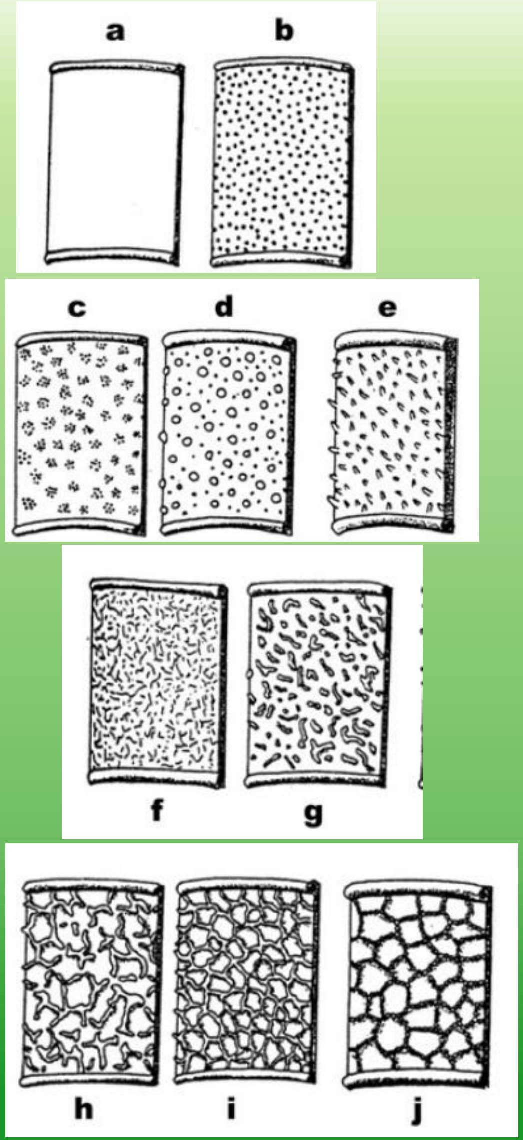

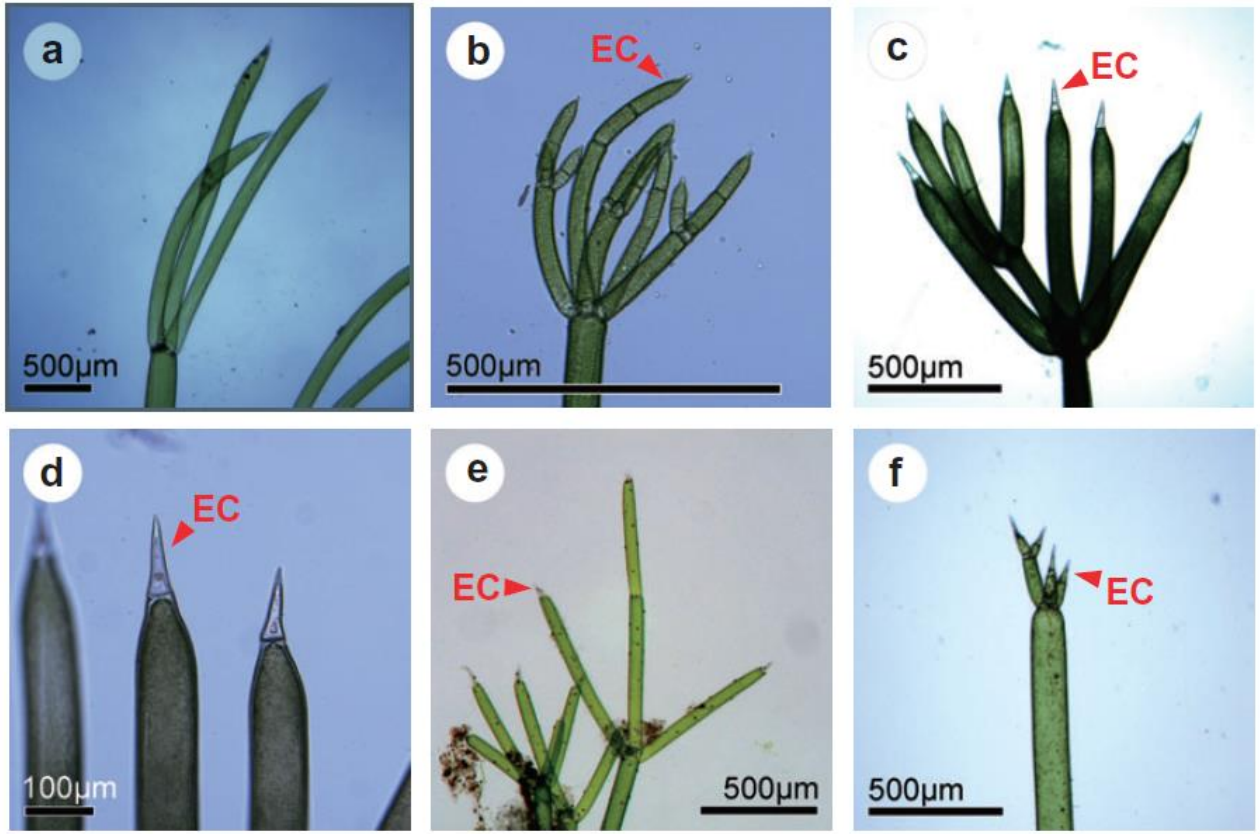

Fig. 4. Dactyl of *Nitella*. (a) Elongated dactyl of *Nitella* (subgen. *Nitella*) *acuminata*, consisting of a single cell. (b) Elongated or abbreviated dactyl of *Nitella* (subgen. *Hyella*) *pulchella*, consisting of two or three cells. Note the end cell (EC) is similar to the penultimate cell. (c) Elongated dactyl of *Nitella* (subgen. *Tieffallenia*) *hyalina*, consisting of two cells. Note the EC is very different from the penultimate cell. (d) Close view of tip of dactyl, showing EC. (e) Elongated dactyl of *Nitella* (subgen. *Tieffallenia*) *oligospira*, consisting of two or three cells. Note the EC is very different from the penultimate cell. (f) Abbreviated dactyl of *Nitella* (subgen. *Tieffallenia*) *axilliformis*, consisting of two cells. Note the EC is very different from the penultimate cell.

Nitella

External and internal morphology of oospore wall as a taxonomic trait

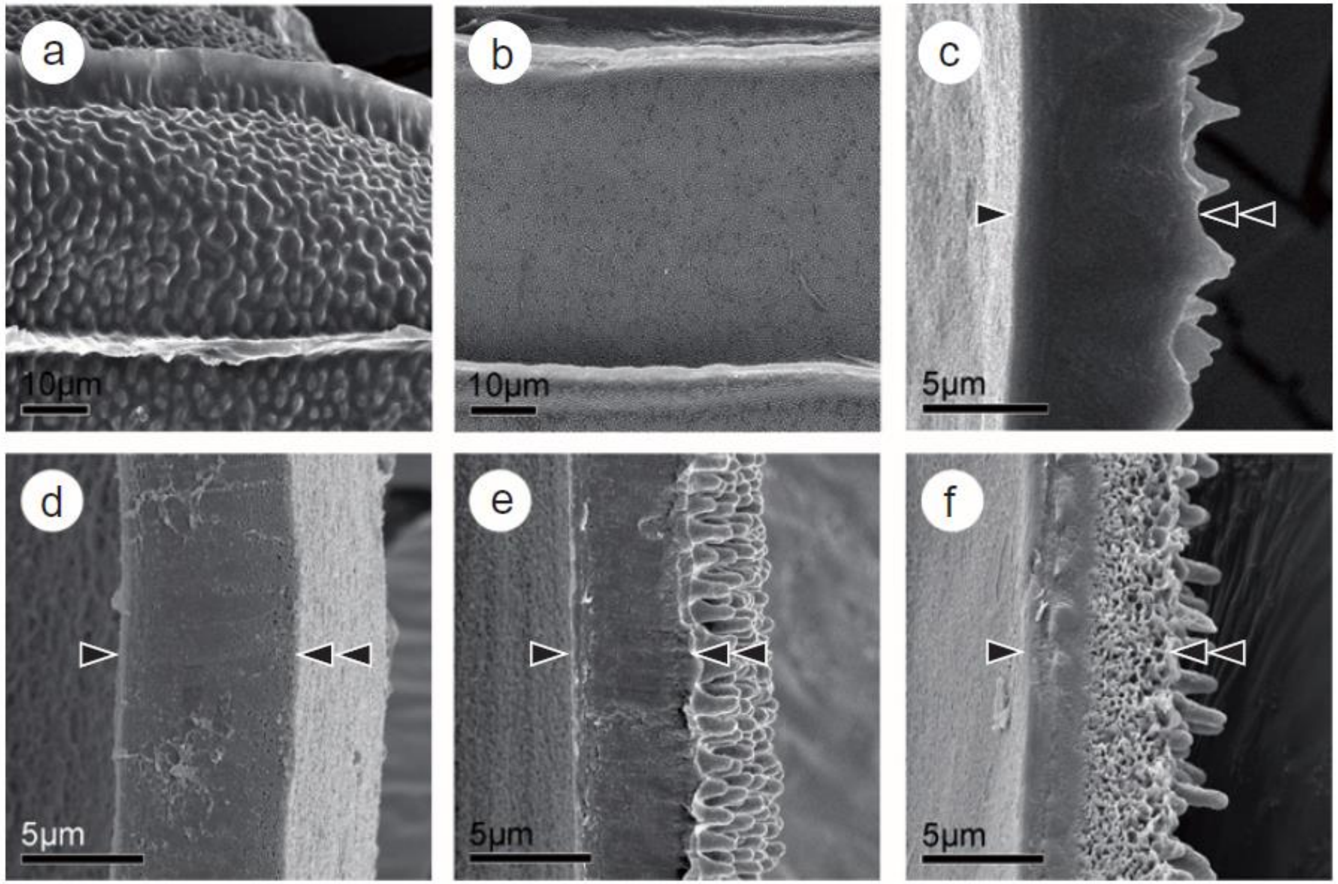

Fig. 6. External and internal morphology of the oospore wall (EMOW and IMOW), scanning electron microscopy (SEM) (b, from Sakayama *et al.* 2002, and d–f, from Sakayama *et al.* 2005; reproduced with permission from the Allen Press Publishing Services and Phycological Society of America, respectively). Single or double arrowhead indicates the inner or outer side of the wall, respectively. (a) EMOW of *Nitella furcata*, showing imperfect reticulate pattern. (b) EMOW of *Nitella gracilens*, showing very fine granulate pattern. (c) IMOW of *Nitella japonica* (S077), showing homogeneous (HG) texture. (d, e) IMOW of *Nitella pseudoflabellata* (S031) and *Nitella megaspora* complex 1 (S054), respectively, showing weakly spongy (W-SG) texture. (f) IMOW of *N. megaspora* complex 2 (S073), showing strongly spongy (S-SG) texture.

Sakayama et al. (2008)

Nitella

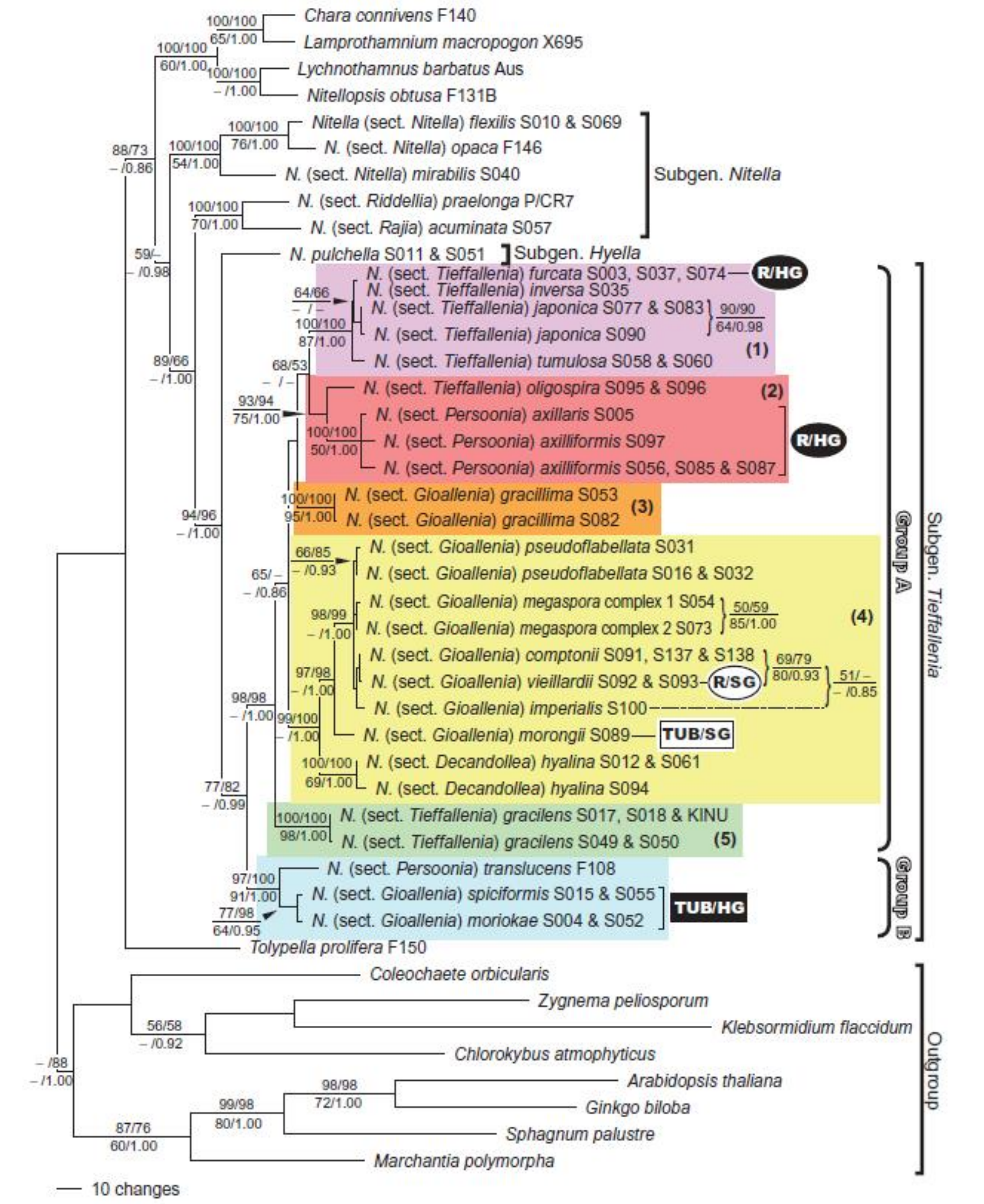

Sakayama et al. (2008)

Genus *Nitellopsis*

- no cortex nor stipuli
- Bulbils (asexual reproduction)

N. obtusa

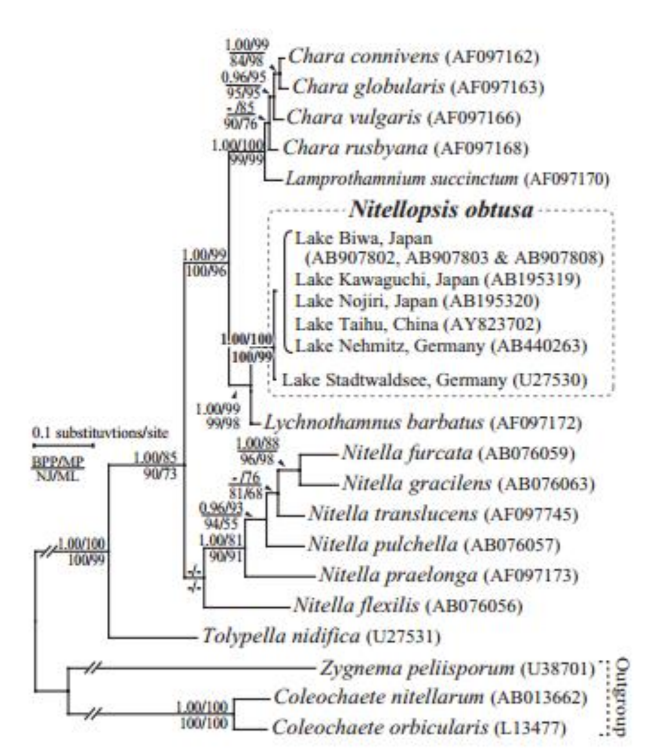

Kato et al. (2014)

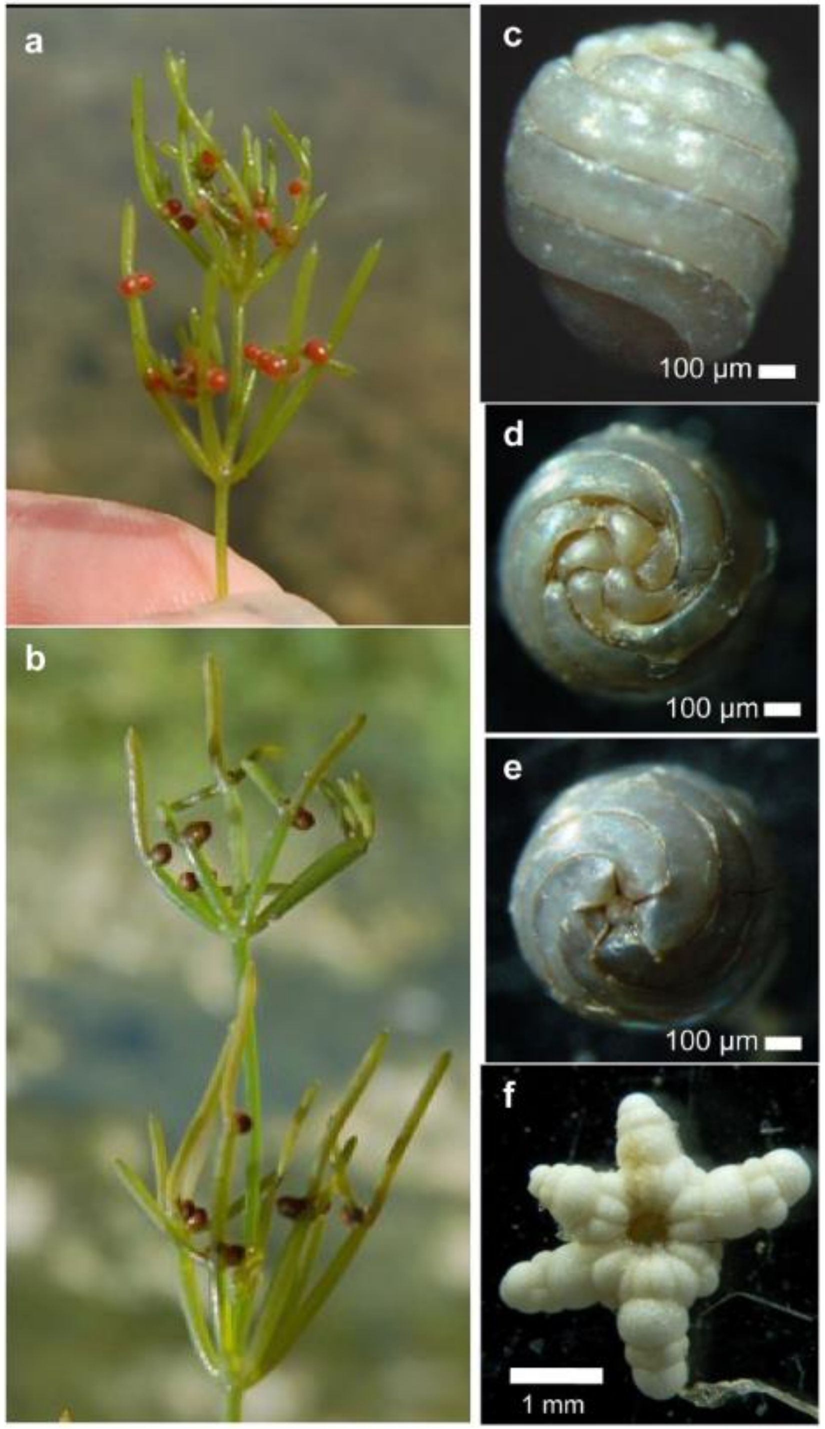

Boissezon et al. (2018)

Genus *Tolypella*

Tlypella

- No cortex nor stipuli, corona with 10 cells

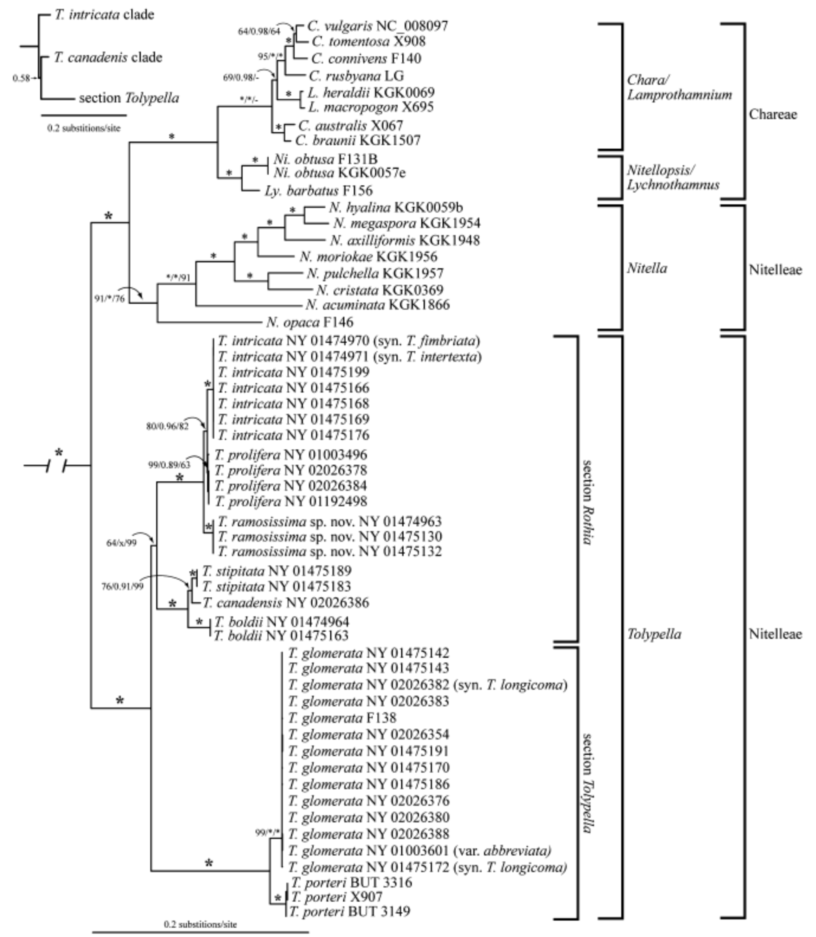

Fig. 4. Phylogeny of Characeae based on combined *atpB*, *psbC*, and *rbcL* data. Maximum likelihood tree with bootstrap values and posterior probabilities above branches (ML, BI, and MP values respectively). An asterisk (*) indicates a bootstrap proportion of 100% or a posterior probability of 1.0. A dash (-) indicates a bootstrap proportion less than 50% or a posterior probability less than 0.5. An "x" indicates an incongruent topology between the BI and the ML and MP analyses and is shown in the inset with the BI posterior probability value.

Pérez et al. (2014)

Tolypella

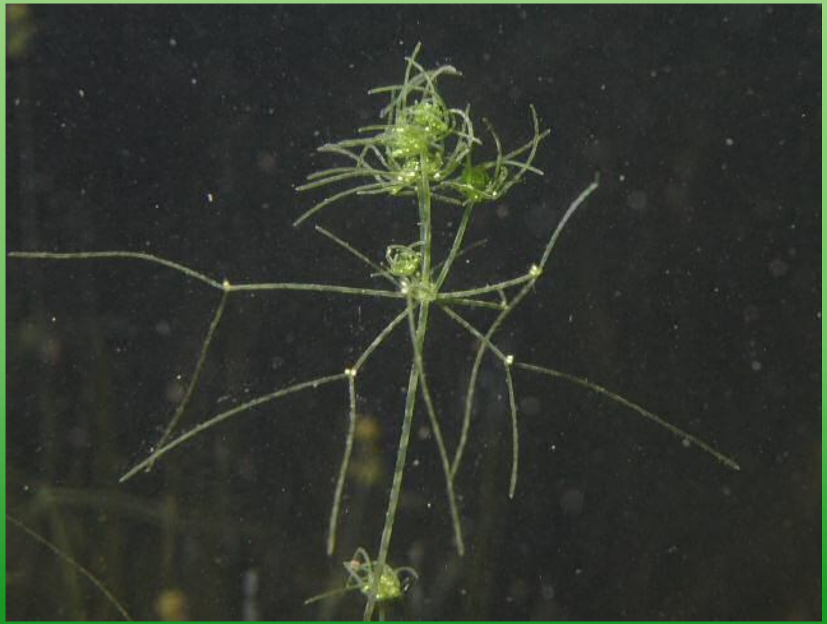

Genus *Lamprothamnium*

- No cortex
- stipuli
- 5 cells of corona

Genus *Lychnothamnus*

L. barbatus

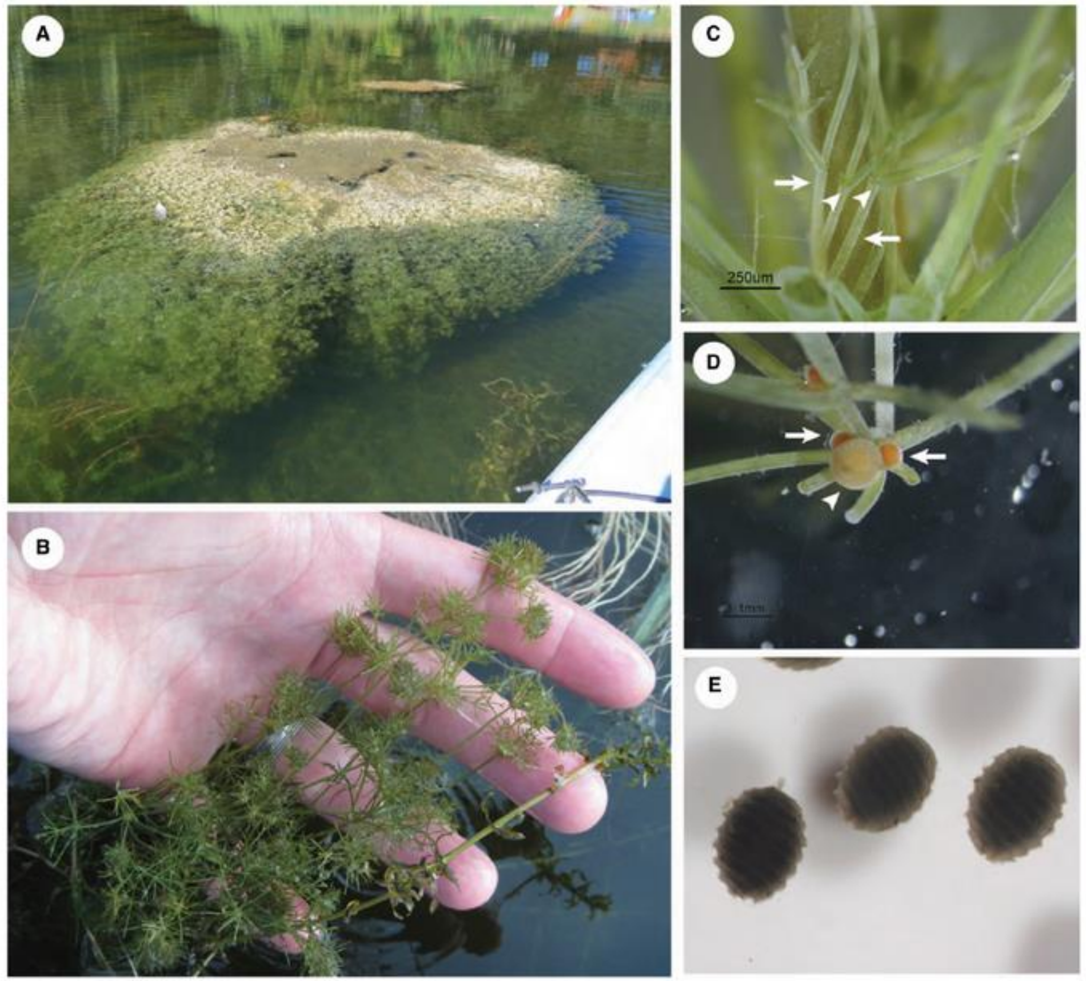

FIGURE 2 *Lychnothamnus barbatus* habit and distinguishing morphological characteristics. (A) *L. barbatus* mat in Wolt Lake, Adams County, Wisconsin. (B) General habit. (C) Detail showing rudimentary axial cortication (arrows) with variable spine cells (arrowheads). (D) Gametangia with antheridia (arrows) lateral oogonia (arrowhead). (E) Oospores with lime shells.

Karol et al. (2001)

Lychnothamnus barbatus

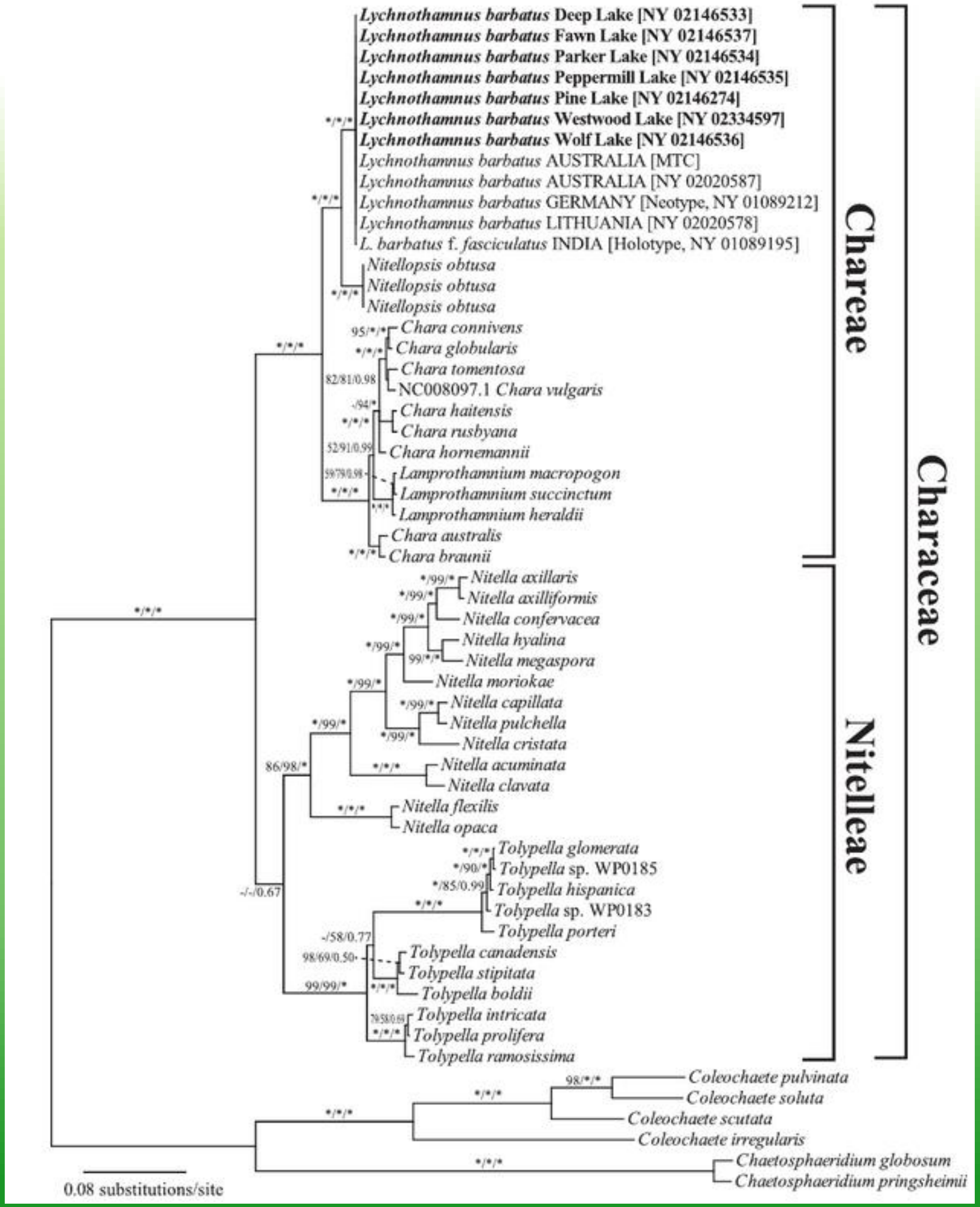

Karol et al. (2001)

Ecology

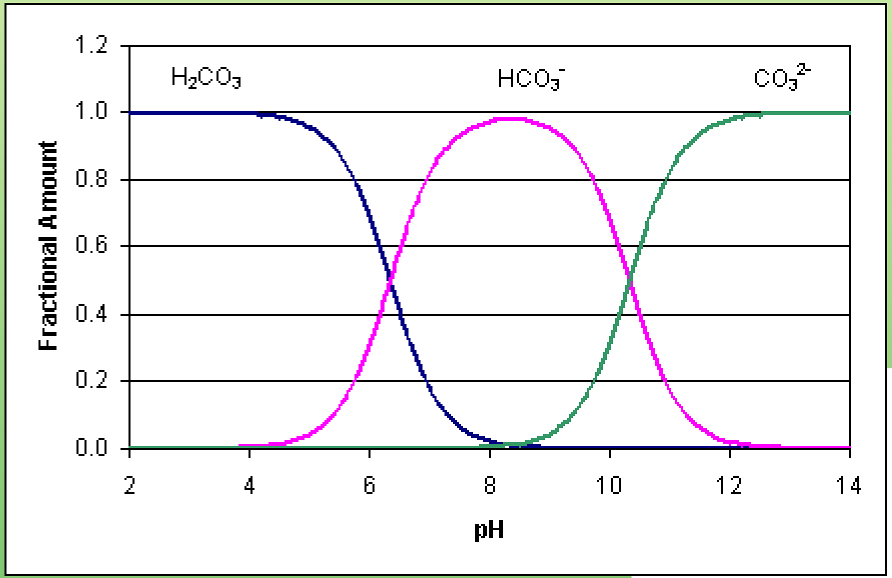

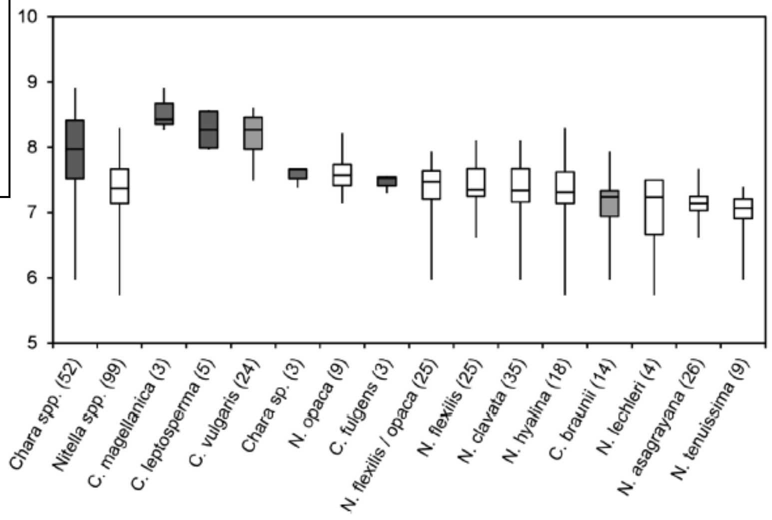

Figure 2. Box-Whisker plot of pH values for taxa with at least 3 values in the water chemistry dataset. Minimum, maximum and median pH are given as well as 50% and 75% quartiles (boxes). Number of values are given in brackets; *Chara* spp. marked in grey.

Schubert et al. (2018)

Ecology

Baltic Sea

A meadow of Chara horrida and Chara tomentosa in the archipelago of Åland, Finland. Photo by Kajsa Rosqvist.

Chara baltica A.Bruzelius (Image Ref. 6684)
Lemkenhafen, Orther Bight (Fehmarn), Baltic Sea; species common at 0,5m depth - 12 Jul 2005
© Dirk Schories (dirk.schories@gmx.de)

CLOSE ✕

Ecology

C. aspera

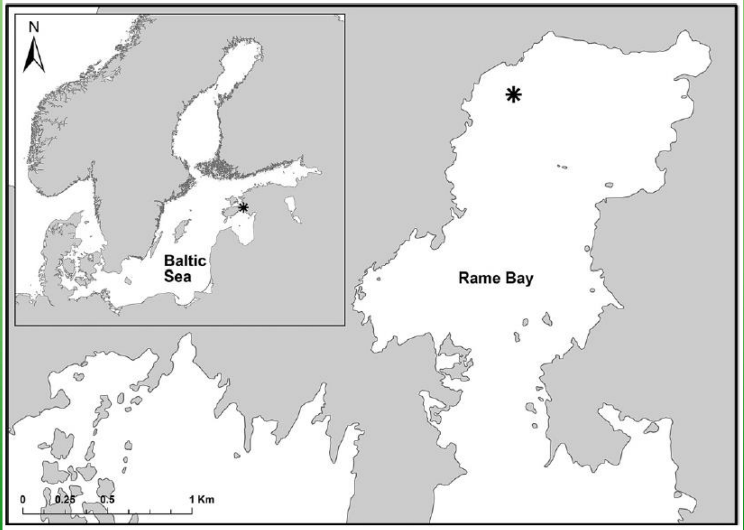

Fig. 1. Location of study area.

Table 1
Timing of disturbances (O) and sample collection (X) in our experiment.

	06 2007	07 2007	08 2007	09 2007	10 2007	07 2008
Timing 1	O	X	X	X	X	X
Timing 2		O	X	X	X	X

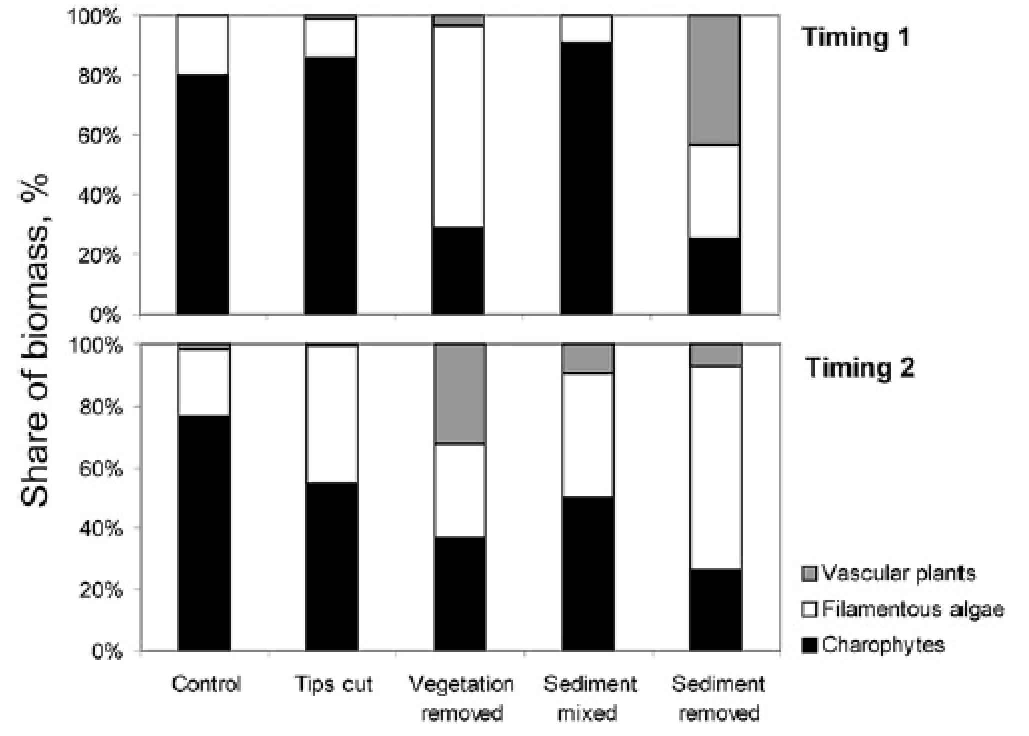

Fig. 3. Biomass share of charophytes, filamentous algae and higher plants for the studied disturbance treatments in 2008.

Torn et al. (2010)

Ecology

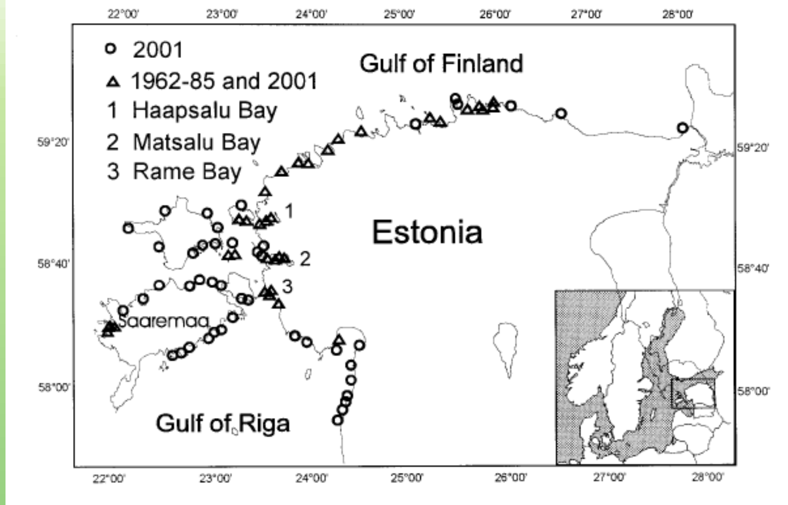

Fig. 1. Location of sampling localities in Estonian coastal waters.

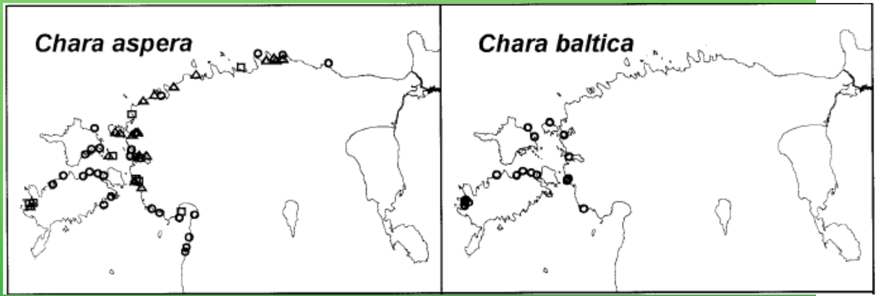

Torn et al. (2004)

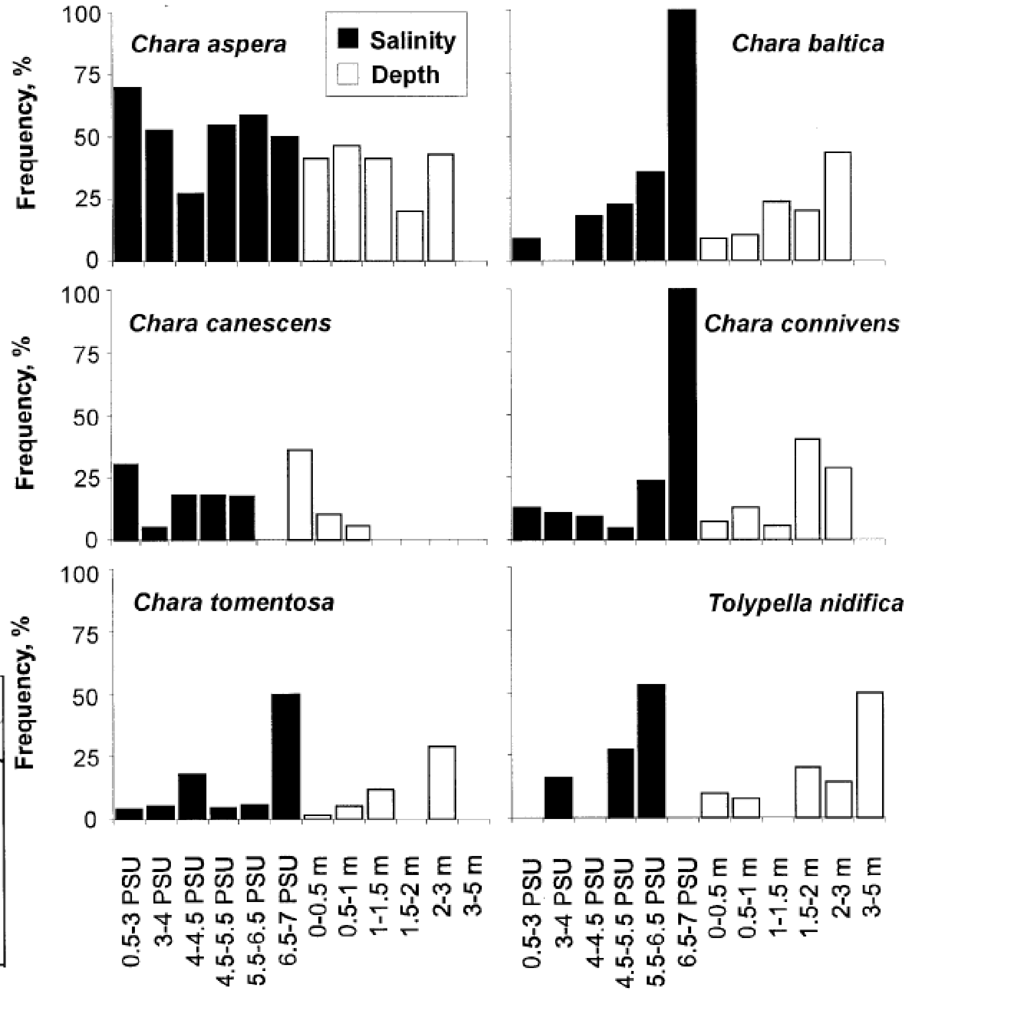

Fig. 2. Frequency of charophyte species findings in different salinity and depth intervals in Estonian coastal waters. Frequency is calculated as occurrence of species in locations with certain salinity or depth interval.

Czech Charophyceae

Table 1. Ecological requirements of Charales in the Czech Republic (according to VILHELM 1914, DĄMBSKA 1964, HAAS 1994, KRAUSE 1997, HUSÁK pers. comm.)

Species	Water factors			Habitats						Substratum				
	Temp	Light	Desicc	Pools/ ponds	Lakes	Ditches	Peat-trenches	Bogs/ fens	Running water	Gravel	Sand	Mud	Peat	Chalk
Chara aspera	RT	IND	x	x	x	x	x	x	x		x	(x)	x	x
Chara braunii	ET	HEL	x	x			x			x	x			
Chara canescens	ET	LOW		x	x		x			x	x			
Chara connivens	ET	IND		x	x				x	x	x	x		
Chara contraria	ET	LOW		x	x	x	x	x	(x)	x	x	x	x	x
Chara delicatula	ET	IND	x	x	x	x	x	x		x	x	x	x	x
Chara globularis	ET	HEL	x	x	x	x	x	x	(x)	x	x	x	(x)	(x)
Chara gymnophylla	ET	LOW												
Chara hispida	ET	LOW		x	x	x	x	x	(x)	x	x	x	x	
Chara polyacantha	ET	LOW		x			x	x		x	x			x
Chara tomentosa	ET	LOW		x	x	x	x		x	(x)	x	x	(x)	(x)
Chara rudis	ET	LOW	x	x	x	x	(x)		x	x	x		x	
Chara vulgaris	ET	LOW	x	x	(x)	x	x	x	x	x	x	(x)	x	
Nitella batrachosperma	ET	LOW		x							x			
Nitella capillaris	ET	HEL	x	x		x	x	x		x	x	x		
Nitella flexilis	ET	LOW	x	x	x	x	x		x	(x)	x	x	x	
Nitella gracilis	ET	IND		x	x	x	x	x	(x)	x	(x)	x		
Nitella mucronata	ET	LOW		x	x	x	x		x	(x)	x	x	x	
Nitella opaca	ET	LOW		x	x	x	x	x	x	x	x	x	x	
Nitella syncarpa	ET	LOW	x	x	x	x	x	x	x	x	x	x		
Nitella tenuissima	ET	LOW	x	x	x	x	x	x	(x)	(x)	x	x	x	
Nitellopsis obtusa	ET	LOW		x	x	x	x		x	x	x	x	x	
Tolypella glomerata	C	HEL		x	(x)		x		(x)	x	x	x		
Tolypella intricata	RT	IND	x	x	(x)				(x)		x			
Tolypella prolifera	ET	IND		x		x		x	x		x			

(Temp) Requirements for temperature: (RT) relativively thermophilic, (ET) eurythermal, (C) cold; (Light) Requirements for light: (IND) indifferent, (HEL) heliophytic, (LOW) tolerant of low light intensity; (Desicc) Desiccation tolerance

Caisová & Gabka (2009)

Czech Charophyceae

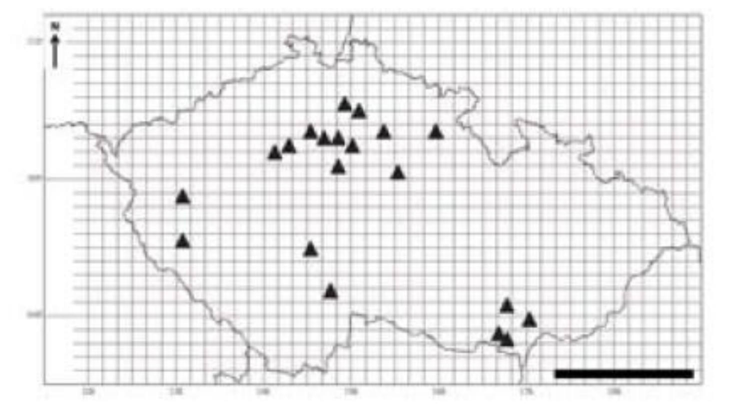

Fig. 13. Distribution of *Chara aspera* in the Czech Republic (scale bar 100 km; for localities see attachment).

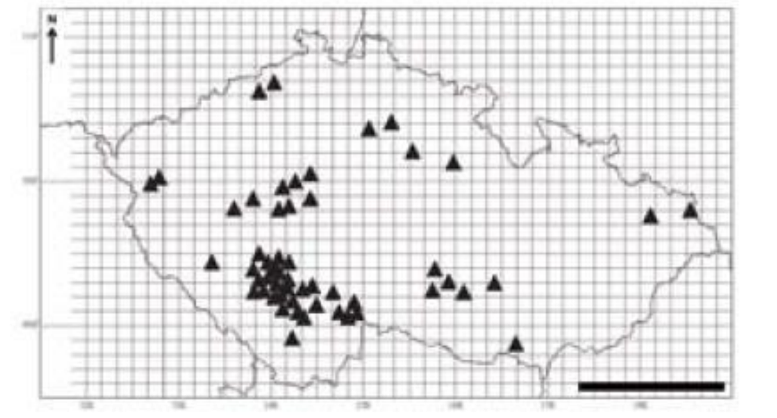

Fig. 22. Distribution of *Chara braunii* in the Czech Republic (scale bar 100 km; for localities see attachment).

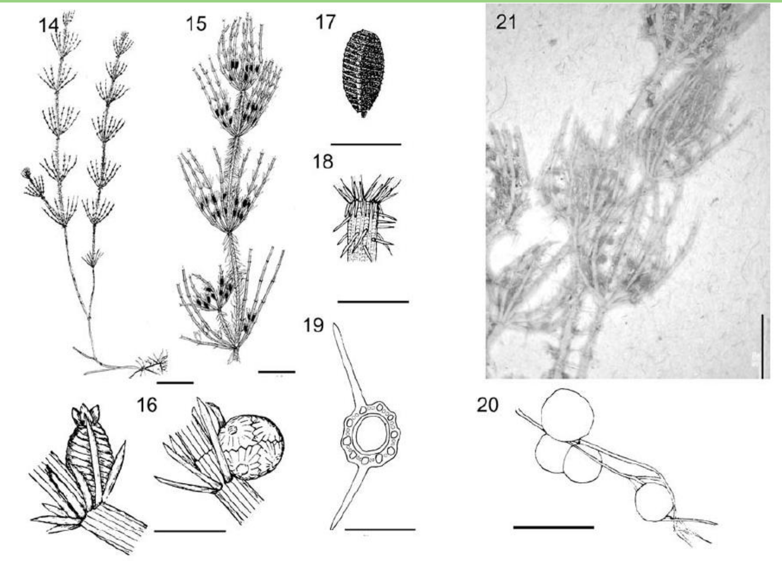

Figs 14–21. *Chara aspera* [(14, 17–19) after KRAUSE (1997); (15–16, 20) after DĄMBSKA (1964); (21) orig. CAISOVÁ]: (14–15, 21) macroscopic habitus; (16) branchlet node with oogonia and antheridia; (17) oospore; (18) stipulodes and spines; (19) internode cross-section; (20) bubils. Scale bars 0.2 cm (Fig. 20), 0.5 cm (Figs 16–19) and 1 cm (Figs 14, 15, 21).

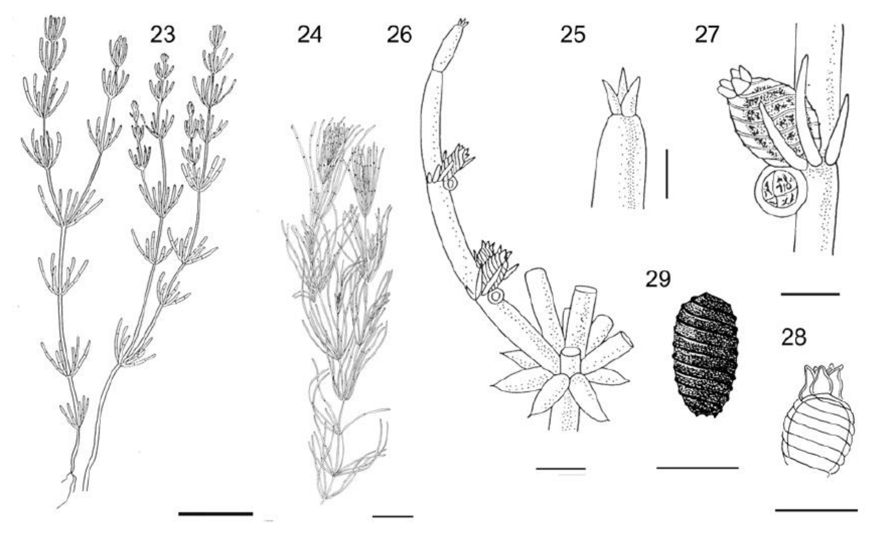

Figs 23–29. *Chara braunii* [(23, 25–27) after WOOD & IMAHORY (1965); (24, 28–29) after KRAUSE (1997)]: (23–24) macroscopic habitus; (25–28) branchlet node with oogonia and antheridia; (29) oospore. Scale bars 0.2 cm (Fig. 28), 0.5 cm (Figs 25, 27, 29) and 1 cm (Figs 23–24, 26).

Czech Charophyceae

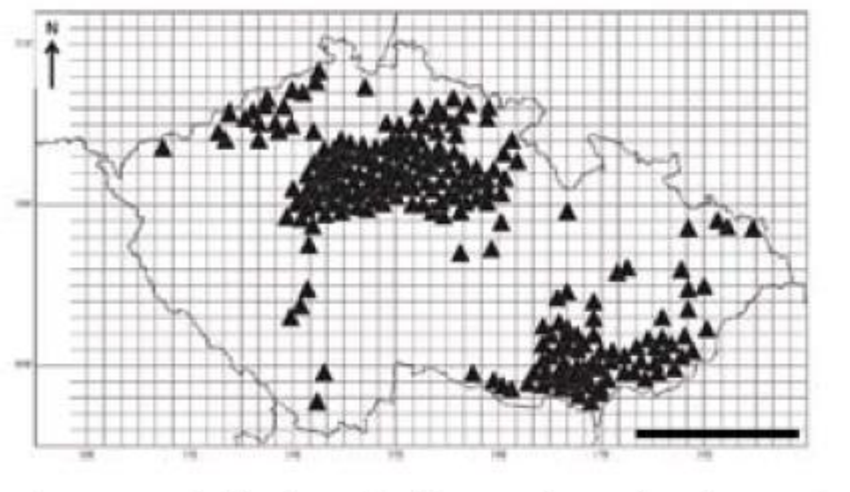

Fig. 126. Distribution of *Chara vulgaris* in the Czech Republic (scale bar 100 km; for localities see attachment).

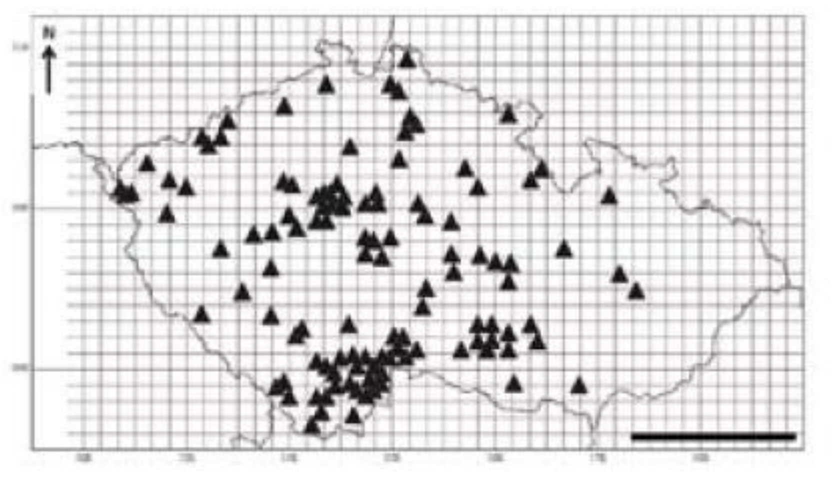

Fig. 151. Distribution of *Nitella flexilis* in the Czech Republic (scale bar 100 km; for localities see attachment).

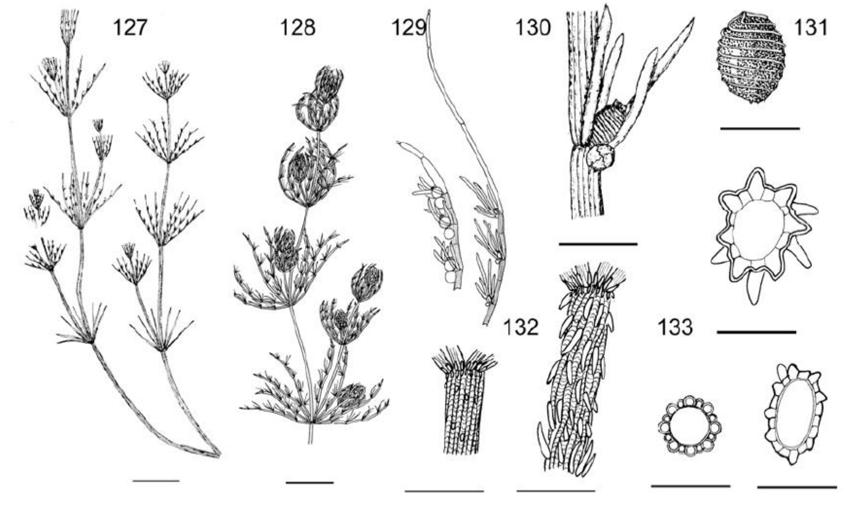

Figs 127–133. *Chara vulgaris* [(127, 130, 133) after DĄMBSKA (1964); (128–129, 131, 133) after KRAUSE (1997)]: (127–128) macroscopic habitus; (129–130) branchlet node with oogonia and antheridia; (131) oospore; (132) internodes, stipuloides and spines; (133) internode cross-section. Scale bars 0.5 cm (Figs 129–133) and 1 cm (Figs 127–128).

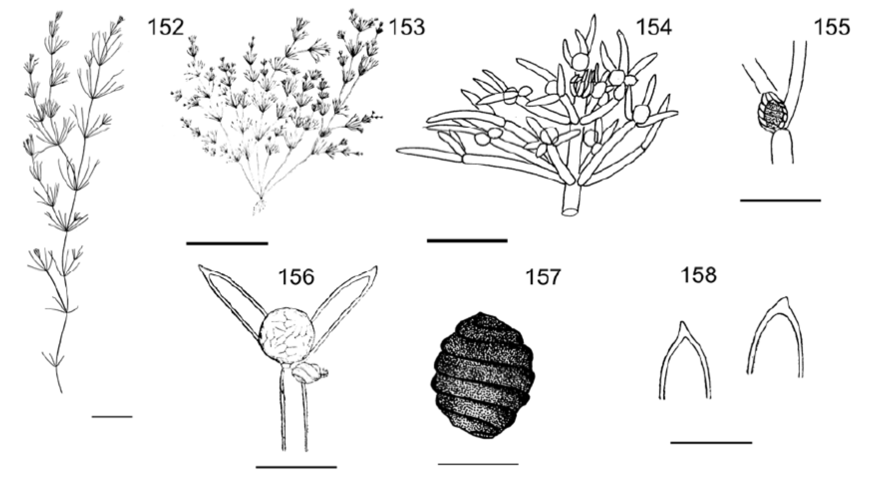

Figs 152–158. *Nitella flexilis* [(152, 154–155, 157) after KRAUSE (1997); (153, 156, 158) after DĄMBSKA (1964)]: (152–153) macroscopic habitus; (154–156) branchlet node with oogonia and antheridia; (157) oospore; (158) ends of branching. Scale bars 0.5 cm (Figs 155–158) and 1 cm (Figs 152–154).

Czech Charophyceae

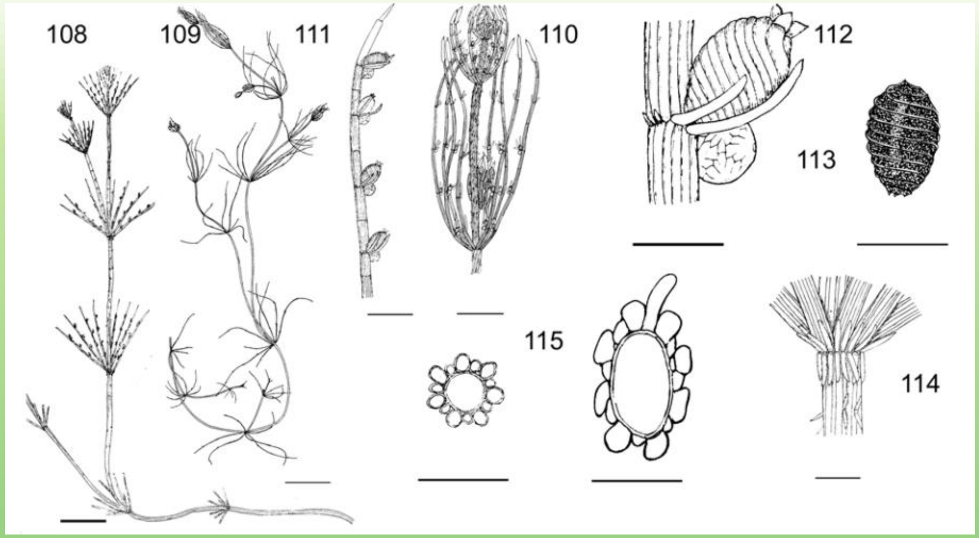

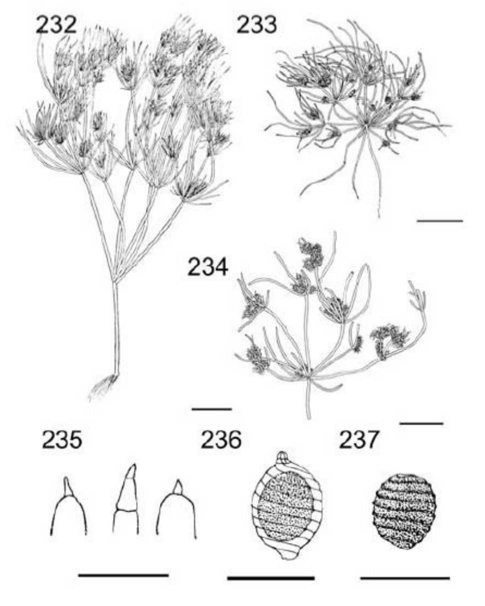

Figs 232–237. *Tolypella prolifera* [(232, 235) after DĄMBSKA (1964); (233–234, 236–237) after KRAUSE (1997)]: (232) macroscopic habitus; (233–234) branching; (235) ends of branching; (236) oogonium; (237) oospore. Scale bars 0.2 cm (Fig. 236), 0.5 cm (Figs 235, 237) and 1 cm (Figs 232–234).

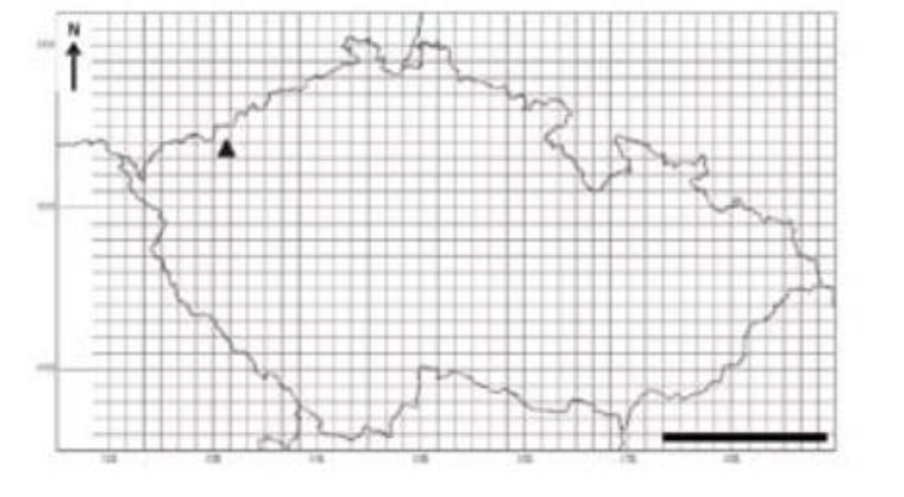

Fig. 107. Distribution of *Chara rudis* in the Czech Republic (scale bar 100 km; for localities see attachment).

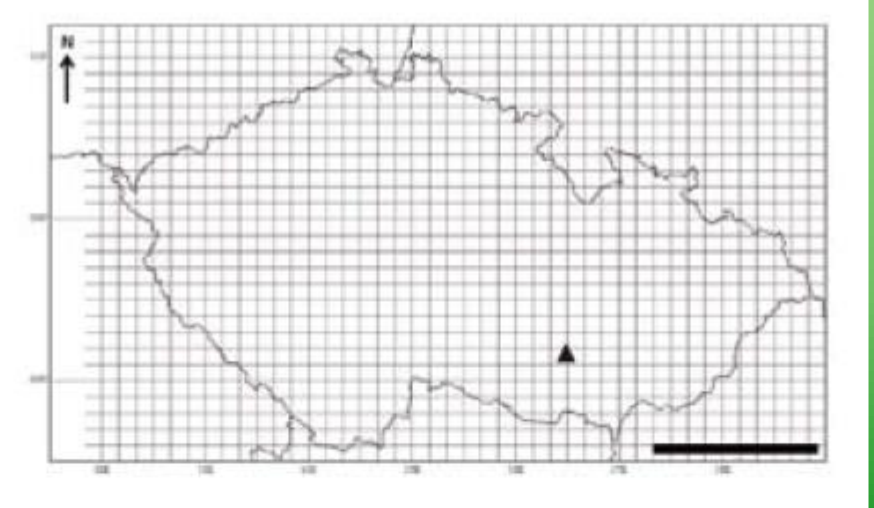

Fig. 231. Distribution of *Tolypella prolifera* in the Czech Republic (scale bar 100 km; for localities see attachment).

fossil Charophyceae

Gyrogonites

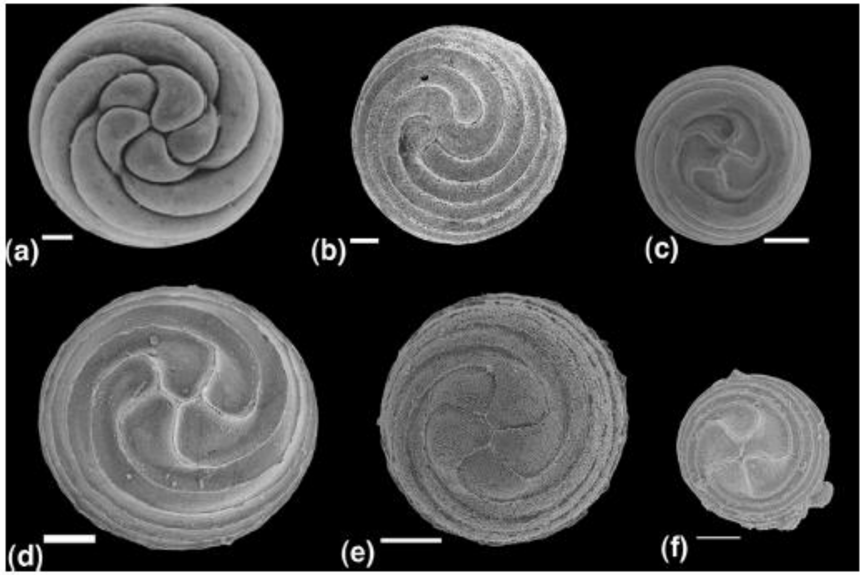

Fig. 6. Apical configuration of gyrogonites. (a) *Nitellopsis obtusa*, strongly developed, massive apical nodes; (b) *Lychnothamnus barbatus*, apical junction of the spiral cells without any change in width or thickness; (c) *Lamprothamnium papulosum*, apex typically deepened below the height of the apical periphery, usually weakly calcified; (d) *Chara hispida*, apical junction of the spiral cells enlarged with strongly protruding intercellular sutures; (e) *Chara globularis*, compact apical rosette, protruding in lateral view; (f) *Chara vulgaris*, greatly enlarged spiral tips create a large dehiscence zone at the apical pole. Scale bars: 100 µm.

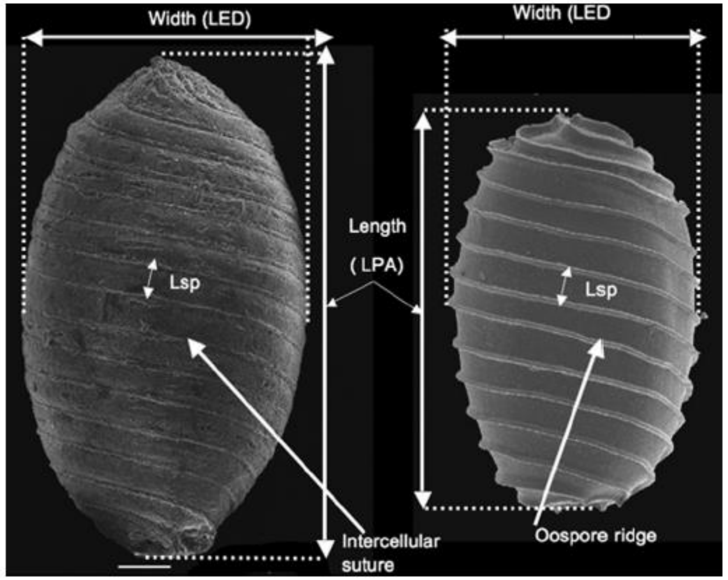

Fig. 9. Parameters for measurements and description of gyrogonites (left) and oospores (right). Scale bar: 10

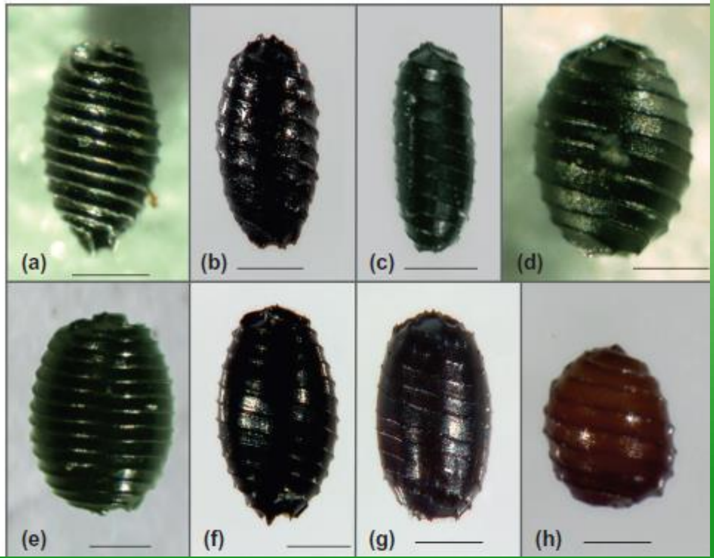

Souillé-Märsche & García (2015)

fossil Charophyceae

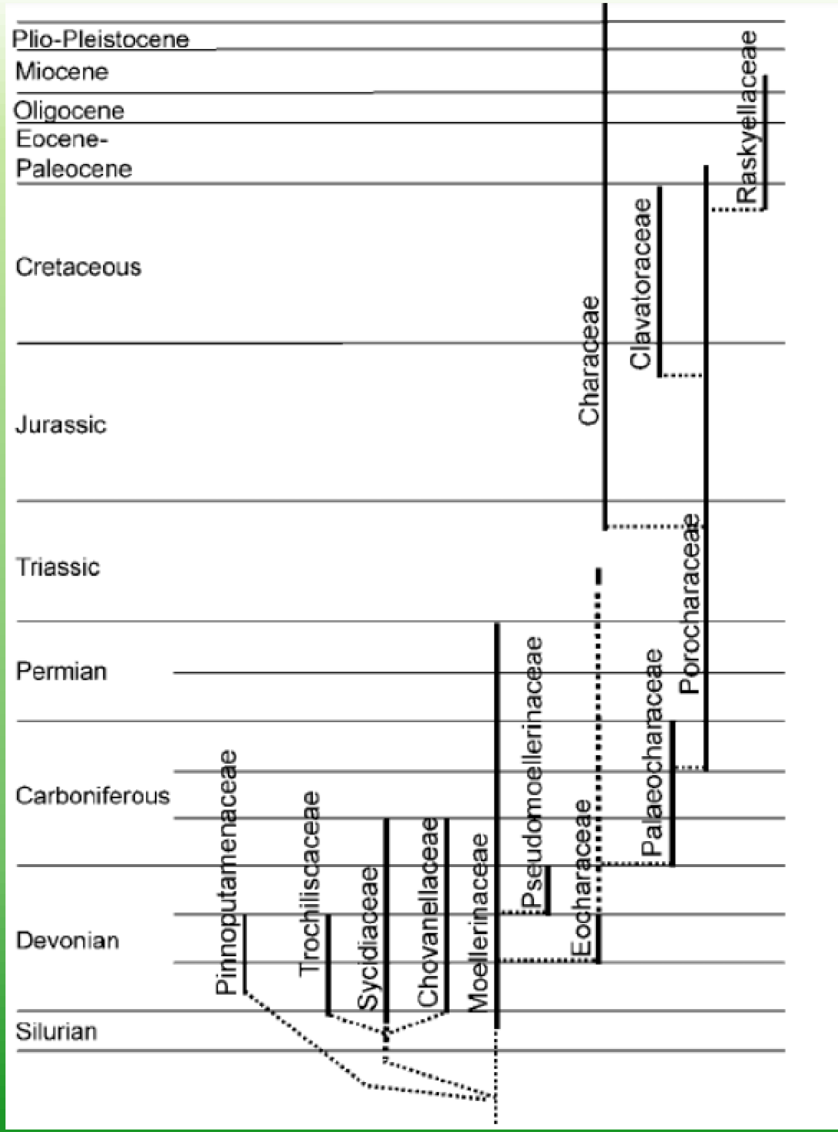

Feist et al. (2005)

fossil Charophyceae

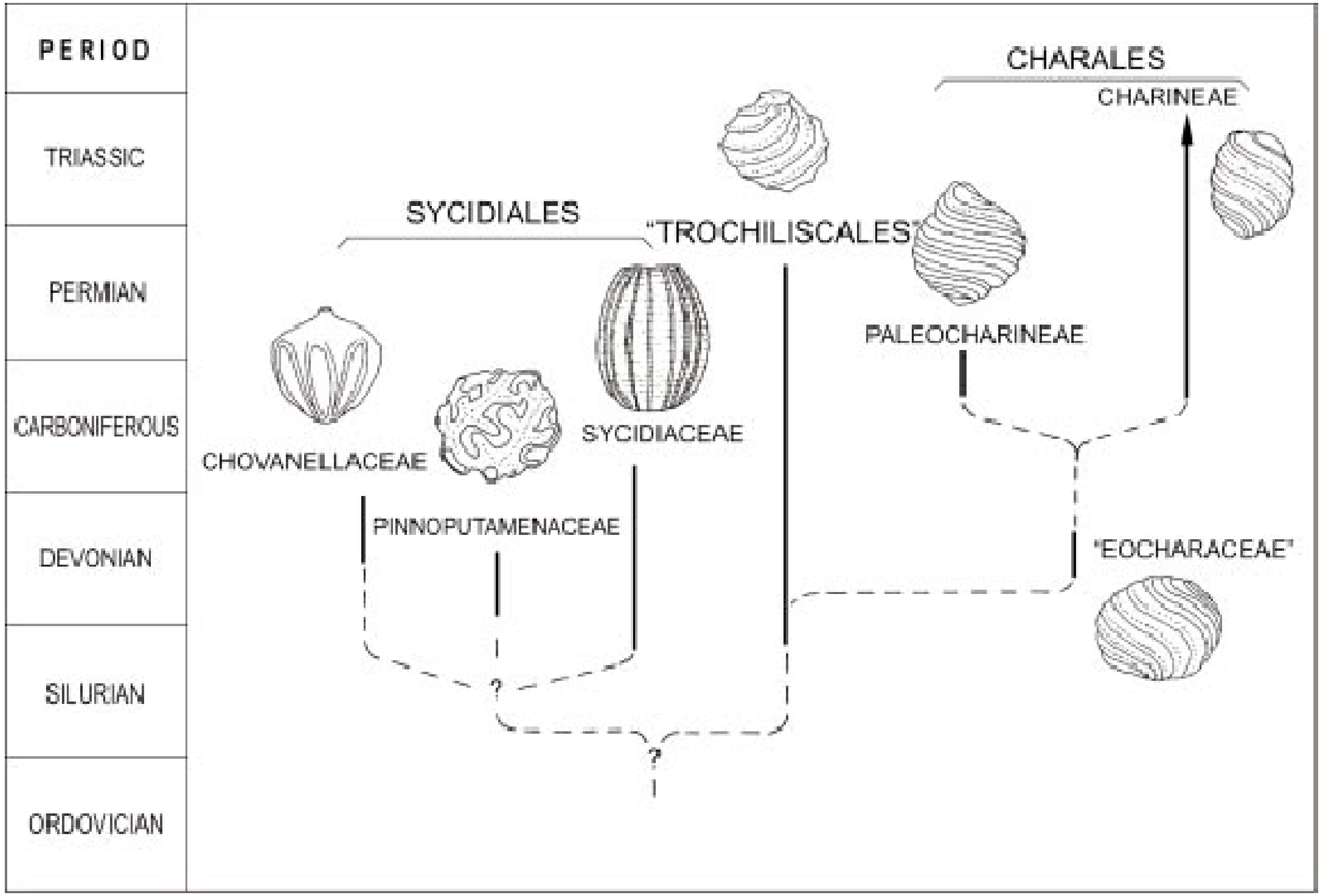

FIGURE 4 | Evolution of Palaeozoic charophyte fructifications (from Martín-Closas et al., 1999).

fossil Charophyceae

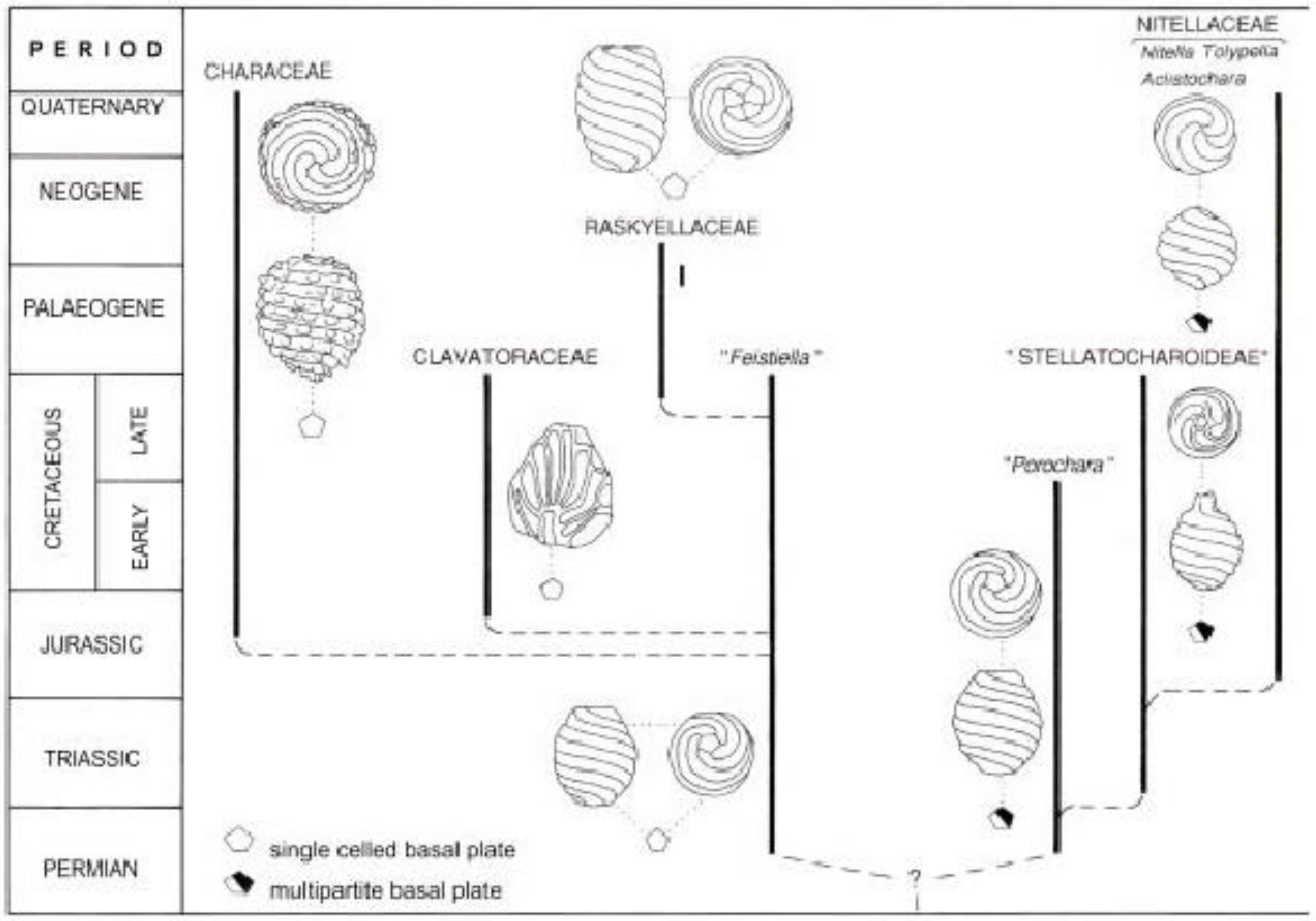

FIGURE 5 | Evolution of post-Palaeozoic charophyte fructifications.

Fosilní Charophyceae

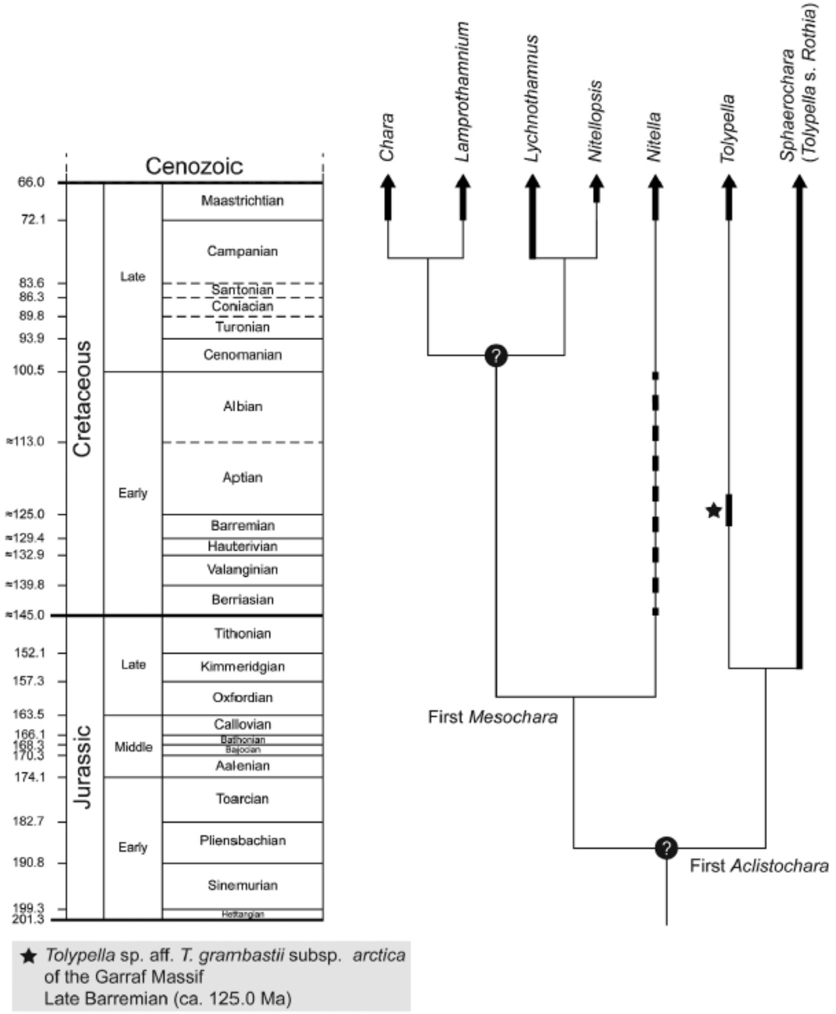

Figure 4. Phylogeny of extant characeans with ages of the main nodes as provided from fossils. The presently known fossil record of extant genera is marked with a bold line on the cladogram. Question marks at nodes indicate uncertainty in the age of the node. Phylogeny modified from Pérez et al. (2014).

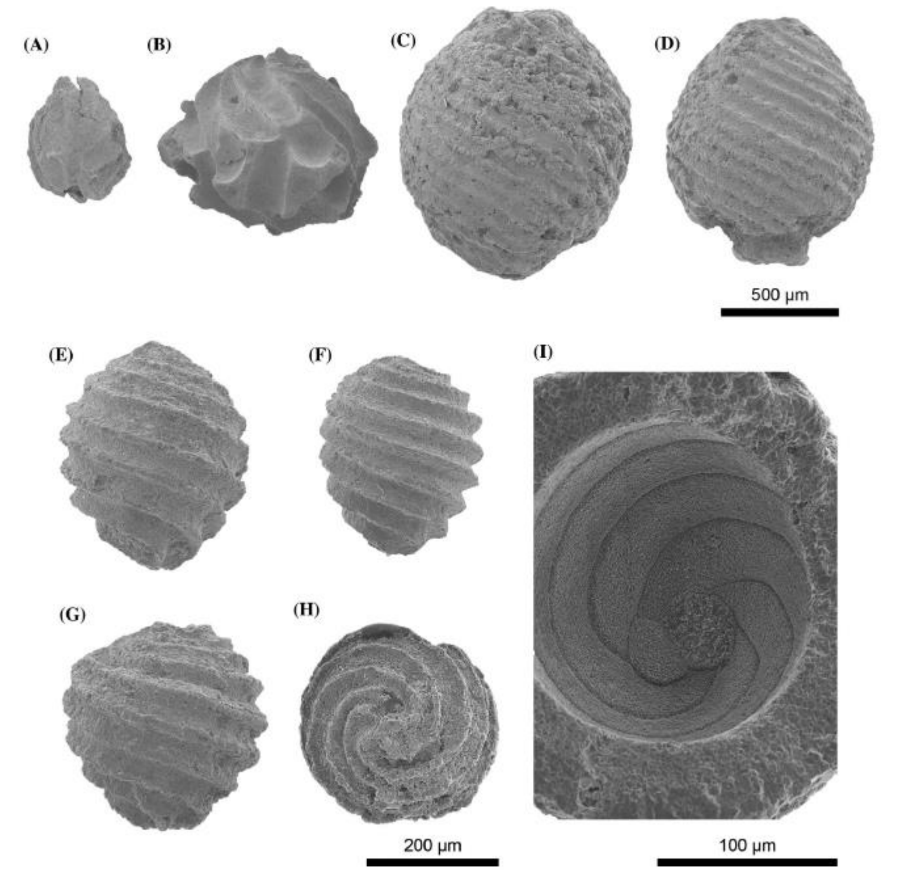

Figure 3. Charophytes from the upper Barremian–lower Aptian of the Garraf Massif. A. *Clavator harrisii*, lateral view of utricle; B. *Atopochara trivolvis triquetra* (advanced morphotype), lateral view of utricle; C. *Globator maillardii trochiliscoides*, lateral view of utricle; D. *Globator maillardii biutricularis*, lateral view of utricle; E–I. *Tolypella* sp. aff. *T. grambastii* subsp. *arctica*; E–G. lateral views of gyrogonite, H. apical view of gyrogonite, I. multipartite basal plate as seen from the inside of an empty gyrogonite.

Martín-Closas et al. (2018)

fossil Charophyceae

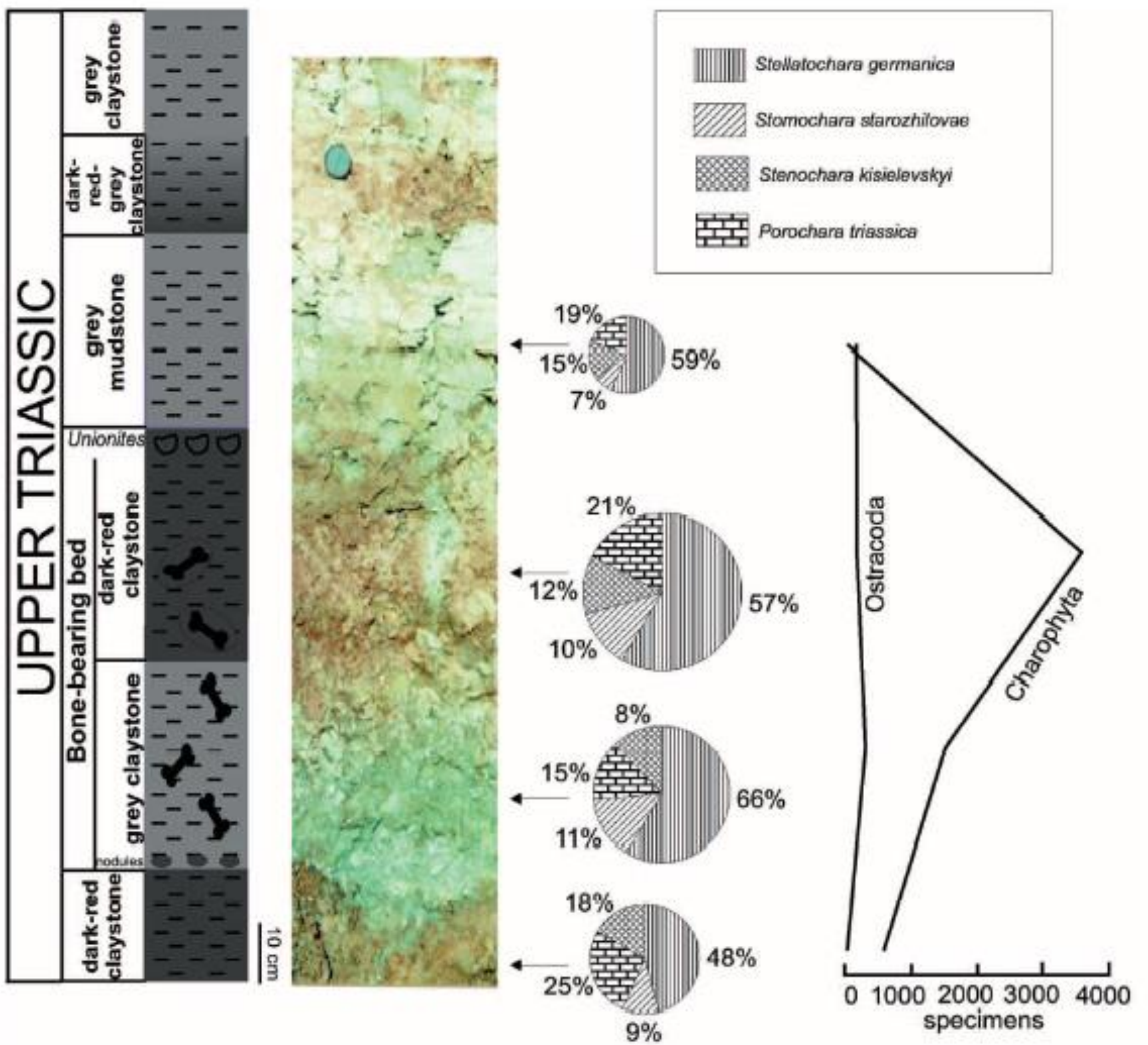

Fig. 2. Stratigraphy of the beds investigated at Krasiejów, with proportions of the charophyte species, and charophyte and ostracod quantities per kilogram of sediment. Photo taken by Dr. Wojciech KRAWCZYŃSKI

Zatoń et al. (2005)

fossil Charophyceae